

Harnessing Chromogenic Bacteria for Eco-Friendly Textile Dyeing: Pigment Production and Process Optimization



Birhanu Zeleke Jima

**A Dissertation Submitted to the Department of Applied Biology,
College of Applied Natural Science**

**Presented in Partial Fulfillment of the Requirement for the Degree of Doctor of
Philosophy in Biotechnology (Specialization in Environmental Biotechnology)**

Office of Graduate Studies

Adama Science and Technology University

January, 2026

Adama, Ethiopia

Harnessing Chromogenic Bacteria for Eco-Friendly Textile Dyeing: Pigment Production and Process Optimization

Birhanu Zeleke Jima

Supervisors

Diriba Muleta (PhD)

Dereje Tsegaye (PhD)

Professor Hunduma Dinka (PhD)

A Dissertation Submitted to the Department of Applied Biology,

College of Applied Natural Science

Presented in Partial Fulfillment of the Requirement for the Degree of Doctor of Philosophy in Biotechnology (Specialization in Environmental Biotechnology)

Office of Graduate Studies

Adama Science and Technology University

January, 2026

Adama, Ethiopia

Declaration

I hereby declare that this dissertation entitled “**Harnessing Chromogenic Bacteria for Eco-Friendly Textile Dyeing: Pigment Production and Process Optimization**” is my original work. That is, it has not been submitted for the award of any academic degree, diploma or certificate in any other university. All sources of materials used for this thesis have been duly acknowledged through appropriate citations.

Birhanu Zeleke



24/10/2025

Name of student

Signature

Date


Recommendation

We, the supervisors of this dissertation, hereby certify that we have read and revised the dissertation entitled “**Harnessing Chromogenic Bacteria for Eco-Friendly Textile Dyeing: Pigment Production and Process Optimization**” prepared under our guidance by Birhanu Zeleke submitted in partial fulfillment of the requirements for the degree of doctor of Philosophy in Biotechnology (specialization in Environmental Biotechnology). Therefore, we recommend the submission of the dissertation to the department for further review and defense.

<u>Diriba Muleta (PhD)</u>	 _____	<u>24/10/2025</u>
Major supervisor	Signature	Date
<u>Dereje Tsegaye (PhD)</u>	 _____	<u>24/10/2025</u>
Co-supervisor	Signature	Date
<u>Prof. Hunduma Dinka (PhD)</u>	 _____	<u>24/10/2025</u>
Co-supervisor	Signature	Date

Approval of Supervisors

We hereby certify that the recommendations and suggestions made by the board of examiners are appropriately incorporated into the final version of the dissertation entitled “**Harnessing Chromogenic Bacteria for Eco-Friendly Textile Dyeing: Pigment Production and Process Optimization**” by Birhanu Zeleke.

<u>Dr. Diriba Muleta</u>	 _____	_____
Major supervisor	Signature	Date
<u>Dr. Dereje Tsegaye</u>	_____	_____
Co-supervisor	Signature	Date
<u>Prof. Hunduma Dinka</u>	_____	_____
Co-supervisor	Signature	Date

Approval of Board of Reviewers

We, the undersigned members of the board of examiners of the dissertation open defense by Birhanu Zeleke have read and evaluated the dissertation entitled “**Harnessing Chromogenic Bacteria for Eco-Friendly Textile Dyeing: Pigment Production and Process Optimization**” and examined the candidate during open defense. This is therefore, to certify that the dissertation is accepted for partial fulfillment of the requirement of the degree of doctor of philosophy in Biotechnology (Specialization in Environmental Biotechnology).

Dr. Tilahun Hailu

Chairperson

Signature

Date

Dr. Zerihun Belay

Internal examiner 1

Signature

Date

Dr. Teshome Geremew

Internal examiner 2

Signature

Date

Dr. Adey Feleke

External examiner 1



Signature

Date

Dr. Mesfin Tadesse

External examiner 2



Signature

Date

Finally, approval and acceptance of the dissertation is contingent upon submission of its final copy to the Office of Postgraduate Studies (OPGS) through the Candidate’s Department Graduate Council (DGC) and College Graduate Committee (CGC)

Department head

Signature

Date

College Dean

Signature

Date

Office of Postgraduate Studies, Dean

Signature

Date

ACKNOWLEDGMENTS

I sincerely express my profound gratitude to my major supervisor, Dr. Diriba Muleta for his invaluable guidance, patience, and encouragement throughout this research. His unwavering support and trust have been truly inspiring. I also extend my heartfelt thanks to my co-supervisors, Dr. Dereje Tsegaye and Prof. Hunduma Dinka, for their close supervision, insightful guidance, and support throughout my research work.

Furthermore, I deeply appreciate Mr. Jemal Hassen in particular, and the Adama Regional Laboratory staff in general for their hospitality and assistance during my laboratory works. I am equally grateful to Adama Science and Technology University (ASTU) for the financial support through the Research University Grant (Grant No ASTU/SP-R/175/22). I extend my heartfelt gratitude to my home institution, Ethiopian Defense University, for generously sponsoring my terminal degree education and supporting my academic journey.

Finally, my special thanks go to my family and colleagues for their firm support, motivation, and help throughout this tough journey.

This research is dedicated to the memory of my beloved daughter, Haymanot Birhanu, whose sudden and untimely departure from us remains a big loss. My darling, may GOD rest your soul in peace. *God is always right.*



Birhanu Zeleke

Zelekebirhanu4@gmail.com

+251 911 101863

TABLE OF CONTENTS

CHAPTER	PAGE
DECLARATION.....	II
RECOMMENDATION.....	III
APPROVAL OF SUPERVISORS.....	IV
APPROVAL OF BOARD OF REVIEWERS.....	V
ACKNOWLEDGMENTS.....	VI
LIST OF TABLES.....	X
LIST OF FIGURES.....	XIII
LIST OF ACRONYMS AND ABBREVIATIONS.....	XVIII
ABSTRACT.....	XX
PUBLICATIONS ARISING FROM THIS DISSERTATION.....	XXI
CHAPTER ONE.....	1
INTRODUCTION.....	1
1.1 BACKGROUND OF THE STUDY.....	2
1.2 STATEMENT OF THE PROBLEM.....	7
1.3 OBJECTIVES.....	8
1.3.1 General objective.....	8
1.3.2 Specific objectives.....	8
1.4 RESEARCH QUESTIONS AND HYPOTHESES.....	9
1.5 SIGNIFICANCE OF THE STUDY.....	10
1.6 DELIMITATIONS AND LIMITATIONS.....	10
CHAPTER TWO.....	11
LITERATURE REVIEW.....	11
INTRODUCTION.....	11

2.1 CONTEXTUAL BACKGROUND	11
2.1.1 Overview of Dyes in the Textile Industry	11
2.1.2 Environmental and Health Concerns of Synthetic Dyes	13
2.2 MICROBIAL PIGMENTS AND CHROMOGENIC BACTERIA	16
2.2.1 Ecological Distribution of Chromogenic Bacteria	16
2.2.2 Isolation and Characterization of Pigment-Producing Bacteria	17
2.2.3 Genes Involved in Pigment Production	18
2.2.4 Strain Improvement in Chromogenic Bacteria	19
2.3 SUBSTRATES AND PRODUCTION APPROACHES	20
2.3.1 Agro-Wastes as Low-Cost Substrate for Culture Growth and Pigment Production	20
2.4 APPLICATIONS AND MARKET POTENTIAL	22
2.4.1 Broader Applications of Bacterial Pigments	22
2.4.2 Textile Dyeing with Bacterial Pigments	22
2.4.3 Merits and Demerits of Microbial Pigments	24
2.4.4 Global Market of Bacterial Pigments	24
2.5 SYNTHESIS AND RESEARCH POSITIONING	25
2.5.1 Gaps in the Literature	25
2.5.2 Theoretical Framework	26
2.5.3 Conceptual Framework Overview	27
CHAPTER THREE	29
MATERIALS AND METHODS	29
3.1 RESEARCH DESIGN	29
3.2 STUDY AREA AND SAMPLING SITES	30
3.3 CHEMICALS AND EQUIPMENT USED IN THE EXPERIMENT	32
3.4 ENVIRONMENTAL SAMPLING, MICROBIAL ISOLATION, AND PRIMARY SCREENING	33
3.5 CHARACTERIZATION OF THE POTENTIAL PIGMENT-PRODUCING ISOLATES	35
3.5.1 Biochemical characterization	35
3.5.2 Biomolecular characterization	35
3.6 ECO-PHYSIOLOGICAL TOLERANCE ASSESSMENT OF SELECTED BACTERIAL ISOLATES	36
3.6.1 Temperature tolerance test	37
3.6.2 pH tolerance test	37

3.6.3 Salt tolerance test	38
3.6.4 Agitation tolerance test.....	38
3.6.5 Carbon and Nitrogen utilization test	38
3.7 FORMULATION OF AGRO-WASTE BASED SUBSTRATES FOR BACTERIAL CULTIVATION.....	38
3.8 OPTIMIZATION OF GROWTH CONDITIONS FOR ENHANCED PIGMENT-PRODUCTION	40
3.8.1 Statistical screening of growth conditions	40
3.8.2 Statistical optimization of significant growth conditions.....	42
3.8.3 Experimental validation of statistically optimized growth conditions.....	43
3.9 EXTRACTION AND QUANTIFICATION OF BACTERIAL BIO-PIGMENTS	43
3.10 ANALYTICAL CHARACTERIZATION OF EXTRACTED PIGMENTS	44
3.10.1 UV-visible Analysis	45
3.10.2 LC-MS Analysis.....	45
3.10.3 ATR-FTIR Analysis.....	46
3.10.4 Pigment stability test	46
3.11 APPLICATION OF BIO-PIGMENTS IN TEXTILE DYEING AND PERFORMANCE EVALUATION ..	47
3.11.1 Pigment solution preparation and dyeing fabrics	47
3.11.2 Evaluation of dyeing performance	48
3.12 DATA ANALYSIS	49
CHAPTER FOUR	50
RESULTS AND DISCUSSION.....	50
4.1 SCREENING AND PROFILING OF PIGMENT-PRODUCING MICROBIAL ISOLATES.....	50
4.2. STRESS TOLERANCE PROFILING OF PIGMENT-PRODUCING BACTERIA	58
4.2.1 Temperature tolerance and growth pattern analysis.....	58
4.2.2 pH tolerance and growth pattern analysis	60
4.2.3 Salt tolerance and growth pattern analysis	63
4.2.4 Agitation tolerance and growth pattern analysis	66
4.2.5 Nutrient utilization and growth pattern analysis	68
4.3. GROWTH PERFORMANCE OF PIGMENT-PRODUCING BACTERIAL ISOLATES ON AGRO-WASTE EXTRACTS	74
4.4. ENHANCED PIGMENT YIELD THROUGH GROWTH CONDITIONS OPTIMIZATION	80
4.4.1 Evaluation of growth parameters	80

4.4.2 Optimization of selected growth parameters.....	84
4.5. ANALYSIS OF THE EFFECTS OF SIGNIFICANT PREDICTORS ON OUTCOME VARIABLES.....	87
4.5.1 Effect on OD value.....	88
4.5.2 Effect on cell biomass	91
4.5.3 Effect on pigment yield	93
4.6 YIELD AND EFFICIENCY OF PIGMENT RECOVERY	94
4.7 CHARACTERIZATION OF EXTRACTED BIO-PIGMENTS	102
4.7.1 Spectral and Structural Characterization of Bio-Pigments Using UV-Vis, LC-MS, and ATR-FTIR	103
4.7.2 Pigment stability analysis.....	110
4.8 DYEING PERFORMANCE OF BIO-PIGMENTS ON TEXTILE MATERIALS	120
CONCLUSIONS AND RECOMMENDATIONS.....	124
REFERENCES	128
APPENDICES	149

LIST OF TABLES

TABLE	PAGE
Table 1 Widely studied micro-organisms for natural pigment production	14
Table 2 Sample data sources, types, characteristics, and geographical coordinates	30
Table 3 Key Independent Variables Identified for Screening Using PBD.....	41
Table 4 Experimental Design Matrix: Significant variables and their optimization levels.....	42
Table 5 Morphological characteristics of pigment-producing potential isolates (PPPI).....	53
Table 6 Biochemical characteristics of pigment-producing potential isolates (PPPI)	54
Table 7 Bio-molecular characteristics of pigment-producing potential isolates (PPPI)	55
Table 8 Summary table of match quality: MALDI-TOF consistency with morphological and biochemical test results	57
Table 9 Summary statistics (Mean, SD, CV%) of OD ₆₀₀ for potential pigment-producing bacterial isolates across culture temperature conditions	59
Table 10 ANOVA summary for differences in mean OD ₆₀₀ values among six potential pigment-producing bacterial isolates in relation to temperature.....	59
Table 11 Pearson's correlation between temperature and OD ₆₀₀ for potential pigment- producing isolates.....	60
Table 12 Summary statistics (Mean, SD, CV%) of OD ₆₀₀ for potential pigment-producing bacterial isolates across different culture medium pH conditions	62
Table 13 ANOVA summary for differences in mean OD ₆₀₀ values among six potential pigment-producing bacterial isolates in relation to variation in pH.....	62
Table 14 Pearson's correlation between medium pH and OD ₆₀₀ for potential pigment- producing isolates.....	63
Table 15 Summary statistics (Mean, SD, CV %) of OD ₆₀₀ for potential pigment-producing bacterial isolates across culture medium salt concentration (% NaCl)	64
Table 16 ANOVA summary for differences in mean OD ₆₀₀ values among six potential pigment-producing bacterial isolates in relation to variation in salt concentration	65
Table 17 Pearson's correlation between salt concentration and OD ₆₀₀ for potential pigment- producing isolates.....	66

Table 18 Summary statistics (Mean, SD, CV %) of OD ₆₀₀ for potential pigment-producing bacterial isolates across culture medium agitation rate (rpm).....	67
Table 19 ANOVA summary for differences in mean OD ₆₀₀ values among six potential pigment-producing bacterial isolates in relation to variation in culture agitation rate	67
Table 20 Pearson's correlation between culture agitation and OD ₆₀₀ for potential pigment-producing isolates.....	68
Table 21 Summary statistics (Mean, SD, CV %) of OD ₆₀₀ for potential pigment-producing bacterial isolates across culture medium carbon sources (1% each).....	70
Table 22 Summary statistics (Mean, SD, CV %) of OD ₆₀₀ for potential pigment-producing bacterial isolates across culture medium nitrogen sources (0.1 % each)	70
Table 23 ANOVA summary for differences in mean OD ₆₀₀ values among six potential pigment-producing bacterial isolates grown on different carbon sources	71
Table 24 ANOVA summary for differences in mean OD ₆₀₀ values among six potential pigment-producing bacterial isolates grown on different nitrogen sources	71
Table 25 Pearson's correlation between carbon sources and OD ₆₀₀ for potential pigment-producing isolates.....	72
Table 26 Pearson's correlation between nitrogen sources and OD ₆₀₀ for potential pigment-producing isolates.....	72
Table 27 ANOVA depicting average OD ₆₀₀ values of <i>M. luteus</i> cultured in different AWEs .	75
Table 28 Group-wise OD ₆₀₀ measurements of <i>E. aurantiacum</i> broth culture and ANOVA summary.....	78
Table 29 PBD experimental run matrix with the corresponding response, mean values of triplicate OD ₆₀₀ for <i>E. aurantiacum</i> cultured in TWE.....	80
Table 30 ANOVA table for selected factorial model: Statistical significance assessment	83
Table 31 Fit Statistics Table: Model evaluation and Goodness-of-Fit Metrics.....	83
Table 32 Regression coefficients expressed in terms of factors.....	84
Table 33 Face-Centered Central Composite Design (FCCCD): Experimental matrix and response values.....	85
Table 34 ANOVA Results for Responses: Statistical Significance and Model Evaluation	86
Table 35 ANOVA results for quadratic model: Evaluating OD ₆₀₀ response	88
Table 36 ANOVA results for quadratic model: Statistical evaluation of biomass response....	92

Table 37 ANOVA Results for 2FI Model: Statistical evaluation of pigment yield response ...	94
Table 38 ANOVA summary table illustrating measured average OD values using different organic solvents for pigment extraction from <i>M. luteus</i>	95
Table 39 ANOVA summary table depicting average pigment yield recovered from <i>M. luteus</i> using different organic solvents	96
Table 40 Software generated solutions for verification experiment.....	98
Table 41 Predicted versus experimental response values from cultivating <i>E. aurantiacum</i> in TWE as substrate under optimized conditions.....	100
Table 42 Comparison of some recent studies on eco-friendly pigments derived from different microbial sources, highlighting the types of pigments produced and the substrates used to enhance pigment yield	101
Table 43 ANOVA summary table presenting the statistical analysis of variance results	111
Table 44 Summary of regression analysis presenting key statistical parameters.....	112
Table 45 ANOVA summary table presenting the statistical analysis of variance results	114
Table 46 Regression results table summarizing key statistical parameters	115
Table 47 ANOVA summary table presenting the statistical analysis of variance results	117
Table 48 ANOVA summary table presenting the statistical analysis of variance results	118
Table 49 Regression results table summarizing key statistical parameters.....	118
Table 50 Regression results table summarizing key statistical parameters.....	119
Table 51 Pigment's exhaustion and fixation calculation table presenting key parameters used to evaluate dye uptake and retention on fabrics	122

LIST OF FIGURES

FIGURE	PAGE
Figure 1 Schematic representation of how key models interconnect in the transition from synthetic dyes to pigments derived from bacterial sources, highlighting integration points.....	27
Figure 2 Conceptual frameworks illustrating the interconnections between core activities, guiding the research approach.....	28
Figure 3 Media prepared from agro-waste residues to be used as alternative low-cost growth substrate.....	39
Figure 4 Fermentation initiation: inoculation of AWEs with potential chromogenic isolates..	40
Figure 5 Pigment extractions: centrifugation of biomass at stationary growth phase post-fermentation	43
Figure 6 Representative colony morphologies of environmental isolates cultivated on nutrient agar for the recovery of pigment-producing strains. The printed labels on the culture plates denote the respective sources of the environmental samples.....	51
Figure 7 Pure colonies of pigment-producing bacterial isolates (PPPI-1 to PPPI-6) grown on nutrient agar. Panels (A)–(F) show isolates obtained from quarry soil (PPPI-1), hot spring (PPPI-2), oil-contaminated soil (PPPI-3), volcanic ash sediments (PPPI-4 and PPPI-5), and air sample (PPPI-6), respectively	52
Figure 8 Line chart illustrating the effect of incubation temperature variations on culture growth of pigment-producing isolates (PPPI-1 to PPPI-6), evaluated via OD ₆₀₀ measurement	58
Figure 9 Line chart demonstrating the effect of the variation in culture medium pH on culture growth of pigment-producing isolates (PPPI-1 to PPPI-6), evaluated via OD ₆₀₀ measurement	61
Figure 10 Line chart illustrating the effect of the variation in salt concentration on culture growth of pigment-producing isolates (PPPI-1 to PPPI-6), evaluated via OD ₆₀₀ measurement	64

Figure 11 Line chart showing the effect of the variation in culture agitation rate on culture growth of pigment-producing isolates (PPPI-1 to PPPI-6), evaluated via OD₆₀₀ measurement67

Figure 12 Line chart depicting the effect of carbon and nitrogen sources on growth of pigment-producing isolates (PPPI-1 to PPPI-6) evaluated via OD₆₀₀ measurement. Panel (A) shows culture response to various carbon sources supplied at 1%, while Panel (B) illustrates growth under different nitrogen sources provided at 0.1% 70

Figure 13 Heat maps of OD₆₀₀ readings illustrating isolates' tolerance across diverse environmental conditions; rows represent test conditions, columns indicate bacterial isolates. Colors reflect OD values: Green-weak growth, Yellow- medium growth, and Red-high growth.....74

Figure 14 Clustered bar charts depicting the impact of AWEs as growth substrate on the selected potent pigment-producing bacterial isolates. Bar height shows mean and standard deviations of triplicate OD₆₀₀ measurements and error bars show standard deviations75

Figure 15 Regression analyses of incubation temperature and pH effects on OD₆₀₀ based measurements of *M. luteus* growth cultured in orange waste extract. Panel (A) presents the growth trend across temperature gradients, while Panel (B) depicts the growth response to varying pH levels77

Figure 16 Regression analyses of salt concentration and agitation effects on OD₆₀₀ based growth of *M. luteus* cultured in orange waste extract. Panel (A) presents the growth trend across different salt concentrations, and Panel (B) illustrates the growth response to varying culture agitation rates78

Figure 17 Half-normal plot for the standardized effects of process variables on OD₆₀₀ value highlighting critical factors for optimization. The absolute values of the estimated effects were plotted against the expected normal order statistics, gives half-normal distribution.82

Figure 18 Pareto chart depicting the influence of process variables on OD₆₀₀ value in descending order, bars representing each variable's contribution to the overall effect83

Figure 19 Response surface optimization graphs generated by Design Expert Statistical software, version 13. Panels (A)-(F) depicting how changes in independent variables affect output variables. Panel (A) shows the relationship between agitation speed (rpm) and pH on OD value. Panel (B) illustrates effects of yeast extract concentration and initial medium pH on OD value. Panels (C) and (D) elucidate the combined effects of agitation versus pH and yeast extract versus pH on culture biomass yield, and Panels (E) and (F) demonstrates how pigment yield was influenced by agitation rate, pH, and yeast extract concentration	91
Figure 20 Cultivation and pigment extraction processes from <i>M. luteus</i> . (A) cultivation of an isolate in different AWEs at optimized culture conditions, (B) fermented culture in orange waste extract, (C) pigment pellet after centrifugation, (D) methanolic pigment extract, (E) concentration process in biosafety cabinet for solvent evaporation, and (F) solidified pigment.....	98
Figure 21 Smooth line graph showing OD ₆₀₀ variation over time of <i>E. aurantiacum</i> at optimized process conditions using TWE as cultivation substrate with standard deviation represented as error bars around the line.....	100
Figure 22 Pure cultures of three bacterial isolates alongside their respective extracted pigments: (A) <i>M. luteus</i> , producing a bright-yellow pigment, (B) <i>E. aurantiacum</i> , yielding an orange-yellow pigment, and (C) <i>Kocuria</i> sp., exhibiting a creamy light-yellow pigment.....	103
Figure 23 Absorption spectra of pigments extracted from three bacterial isolates from left to right: (A) <i>M. luteus</i> , (B) <i>E. aurantiacum</i> , and (C) <i>Kocuria</i> sp.....	104
Figure 24 Mass spectra of pigmented compounds extracted from three bacterial isolates from left to right: (A) <i>M. luteus</i> , (B) <i>E. aurantiacum</i> , and (C) <i>Kocuria</i> sp.	106
Figure 25 The structural information of bioactive compound responsible for pigmentation. (A) TIC of the pigmented compound extracted from <i>M. luteus</i> and (B) mass spectra of psi,psi.-carotene,1,1',2,2'-tetrahydro-1,1'-bis[(trimethylsilyl)oxy]-, having multiple peaks with the most abundant fragment ion at ($m/z=716$)	106
Figure 26 LC-MS analysis of carotenoid compounds extracted from <i>E. aurantiacum</i> : Panel (A) illustrates the ion intensity detected over time, Panels (B) and (C) reveal peaks	

	corresponding to the mass-to-charge ratios (m/z) of the detected carotenoid molecules	107
Figure 27	The IR spectrum of pigmented compound extracted from <i>M. luteus</i> . The IR spectrum corresponds to the O-H, C-H and C=C stretching vibrations showed the presence of hydroxyl, alkane and alkene groups.....	109
Figure 28	IR spectrum of pigmented compound extracted from <i>E. aurantiacum</i> , depicting characteristic absorption peaks corresponding to various functional groups present in the compound.....	110
Figure 29	Influence of pH on the stability of the pigment extracted from <i>M. luteus</i> : (A) A line graph showing changes in absorbance of the pigment as a function of change in pH level, (B) Color intensity of the pigment across different pH levels, with labeled test tube vials indicating the respective pH values. The labels on each test tube vials indicate the pH value of the respective pigment solutions.....	112
Figure 30	Line fit plot showing the relationship between pH and the pigment stability, illustrating how changes in pH influence absorbance. The fitted line represents the trend in pigment behavior across different pH levels, providing insights into its stability.....	113
Figure 31	Influence of temperature on the stability of the pigment extracted from <i>M. luteus</i> : (A) A line graph illustrating changes in absorbance across different temperature levels, showing trends and variation patterns of the pigment as a function of temperature change, and (B) Visual representation of pigment color intensity at various temperatures. The labels on each test tube vials indicate the temperature of the respective pigment solutions	114
Figure 32	Line fit plot illustrating the relationship between temperature and pigment stability, showing how changes in temperature affect absorbance. The fitted line represents the trend in pigment behavior across different temperature levels, providing insights into its thermal stability.....	116
Figure 33	Influence of oxidizing and reducing agents on the stability of the pigment extracted from <i>M. luteus</i> : (A) Absorbance pattern and color intensity of the pigment solution as a function of varying concentrations of H ₂ O ₂ , and (B) Absorbance pattern and color	

intensity of the pigment solution as a function of varying concentrations of glucose 117

Figure 34 Line fit plot illustrating the effect of hydrogen peroxide (H_2O_2) and glucose concentrations on the stability of the extracted pigment. The fitted lines represent the trends in absorbance as a function of oxidizing (H_2O_2) and reducing (glucose) agents, providing insights into the pigment's chemical stability under varying conditions.. 120

Figure 35 Actual images of cotton and Tetron 6000 fabrics before and after dyeing tests showing color difference. Panels (A) and (B) show pigment uptake by cotton and Tetron 6000 fabrics, respectively. Panels (C) and (D) show un-dyed cotton and Tetron 6000 fabrics, respectively, used as negative control for pigment uptake and retention comparison. Panels (E) and (F) depict color retention comparison between cotton and Tetron 6000 fabrics, respectively, after washing with detergent and exposure to sunlight 122

LIST OF ACRONYMS AND ABBREVIATIONS

ANOVA	Analysis of Variance
ATR	Attenuated Total Reflectance
AWE	Agro-Waste Extract
BSC	Biosafety Cabinet
CCD	Central Composite Design
CHCA	Cyano Hydroxycinnamic Acid
CSA	Central Statistics Authority
ESI	Electrospray Ionization
FTIR	Fourier Transform Infrared
GNB	Gram Negative Bacilli
GPB	Gram Positive Bacilli
GPC	Gram Positive Cocci
GPS	Geographical Positioning System
IR	Infrared
LC	Liquid Chromatography
LC-MS	Liquid-Chromatography-Mass Spectrometry
MALDI-TOF	Matrix Assisted Laser Desorption/Ionization Time-of-Flight
MR	Methyl Red
MS	Mass Spectra
NA	Nutrient Agar
OD	Optical Density
OVAT	One-Variable-at-a-Time
OWE	Orange waste Extract
PBD	Plackett-Burman Design
PPPI	Potential Pigment-Producing Isolate
PSI	Pound Square Inch
REACH	Registration Evaluation Authorization and Restriction of Chemicals
RPM	Revolution Per Minute

RSM	Response Surface Methodology
SmF	Submerged Fermentation
TWE	Tomato Waste Extract
UV-Vis	Ultra Violet-Visible
VP	Voges Proskauer

ABSTRACT

*Microbial pigments are emerging as sustainable alternatives to synthetic dyes due to their environmental compatibility and potential for circular bio-economy applications. This study focused on the identification of potent pigment-producing bacterial isolates, the use of agro-waste substrates as low-cost substrates, and the optimization of culture parameters to enhance pigment yield. The study systematically explored pigment-producing bacterial isolates from environmental samples, employing morphological, biochemical, and MALDI-TOF analyses for identification. Eco-physiological tolerance was assessed using the one-variable-at-a-time approach, while culture optimization was conducted through Plackett–Burman Design followed by response surface methodology. Agro-waste extracts as low-cost substrates were evaluated via optical density measurements, and pigments were extracted using organic solvents. Pigments were characterized using UV-Vis spectroscopy, LC-MS, and ATR-FTIR. The pigments' stability under varying stressor conditions was assessed by monitoring absorbance at their characteristic wavelengths. Fabrics dyeing were conducted using immersion technique. Dye exhaustion and fixation to fabrics were evaluated via absorbance method after washing and exposure to sunlight. From purified colonies on streak plates, six isolates; namely: *Acinetobacter* sp., *Exiguobacterium aurantiacum*, two *Kocuria* spp. (from different samples), *Micrococcus luteus*, and one unidentified strain, exhibited chromogenic potential. Among the chromogenic isolates screened, *Micrococcus luteus* exhibited the highest pigment yield (1.47 g/L) under orange-waste extract cultivation, likely due to the isolate's inherent carotenoid biosynthetic capacity, stress tolerance, and efficient substrate utilization. Optimization of pigment production by *Exiguobacterium aurantiacum* using tomato-waste extract revealed that agitation rate, pH, and yeast extract concentrations were the most significant factors influencing culture growth ($p < 0.001$), leading to 1.6-fold yield increment compared to un-optimized conditions. The characteristic UV-Visible absorbance peaks (400–550 nm) indicated the pigments are likely carotenoid compounds with functional group signatures (O–H, C–H, C=C, C=O) from infrared spectra analyses. The LC-MS analyses further resolved pigment mixtures, provided molecular weights and fragmentation patterns, indicating pigment heterogeneity. Stability assays of *Micrococcus luteus* pigment indicated susceptibility to oxidative and thermal stress, while dyeing trials demonstrated vibrant and uniform coloration with moderate fixation on fabrics. While microbial pigment production has been widely reported, existing studies predominantly rely on synthetic media. The present study is fundamentally novel, integrating systematic screening, agro-waste valorization, and multivariate statistical optimization, marking the first such effort in Ethiopia. The findings highlight *Micrococcus luteus* as a robust candidate for scalable, eco-friendly pigment production under low-cost sustainable culture conditions. The findings highlight the feasibility of low-cost, eco-friendly microbial pigments for industrial applications as promising alternatives to synthetic dyes.*

Keywords: Agro-waste extracts, Carotenoid, Eco-friendly dyeing, Exiguobacterium aurantiacum, Micrococcus luteus, Pigment production,

Publications arising from this dissertation

Zelege B, Muleta D, Dinka H, Tsegaye D, Hassen J (2025) Enhancing pigment production by a chromogenic bacterium (*Exiguobacterium aurantiacum*) using tomato waste extract: A statistical approach. PLoS One 20(6): e0312922.

<https://doi.org/10.1371/journal.pone.0312922>

Zelege, B., Muleta, D., Dinka, H. *et al.* Stability and dyeing performance of *Micrococcus luteus* pigment on cotton and polyester fabrics. *Discov Biotechnol*, 2, 31(2025).

<https://doi.org/10.1007/s44340-025-00038-7>

B. Zelege, D.Muleta. H.dinka, D.Tsegaye, and J.Hassen, Characterization of chromogenic bacteria using agro-waste extracts as substrate for pigments production, *Heliyon*, vol 12, no.1, p. e44470, Jan. 2026.

<https://doi.org/10.1016/j.heliyon.2025.e44470>

CHAPTER ONE

INTRODUCTION

Synthetic dyes derived from petroleum continue to dominate industrial applications particularly in the textile sector due to their color fastness, ease of application, and economic viability. However, their extensive use has become major contributor to global environmental pollution with dyeing processes consuming large volumes of water and generating toxic effluents rich in residual dyes and salts. The persistence of synthetic dyes, especially azo and nitro compounds in aquatic ecosystems pose serious ecological and health risks including carcinogenicity, oxygen depletion, and biodiversity loss. Emerging textile hubs such as Ethiopia reflect the growing reliance on synthetic dyes, further intensifying concerns over sustainability.

Driven by growing regulatory pressures and rising consumer demand for eco-friendly products, interest in natural pigments particularly those derived from microorganisms has intensified. Unlike synthetic dyes, microbial pigments provide clear environmental, health, and economic advantages, positioning them as viable candidates for industrial adoption within a circular bio-economy framework.

Microbial pigments combine biodegradability, non-toxicity, and functional bioactivities such as antioxidant and antimicrobial properties, making them attractive alternatives to synthetic dyes. Advances in biotechnology, including strain improvement, fermentation optimization, and the use of agro-waste substrates have enhanced pigment yield and reduced production costs, aligning pigment production with circular economy principles. Despite challenges related to stability, scalability, and regulatory compliance, microbial pigments are gaining attraction in textiles, cosmetics, and food industries, supported by innovations in nanoparticle technology, waterless dyeing, and statistical optimization methods.

Against this background the present study explored eco-friendly pigment production from chromogenic bacteria cultivated on agro-waste substrates with focus on their dyeing potential

for cotton and polyester fabrics. By evaluating culture growth, pigment stability, and dyeing performance under optimized conditions, this research aimed to address key challenges and contribute to the development of sustainable, scalable, and environmentally responsible dyeing practices.

1.1 Background of the study

Petroleum based synthetic dyes dominate industrial applications with the textile sector being a major contributor to global environmental pollution mainly due to their color fastness, ease of application, and economic viability (Akter et al., 2023; Slama et al., 2021). Moreover, dyeing processes consume huge amounts of water, 30-50 liters per kg of fabric (Khattab et al., 2020; Pei et al., 2024), generating toxic wastewater loaded with residual dyes and salts, contributing for significant water pollution. The textile industry still accounts for 20% of global wastewater, 40% of which are carcinogenic (Khattab et al., 2020).

Globally, synthetic dyes production exceed 800,000 tons annually with over 10,000 variants in use (Islam et al., 2022). Due to their stable structures and resistance to natural degradation, dyes can persist in the environment for many years (Mehta et al., 2021). Recent study shows that synthetic dyes especially azo and nitro compounds remain the dominant pollutants in textile effluents, with over 280,000 tons released annually into water bodies (Kusumlata et al., 2024). Textile wastewater, especially in low and middle-income countries is frequently released untreated, compounding ecological degradation.

The widespread use of synthetic dyes poses a serious threat to ecosystem productivity and environmental sustainability. When discharged into aquatic environments these dyes intensify pollution and create unpleasant odors that degrade water quality. Their dense coloration reduces sunlight penetration which in turn limits photosynthesis in aquatic plants and algae. This disruption impairs oxygen exchange within water bodies, leading to depleted oxygen levels that endanger fish and other aquatic organisms. Increased turbidity further destabilizes ecological balance, while persistent dye compounds contribute to long-term oxygen depletion. Beyond ecological impacts many synthetic dyes carry potential carcinogenic risks, raising concerns for both environmental health and human safety (Islam et al., 2022).

Countries like China, India, Bangladesh, and Vietnam dominate global textile production, while Ethiopia and Egypt are emerging hubs due to cost advantages and government incentives (Sanghvi & Sekhar, 2025). Ethiopia in particular has prioritized textile manufacturing as a key industrial strategy, attracting foreign investment and fostering sectoral growth. Ethiopia's textile sector has grown significantly with over a hundred firms engaged in manufacturing as of the 2012/13 survey by the Central Statistical Agency (CSA). In 2015, Ethiopian textile processing units consumed approximately 1,425 tons of various dyes and chemicals, reflecting the industry's reliance on synthetic dyes and excessive water usage.

Ethiopia's textile and garment industries rely heavily on synthetic dyes and chemicals particularly azo, reactive, and disperse dyes with dyeing processes consuming large amounts of salts, alkalis, and fixing agents that contribute to untreated wastewater discharges near industrial parks, worsening ecological and public health concerns. Despite global shifts toward bio-based pigments, the sector remains dominated by synthetics though increasing pressure from the government side and international buyers underscores the urgent need for sustainable alternatives (Fobiri GK, 2022; Slama et al., 2021).

Concerns over the environmental and health hazards of synthetic dyes, particularly in textiles, food, and cosmetics have driven interest in sustainable alternatives. Regulatory bodies like the European Union regulation for the Registration, Evaluation, Authorization and Restriction of Chemicals (REACH) are enforcing stricter chemical controls alongside increasing consumer demand for eco-friendly products (Negi, 2025). Hence, the transition toward greener practices using natural pigments sourced from microorganisms has gained momentum to curb the problems.

Waterless dyeing technologies such as supercritical CO₂ and air dyeing significantly reduce water consumption, while low-liquor ratio methods lower salt requirements and thereby minimize wastewater generation and environmental impact (Mahmud and Kaiser, 2020). Moreover, advancements in nanoparticle technology have enhanced pigment binding with improved color vibrancy and stability, expanding the potential of microbial pigments as the most promising alternative to synthetic dyes for scalable and eco-friendly textile dyeing applications (Abdelgawad et al., 2025).

Advances in fermentation technology and genetic engineering are improving pigment yield and scalability (Devi, et al., 2020). Microorganisms can be rapidly and efficiently cultured on minimal space through fermentation on low-cost agro-waste substrates, offering dual benefits of pigment synthesis and waste reduction (Kamble et al., 2022; Geyik et al., 2024; Devi, et al., 2020), making microbial pigments viable alternatives to synthetic dyes.

Transitioning from shake-flask cultivation to controlled pilot-scale bioreactors is essential to ensure reproducibility and scalability of microbial pigment production. Continuous fermentation systems further enhance productivity by maintaining steady-state cultures and reducing downtime (Basto et al., 2025). Achieving industrial scalability, however, requires a reliable and consistent supply of agro-waste substrates, which can be secured through strategic partnerships with agro-industries such as tomato processors and breweries. Integrating these waste streams not only stabilizes substrate availability but also strengthens the economic feasibility of large-scale operations. Moreover, valorizing agro-waste directly supports circular economy policies, thereby increasing the attractiveness of microbial pigment technologies to both governments and investors (Możejko-Ciesielska, 2025).

Key innovations in microbial pigment production center on optimizing fermentation processes, harnessing agro-industrial waste as cost-effective substrates, enhancing pigment yields, and advancing bioreactor technologies to achieve economic scalability. Pigments derived from agro-waste substrates demonstrate strong potential for both economic feasibility and industrial adoption. However, realizing this potential requires systematic bioprocess optimization, consistent yield performance, and the establishment of resilient supply chains that integrate waste valorization with downstream textile and related applications (Możejko-Ciesielska, 2025).

Enhanced filtration and chromatographic techniques have refined pigment purity. Regulatory approved pigments like carotenoids are now incorporated into textiles, cosmetics, and food products (Harshini et al., 2025). However, challenges including stability issues, production costs, and scalability hurdles needs to be addressed for broader adoption. Environmental sensitivity (e.g., pH, temperature, light exposure, etc.,) also affects pigment shelf life.

Regulatory approvals also require extensive safety testing and compliance (Agarwal et al., 2023).

Recent progresses indicate bacterial pigments could revolutionize sustainable textile dyeing, offering both functional and ecological benefits. Advances in strain selection, fermentation optimization, metabolic engineering, and eco-friendly processing are enhancing the feasibility of bacterial pigments. Research is progressing toward improving color fastness, addressing wash resistance, and integrating bacterial dyeing methods into textile designs. Despite promising advances, pigment stability and production efficiency remain big challenges, limiting scalability (Sen et al., 2019). Maximizing microbial pigment yield and minimizing production costs are critical for economic viability.

The use of low-cost agro-wastes as substrates for microbial culture growth extends agro-waste valorization beyond simple substitution, transforming low-value residues into functional inputs that drive biological innovation, sustainability, and circular bio-economy outcomes (Huang et al., 2024). Continued screening of novel microbial isolates holds promise for identifying pigments with greater stability, expanded color ranges, and improved compatibility with diverse textile substrates. In parallel, systematic optimization of dyeing parameters including temperature, pH, and chemical interactions remain essential to enhance color fastness and durability, thereby strengthening the industrial applicability of microbial pigments (Coccatto et al., 2017; Gong et al., 2017; Molina et al., 2023).

The one-variable-at-a-time (OVAT) optimization method has traditionally been employed in microbial process development; however, it is constrained by the need for numerous experimental trials, high labor intensity, and its inability to account for interactions among variables. In contrast, statistical experimental design approaches such as Plackett-Burman Design (PBD) and Response Surface Methodology (RSM) provide more efficient pathways to optimization. These methods enable systematic identification of critical factors influencing pigment yield, capture variable interactions, and reduce the number of required experiments. By enhancing process efficiency and maximizing pigment output, they contribute directly to lowering production costs per unit and improving the economic feasibility of microbial pigment production (Basto et al., 2025)

Plackett-Burman design which enables rapid screening of influential process variables and minimize unnecessary trials has been widely applied in enzyme production, bio-surfactant optimization, and liposome formulation (Chaudhari & Shirkhedkar, 2020). Furthermore, RSM reduces complexity by evaluating multiple factors and their interactions simultaneously, optimizing fermentation parameters, pH stability, and biomass production in bacterial pigments (Oliveira et al., 2019). Various factors including agitation, nutrient sources, substrate type, inoculum age, temperature, and pH affect microbial pigment yield and hence, optimizing these parameters enhances productivity, improving pigment stability and fastness for textile dyeing applications.

The rapid expansion of textile and garment industries in Ethiopia has intensified concerns over environmental pollution particularly due to the widespread use of synthetic dyes and chemicals. Most industries lack efficient wastewater treatment facilities, resulting in untreated effluent discharges that pose serious ecological and public health risks. Despite global advances in eco-friendly alternatives, no remedial trials have been undertaken locally to replace synthetic dyes with eco-friendly pigments. Furthermore, there has been no isolation, screening, or evaluation of pigment-producing microbial isolates for textile applications, and no successful case studies have been reported. This highlights a clear research gap in Ethiopia regarding sustainable pigment production and its potential role in reducing the environmental footprint of the textile sector.

This study investigated the dyeing potential of bacterial pigments on cotton and polyester fabrics with isolates recovered from diverse environmental samples across ecological zones of Ethiopia. Potent strains were screened for eco-physiological tolerance and cultivated using agro-waste extracts; an innovative, low-cost, and eco-friendly substrate strategy that marks significant progress in sustainable dyeing practices. By optimizing culture and dyeing conditions, this research addressed key challenges related to microbial growth, pigment stability, and dyeing performance, thereby paving the way for scalable and environmentally responsible textile applications. The originality of this work lies in its integrated approach, combining microbial screening, agro-waste valorization, statistical optimization, and application validation within a single framework. Notably, *Micrococcus luteus* emerged as a

robust pigment producer under low-cost sustainable conditions, underscoring its potential as a candidate organism for industrial-scale bio-based dye production.

1.2 Statement of the problem

Synthetic dyes have long been dominated dyeing industries due to their efficiency, stability, and cost-effectiveness. However, growing concerns about safety and consumer preference have led to increased interest in natural colorants, driving research into sustainable alternatives. This shift highlights the need for safer, eco-friendly solutions in the dyeing industry.

The textile industry is heavily reliant on synthetic dyes, contribute to environmental pollution and pose health risks due to their non-biodegradable toxic waste products. Despite the promising potential of bacterial pigments as natural alternatives, commercialization is limited by low yields, high production costs, unstable color properties, and the lack of cost-effective substrates for large-scale production. Synthetic culture media are expensive and unsustainable, making large-scale microbial dye production economically unfeasible (Negi, 2025).

Simultaneously, the agro-industrial sectors generate large volumes of organic wastes, rich in carbon and nitrogen which can serve as nutrient-rich substrates for microbial fermentation (Astudillo et al., 2023). Therefore, integrating bacterial pigment production with agro-waste valorization presents a dual opportunity to reduce the environmental burden of waste and to lower the cost of bio-pigment production.

The growing global demand for textiles, particularly those reliant on synthetic dyes has contributed to severe environmental pollution from textile effluents containing acids, alkalis, solvents, heavy metals, and excessive water usage (Yuan et al., 2016). These concerns have intensified interest in alternative colorants derived from microorganisms which are natural, cost-effective, and readily biodegradable, avoiding the formation of recalcitrant intermediates upon environmental release. The rising demand for eco-friendly dyes across industries has created a promising market niche where microbial pigments can compete, despite higher initial production costs, by offering sustainable and environmentally responsible solutions (Możejko-Ciesielska, 2025).

While microbial pigments are in early research stages of industrial application, their easy cultivation on an inexpensive media, wide color spectrum, and environmental compatibility make them attractive substitutes for synthetic dyes. Utilizing agro-wastes as substrate for microbial growth offers a cost-effective solution for natural pigment production. This study addressed the absence of prior efforts in Ethiopia to integrate microbial pigment synthesis with agro-waste valorization by screening potent pigment-producing bacterial isolates, optimizing pigment production, evaluating pigment stability under environmental stressors, and assessing dyeing performance. In doing so, it directly responded to the lack of eco-friendly alternatives to synthetic dyes and demonstrated a pathway toward reducing the environmental footprint of textile dyeing.

1.3 Objectives

1.3.1 General objective

The main objective of this research was to investigate bacterial pigments as sustainable alternatives to synthetic dyes for textile dyeing applications by utilizing agro-waste extracts as cost-effective growth substrate.

1.3.2 Specific objectives

The specific objectives of this study were:

- To isolate, characterize and identify pigment-producing bacteria from diverse environmental samples.
- To evaluate eco-physiological tolerance of the identified pigment-producing bacterial isolates to temperature, pH, agitation, salt concentration, and nutrient concentration
- To optimize growth conditions of the pigment-producing bacterial isolates using agro-waste extracts as substrate
- To characterize the bio-pigments, evaluate their stability and dyeing performance on textile materials

1.4 Research questions and hypotheses

The research questions define the core inquiry and guide the direction of this research, reflecting the overall research aim to explore bacterial pigments as sustainable alternatives to synthetic dyes in textile applications. Therefore, the following research questions were formulated to establish the investigative focus of this study.

1. Do environmental bacterial strains produce pigments when cultured on agro-waste extracts?
2. Is there any difference between agro-waste extracts in promoting bacterial pigment production?
3. What environmental factors influence culture growth and pigment production? and
4. How stable are bacterial pigments under varying environmental factors such as temperature, light exposure, and pH variations?

Based on the above research questions, null hypotheses were formulated to provide testable statements that assume no effect, no difference or no relationship between variables, thereby establishing the statistical framework for hypothesis testing. The underlying assumptions were that chromogenic bacteria may not express pigment biosynthesis pathways when cultivated on agro-waste substrates as these extracts could lack essential precursors or balanced nutrients compared to synthetic media. It was further assumed that pigment yield is constitutive and not significantly influenced by optimized culture parameters such as temperature, pH, or nutrient availability. Finally, the hypotheses presupposed that bacterial pigments are chemically unstable under diverse environmental conditions, thereby restricting their potential for industrial applications.

In complement to the null hypotheses, alternative hypotheses were formulated to directly challenge the assumptions of no effect, no difference, and no relationship between variables, thereby providing testable, research-driven statements. First, it was hypothesized that chromogenic bacteria are capable of activating pigment biosynthesis pathways when cultivated on agro-waste substrates as these extracts may supply sufficient precursors and nutrients comparable to synthetic media. Second, pigment yield was hypothesized to be non-constitutive but significantly influenced by optimized culture parameters including

temperature, pH, and nutrient availability, demonstrating that production levels can be enhanced under controlled environmental conditions. Finally, it was proposed that bacterial pigments exhibit chemical stability across diverse environmental stressors, maintaining their structural integrity and functional properties which supports their potential applicability in industrial dyeing and bioprocesses.

1.5 Significance of the Study

This study contributes to sustainable pigment production for textile dyeing by harnessing bacterial pigments, a renewable biological resource. It promotes agro-waste valorization, reducing production costs while minimizing environmental impact. By advancing eco-friendly dyeing technique, this research supports global efforts toward green manufacturing and environmental conservation. Additionally, optimizing microbial pigments may open new possibilities for industrial-scale production, benefiting textile industries, farmers, researchers, and society at large.

1.6 Delimitations and limitations

This study focused on isolating and characterizing bacterial strains from environmental sources (soil, water, air) and utilizing some locally available agro-waste residues as growth substrate based on availability. While this research emphasized pigment production optimization and textile dyeing potential of bacterial pigments, it did not extend to large-scale industrial trials and long-term environmental impact assessments.

Variability in agro-waste extract composition may affect pigment production consistency and reproducibility. Additionally, culture optimization and pigment stability tests were conducted under laboratory conditions, which might not fully replicate real-world industrial environments due to differences in equipment and process conditions. Furthermore, bacterial pigment color fastness may not match synthetic dyes, potentially impacting commercial viability in the textile industry.

CHAPTER TWO

LITERATURE REVIEW

Introduction

The textile industry has long relied on synthetic dyes to meet global demands for coloration. Nevertheless, increasing awareness of their environmental and health impacts has triggered the search for sustainable alternatives. Natural pigments, particularly those derived from microorganisms have emerged as promising eco-friendly substitutes due to their diverse bioactivities as potential industrial applications.

Chromogenic bacteria represent unique source of microbial pigments with their ecological distribution, genetic basis of pigment biosynthesis, and capacity for strain improvement, offering valuable insights into biotechnological exploitation. Furthermore, agro-waste substrates provide cost-effective and sustainable medium for pigment production that align with circular economy principles.

This review synthesizes current knowledge on microbial pigment production, beginning with the broader context of dyes in the textile industry and the limitations of synthetic dyes before narrowing to bacterial pigments, their biosynthetic pathways, and production strategies. It then explores applications in textile dyeing and other industries, evaluates the merits and demerits of microbial pigments, and considers their global market potential. Finally, the review outlines the theoretical and conceptual frameworks guiding this research and highlights gaps in the literature that justify this study.

2.1 Contextual Background

2.1.1 Overview of Dyes in the Textile Industry

The textile industry has historically relied on dyes to achieve vibrant and durable coloration with synthetic dyes emerging as the dominant choice since their introduction in the 19th

century. Prior to this, natural pigments sourced from plants, insects, and marine organisms provided unique hues but were limited by high production costs and restricted availability (Pizzicato et al., 2023). The discovery of mauveine, the first synthetic organic dye, by William Henry Perkin in 1856 and subsequent advances such as diazotization reactions revolutionized textile coloration, making synthetic dyes cheaper, more accessible, and widely applicable across industrial sectors (Nagendrappa, 2010).

Today, synthetic dyes account for more than 90% of global usage with annual production exceeding 800,000 tons and over 10,000 variants in circulation (Slama et al., 2021; Yaseen & Scholz, 2019). Their popularity stems from superior color fastness, intensity, and cost-effectiveness particularly in the textile sector. Among these azo dyes represent the largest class, comprising 60–70% of consumption due to their stability and efficient fiber binding properties (Alzain et al., 2023).

Despite their economic advantages, synthetic dyes pose significant environmental challenges. Derived primarily from petrochemical sources such as coal tar and petroleum intermediates, they are often non-biodegradable and contain hazardous compounds including aromatic amines and heavy metals. Textile dyeing processes also consume vast amounts of water and releasing untreated effluents that contribute to approximately 20% of global industrial water pollution (Islam et al., 2022; Yaseen & Scholz, 2019). These discharges impair aquatic ecosystems, reduce oxygen exchange, and introduce carcinogenic risks to both humans and wildlife (Dutta et al., 2022; Khattab et al., 2020).

Addressing these concerns require sustainable alternatives and practices. Biodegradable dyes derived from natural sources coupled with innovations such as water-efficient dyeing, non-toxic mordants, and closed-loop recycling systems offer promising solutions to minimize environmental degradation. Furthermore, stricter regulatory frameworks and industry-led sustainability initiatives are essential to foster responsible transition toward eco-friendly pigment use in textiles (Akter et al., 2023).

2.1.2 Environmental and Health Concerns of Synthetic Dyes

The extensive use of synthetic dyes in the textile industry has raised significant environmental and health concerns due to their persistence, petrochemical origin, and toxic composition. Large volumes of untreated effluents are discharged into aquatic environments, reducing light penetration, disrupting photosynthesis, and introducing hazardous compounds that threaten biodiversity (Islam et al., 2022). Many synthetic dyes contain mutagenic and carcinogenic substances including azo groups, aromatic amines, and heavy metals which accumulate in ecosystems and pose long-term risks to both aquatic life and human health (Lellis et al., 2019; Singha et al., 2021).

Inadequate wastewater treatment facilities particularly in developing countries exacerbate these impacts by increasing biochemical and chemical oxygen demands, inhibiting plant growth, and promoting microbial resistance, ultimately leading to bioaccumulation within the food chain (Wang et al., 2022). Human exposure occurs through contaminated water, inhalation, or direct skin contact with reported effects ranging from allergic reactions and respiratory disorders to organ damage and genetic mutations (Ramamurthy et al., 2024).

Addressing these challenges require the adoption of sustainable practices including the development of biodegradable dyes, advanced wastewater treatment technologies, and strict regulatory frameworks to minimize discharge and safeguard environmental and public health.

2.1.3 Natural Pigments as Alternatives

Natural pigments have emerged as sustainable alternatives to synthetic dyes, valued for their safety, biodegradability, and reduced environmental impact (Salvo et al., 2023). Historically, pigments derived from plants, insects, and minerals provided coloration, but their limited availability and sustainability challenges restricted widespread use. Within the broader category of natural pigments, plant-based dyes are widely available and have a long history of use. However, they are often constrained by poor color fastness, variable yields, and strong dependence on agricultural resources, requiring extensive land, water, and seasonal harvesting that introduces yield variability (Amutha, 2025; Islam et al., 2024). Although considered eco-friendly, large-scale cultivation of dye crops compete directly with food production,

undermines sustainability, and poses risks to biodiversity, factors that run counter to the principles of the strategies of sustainable development goals.

In contrast microbial pigments offer structural diversity, eco-friendly properties, and scalability, making them promising candidates for industrial applications (Pizzicato et al., 2023; Anshi et al., 2024). Microbial pigments, though still developing, offer sustainable and eco-friendly alternatives to synthetic dyes combining the benefits of biodegradability, non-toxicity, and vibrant color diversity with strong market potential (Mouro et al., 2023). Research findings have shown that pigments from different strains of microorganisms demonstrated effective dyeing performance (Table 1).

Table 1 Widely studied micro-organisms for natural pigment production

Organism	Pigment(s)	Applications	Features	Challenges/Importance	Reference
<i>Serratia marcescens</i>	Prodigiosin (red)	Textile dyeing, antimicrobial coatings, anticancer research	High pigment yield	Some strains are opportunistic pathogens, requiring biosafety measures	(Venil et al., 2021)
<i>Streptomyces</i> spp.	Actinorhodin (blue), undecylprodigiosin, melanin	Textile dyes, pharmaceuticals	Produces multiple pigments	Pivotal in industrial microbiology	(Sebastian et al., 2022)
<i>Chromobacterium violaceum</i>	Violacein (violet)	Biomedical, cosmetics	High antioxidant and antibacterial activity	Requires careful handling due to potential pathogenicity	(Venil et al., 2016)
<i>Pseudomonas aeruginosa</i>	Pyocyanin (blue), pyoverdine (yellow-green)	Biomedical, potential textile applications	Strong pigmentation, bioactivity	Opportunistic pathogen	(Sengupta & Bhowal, 2022)

Organism	Pigment(s)	Applications	Features	Challenges/Importance	Reference
<i>Bacillus</i> spp.	Melanin, Carotenoids	Textile and leather dyeing, cosmetics, sunscreens	Non-pathogenic strains available; stable in extreme environments	Environmentally robust pigments	(Fatima & Anuradha, 2022)
<i>Rhodococcus</i> spp.	Carotenoids (yellow, orange, red)	Food, nutraceuticals, bioplastic coloring	High stress tolerance; naturally pigment-rich	Valuable for biotechnological applications	(Çobanoğlu & Yazıcı, 2022)
<i>Janthinobacterium lividum</i>	Violacein	Cosmetics, pharmaceuticals	Psychrotolerant	Potential for cold-environment applications	(Kowalska et al., 2024)
<i>Micrococcus luteus</i>	Carotenoids (yellow)	Food, cosmetic industries	Easy to culture	Widely used in microbial pigment studies	(Kandasamy & Kathirvel, 2024)
Halophilic bacteria (<i>Halomonas</i> , <i>Salinibacter</i>)	Bacterioruberin, Salinixanthin	Textile dyeing in saline conditions, UV protection	Thrive in high-salt environments	Adapted for extreme habitats	(Manjula et al., 2018)

Microorganisms such as bacteria and fungi grow rapidly, require minimal resources, and can be genetically manipulated to enhance pigment yield. Their ability to utilize agro-industrial residues as substrates further reinforces sustainability, while bacterial pigments including carotenoids, melanins, violacein, prodigiosin, and phycocyanin provide not only coloration but also functional benefits such as antimicrobial activity, UV protection, and antioxidant capacity (López et al., 2023; Venil et al., 2020).

Fermentative production of microbial pigments offers advantages of high yield, cost-effectiveness, and reduced dependence on seasonal variability. Optimizing fermentation parameters such as pH, temperature, and nutrient composition enhances pigment output with submerged fermentation (SmF) widely applied for large-scale production (Lee, 2025). Their

diverse chemical structures including carotenoids, pyrroles, indoles, and phenazines, contribute to pigmentation stability and wider application potential.

As industries shift toward greener practices, microbial pigments represent viable eco-friendly alternatives to synthetic dyes. Continued research into strain selection, fermentation optimization, and pigment purification alongside ensuring non-pathogenic properties will be critical for their successful integration into textiles and other industrial sectors (Ramesh et al., 2019).

2.2 Microbial Pigments and Chromogenic Bacteria

2.2.1 Ecological Distribution of Chromogenic Bacteria

Chromogenic bacteria are widely distributed across diverse ecological niches ranging from terrestrial soils to aquatic and extreme environments where environmental pressures often stimulate pigment synthesis. Their ecological diversity reinforces their potential as sustainable sources of natural pigments. Among natural pigment sources, chromogenic bacteria occupy unique niche, thriving in diverse ecological environments and producing wide spectrum of bioactive pigments.

With respects to global distribution, chromogenic bacteria have been isolated from a wide variety of ecosystems including soil, freshwater, seawater, marine sediments, glaciers, algal mats, and contaminated soils. Their ability to thrive in such diverse habitats reflects their adaptability and ecological resilience. Many pigment-producing bacteria are also found in extreme habitats such as hot springs, acid lakes, deserts, and polar regions, where pigments often functions as protection metabolites, enabling survival under stress conditions like UV radiation, oxidative stress, and nutrient limitation (Kirby et al., 2011)

The rate and intensity of pigment production vary with environmental conditions such as nutrient availability, pH, salinity, temperature, and light exposure. For example, bacteria at air-water interfaces often produce pigments to withstand sunlight exposure, while saline environments can alter pigment composition and coloration (Bahram et al., 2021).

Several chromogenic bacterial genera such as *Serratia marcescens* (red pigment, prodigiosin), *Chromobacterium violaceum* (violet pigment, violacein), *Flavobacterium* (yellow pigments), and *Pseudomonas* spp. (blue-green pigments such as pyocyanin) are commonly reported across ecosystems which demonstrate the ecological distribution of chromogenic bacteria and their potential for industrial pigment applications. While distribution studies highlight the ubiquity of chromogenic bacteria, comparative ecological analyses remain limited. Hence, more integrated research is needed to link habitat conditions, pigment diversity, and functional roles to industrial scalability.

2.2.2 Isolation and Characterization of Pigment-Producing Bacteria

The isolation and characterization of pigment-producing bacteria are fundamental for harnessing their potential in industrial applications. These microorganisms inhabit diverse ecological niches ranging from soil and freshwater to extreme environments such as glaciers, saline lakes, and hot springs where environmental pressures often stimulate pigment synthesis (Villa et al., 2022; Ramesh et al., 2019). Pigments act as secondary metabolites that protect bacteria against stressors including UV radiation, oxidative damage, and nutrient limitation, while also contributing to microbial competition, biofilm formation, and ecological interactions (Sajjad et al., 2020; Agarwal et al., 2023)

Isolation typically involves culture-based techniques followed by screening under controlled conditions with pigment yield influenced by substrate composition, pH, temperature, salinity, and nutrient availability. Gene regulation mechanisms further modulate pigment biosynthesis as seen in *Serratia marcescens* where prodigiosin production is operon-controlled, and in *Pseudomonas aeruginosa* where quorum sensing governs pyocyanin synthesis (Jia et al., 2021; Haddix & Shanks, 2018).

Characterization employs complementary approaches. Morphological analysis provides preliminary insights but requires validation through biochemical assays, and bio-molecular and molecular techniques. Enzyme activity profiling and metabolic pathway testing aid species identification, while advanced methods such as MALDI-TOF mass spectrometry and 16S rRNA sequencing enable precise taxonomic classification (Hanina et al., 2018; Haider et al., 2023). Genomic and transcriptomic analyses further reveal regulatory networks controlling

pigment biosynthesis, offering opportunities for biotechnological optimization (Chauhan & Jindal, 2020; Wani et al., 2022).

Pigment-producing bacteria synthesize diverse compounds including carotenoids, melanins, violacein, prodigiosin, and phenazines, each with functional properties such as antimicrobial activity, UV protection, and antioxidant capacity. Species like *Flavobacterium*, *Serratia marcescens*, and *Chromobacterium violaceum* exemplify the industrial relevance of bacterial pigments with applications spanning textiles, food, cosmetics, and pharmaceuticals (Venil et al., 2013; Lee, 2025).

Advancing microbial pigment production requires isolating potent strains and optimizing fermentation processes using cost-effective substrates. Emphasis on agro-industrial residues coupled with improved bioreactor systems and genetic engineering can enhance pigment yield, stability, and scalability, thereby supporting sustainable industrial adoption (Kramar & Kostic, 2022; Wani et al., 2022).

2.2.3 Genes Involved in Pigment Production

Bacterial pigment production is driven by specialized gene clusters such as *crt*, *pig*, and *vioABCDE*. For instance, carotenoid biosynthesis is regulated by the *crt* gene family (*crtE*, *crtB*, *crtI*, *crtY*) which directs the isoprenoid pathway leading to pigment formation. Violacein production in *Chromobacterium violaceum* is directed by the *vioABCDE* gene cluster, encoding enzymes that convert tryptophan into the violet pigment, and prodigiosin biosynthesis in *Serratia marcescens* is controlled by the *pig* gene cluster which regulates the condensation of pyrrole precursors into the red pigment (Ahmed et al., 2025; Y. Wang et al., 2024).

Gene expression is often influenced by environmental signals such as nutrient availability, pH, temperature, and oxidative stress. Quorum sensing systems also play critical role in gene expression. For example, *Pseudomonas aeruginosa* regulates pyocyanin production through quorum sensing pathways that activate pigment biosynthetic genes in response to cell density. Metal ions such as iron can also modulate pigment gene expression by altering biosynthetic activity depending on availability (Castro et al., 2019; Wang et al., 2024).

Pigments act as protective metabolites; shielding bacteria from UV radiation, oxidative stress, and extreme environmental conditions. Pigments also contribute to microbial competition with some pigments exhibiting antimicrobial activity, and to biofilm formation, enhancing survival in hostile environments. Understanding the genetic regulation mechanisms not only ensure microbial survival but also provide foundation for industrial exploitation through metabolic engineering and optimized fermentation strategies to improve pigment yield, stability, and scalability, offering opportunities for biotechnological applications in textiles, food, cosmetics, and pharmaceutical industries (Ahmed et al., 2025).

2.2.4 Strain Improvement in Chromogenic Bacteria

Strain improvement in chromogenic bacteria focuses on enhancing pigment yield, stability, and scalability through genetic and metabolic engineering, making them more viable for industrial applications. Chromogenic bacteria naturally produce diverse pigments such as carotenoids, prodigiosin, and violacein. However, wild-type strains often exhibit low yields, unstable pigment expression, and sensitivity to environmental conditions, limiting their industrial potential. Strain improvement strategies aim to overcome these limitations by enhancing productivity, optimizing substrate utilization, and improving tolerance to stress factors (Konar & Datta, 2022).

Strain improvement in chromogenic bacteria employs mutagenesis, metabolic engineering, and recombinant DNA technologies to enhance productivity and stability (Chavan et al., 2025). As classical approaches to strain improvement, chemical mutagens such as nitrosoguanidine and physical agents like UV radiation have been used to generate genetic variants with improved pigment output followed by screening of the mutant strains under controlled conditions to identify those with enhanced pigment biosynthesis (Konar & Datta, 2022).

Adaptive laboratory evolution leverages the natural ability of microorganisms to adapt to environmental pressures over time whereby microbial populations are cultivated under gradually intensifying selective conditions such as increasing concentrations of substrates, toxins, or environmental stressors like high temperature or pH extremes (Wang et al., 2023).

Over many generations, beneficial mutations accumulate, allowing certain strains to outcompete others under these selective pressures.

Metabolic engineering and recombinant DNA technology are also employed as modern biotechnological approaches for strain improvement. Metabolic engineering is used in redirecting metabolic flows toward pigment biosynthesis by overexpressing key enzymes or knocking out competing pathways. Whereas, recombinant DNA technology is used to introduce foreign genes or modify biosynthetic gene clusters to enhance or introduce specific functions that are not naturally present in the host microorganism (Konar & Datta, 2022).

Improved strains enable cost-effective large-scale pigment production particularly when combined with agro-waste substrates and optimized fermentation systems. Enhanced strains also show better thermal stability, color fastness, and bioactive properties, making them suitable for textile dyeing, food, and pharmaceutical applications. Despite progress, challenges remain in scaling up improved strains, ensuring regulatory compliance, and maintaining genetic stability during prolonged industrial use. Hence, integrated approaches combining strain engineering, substrate optimization, and process control are needed to fully realize the potential of chromogenic bacteria in sustainable pigment production.

2.3 Substrates and Production Approaches

2.3.1 Agro-Wastes as Low-Cost Substrate for Culture Growth and Pigment Production

Industrial-scale microbial pigment production requires cost-effective and sustainable approaches. Conventional synthetic media often composed of pure sugars such as glucose, sucrose, or fructose, are economically unfeasible for large-scale use. Agro-industrial wastes which are rich in carbohydrates, proteins, fibers, minerals, and vitamins provide affordable and renewable alternatives that align with circular economy principles while simultaneously addressing waste management and environmental concerns (Venil et al., 2020 ; Soren et al., 2020).

Efficient pigment biosynthesis depends on optimizing fermentation conditions including temperature, pH, oxygen availability, agitation, and nutrient composition. These parameters

influence microbial metabolism, shifting cells toward secondary metabolite production such as pigments under stress conditions (Fouillaud & Dufossé, 2022). For instance, *Monascus* spp. yield pigments optimally at 25–28 °C, while *Pseudomonas* spp. require 35–36 °C. Most pigment-producing bacteria favor acidic conditions (pH 4.5–6.5) though variations exist depending on species and pigment type (Abdollahi et al., 2021; Rehman & Dixit, 2020).

Submerged fermentation is widely applied by utilizing sugar-rich by-products such as molasses, fruit juices, and whey filtrates as nutrient sources. Carbon and nitrogen sources strongly affect pigment yield with starch, sucrose, and xylose enhancing production, while simple sugars like glucose may inhibit synthesis (Ngamwonglumlert et al., 2017).

Pretreatment of agro-waste is often necessary to improve nutrient accessibility. Hydrolysis of cellulosic materials releases fermentable sugars, while cooking starch-rich substrates produce liquors suitable for microbial growth. Examples include potato extract supplemented with xylose and glycine, which outperformed commercial potato dextrose broth in pigment yield from *Penicillium* strains, and hydro-distilled orange residues used for pigment production (Chua et al., 2021; (Kantifedaki et al., 2018). Agro-wastes such as bagasse can also serve as inert supports for fermentation, demonstrated in prodigiosin production by *Serratia marcescens* (Paul et al., 2024).

Numerous studies confirmed the feasibility of agro-waste utilization in microbial pigment synthesis. Pineapple peels, orange peels, and wheat bran have supported pigment production in *Serratia marcescens*, *Chromobacterium violaceum*, and *Streptomyces* spp. Beta-carotene has been synthesized from *Blakeslea trispora* using citrus waste, while astaxanthin has been extracted using grape juice-based substrates (Ciegler et al., 1963; Omar et al., 2019; (Grewal et al., 2022; Ramesh et al., 2022). These examples highlight the dual benefits of reducing production costs and valorizing agricultural residues.

To maximize industrial viability, modern optimization strategies are essential. While traditional one-variable-at-a-time (OVAT) methods are labor-intensive and limited in scope, statistical designs such as Plackett-Burman and response surface methodology (RSM) enable efficient screening of multiple parameters, reduce variability, and enhance pigment yield (Chaudhari & Shirkhedkar, 2020). Integrating agro-waste substrates with advanced

fermentation optimization thus offers a scalable, eco-friendly pathway for microbial pigment production.

2.4 Applications and Market Potential

2.4.1 Broader Applications of Bacterial Pigments

Microbial pigments can also provide multi-functional bioactive benefits such as antioxidant, UV protection, and antimicrobial properties besides its coloring effect, increases the value of the final products due to their bioactivity and safety profiles (Choi et al., 2021; Venil et al., 2013). Natural colorants from bacteria including carotenoids and prodigiosin derivatives are being investigated as food additives due to their safety and antioxidant properties. Unlike synthetic food dyes, microbial pigments offer nutritional and bioactive benefits, aligning with consumer demand for clean-label products (Venil et al., 2020). Moreover, bacterial pigments such as melanins and carotenoids are applied in cosmetics for their UV-protective, antioxidant, and antimicrobial functions. Their stability and bioactivity enhance formulations for sunscreens, skin and hair care products, while reducing reliance on synthetic chemicals (López et al., 2023).

Several bacterial pigments exhibit antimicrobial, anticancer, and immune-modulatory activities, making them promising candidates for drug development too. For example, violacein from *Chromobacterium violaceum* showed potent anticancer properties, while prodigiosin demonstrated immunosuppressive and antibacterial effects. These bioactivities expand their potential beyond coloration into therapeutic applications (Venil et al., 2013). Microbial pigments also play roles in bio-sensing and bioremediation. Their ability to respond to environmental stressors enables use in microbial biosensors, while pigment-producing strains can contribute to pollutant degradation and eco-friendly waste valorization strategies (Fouillaud & Dufossé, 2022).

2.4.2 Textile Dyeing with Bacterial Pigments

Bacterial pigments represent one of the most promising eco-friendly alternatives to synthetic dyes in textile applications. Unlike conventional dyes derived from fossil fuels which generate

toxic effluents and rely on hazardous chemicals, microbial pigments are biodegradable, non-toxic, and often possess functional properties such as antimicrobial activity and UV protection (Kamble et al., 2022; Repon et al., 2024). Their bioactive nature enhances textile durability by protecting fabrics against microbial degradation while simultaneously reducing environmental pollution associated with dyeing processes (Ghosh & Banerjee, 2023).

Recent studies have demonstrated the successful application of bacterial pigments on cotton, silk, and wool, showing favorable affinity, wash fastness, and light stability (Anshi et al., 2024). Mordanting techniques further improve dye uptake and retention, making microbial pigments viable for diverse textile substrates. However, efficient pigment recovery remains a challenge. While extracellular pigments are relatively easy to extract, intracellular pigments require cell disruption and solvent-based methods followed by purification through chromatography and spectroscopic techniques to ensure stability and quality (Rifna et al., 2023)

Despite their advantages, bacterial pigments face scalability and standardization challenges as extraction methods consume large amounts of solvents and require optimization for industrial feasibility. To address these challenges, researchers are exploring agro-waste substrates as low-cost growth media, thereby reducing expenses and supporting circular waste management (Gemelli et al., 2024). Additionally, pigment formulations must be optimized for stability such as thermal conditions as textile dyeing typically occurs at 50–80 °C for extended durations (Kramar & Kostic, 2022).

With ongoing advances in fermentation optimization, substrate utilization, and pigment stabilization, bacterial pigments hold significant potential to revolutionize sustainable textile dyeing. Their dual role in providing coloration and functional benefits positions them as viable alternative to synthetic dyes, supporting both environmental sustainability and industrial innovation. Their multifunctional properties such as coloration, bioactivity, and sustainability make microbial pigments valuable across industries, though challenges in scalability, stability, and regulatory approval remain.

2.4.3 Merits and Demerits of Microbial Pigments

Microbial pigments offer significant ecological and functional advantages including sustainability, safety, and bioactivity. Bio-pigments are naturally degradable, reducing environmental pollution compared to synthetic dyes (Venil et al., 2020). Moreover, many bacterial pigments lack carcinogenic compounds, making them safer for textiles, food, and cosmetics (López et al., 2023).

The diverse chemical structures of pigments allow use in textiles, pharmaceuticals, cosmetics, and food industries (Fouillaud & Dufossé, 2022). For example, pigments such as carotenoids, violacein, and prodigiosin exhibit antioxidant, antimicrobial, and UV-protective properties, adding their value beyond coloration (Venil et al., 2013). The rapid growth of chromogenic microorganisms on low-cost substrates support circular economy principles (Kamble et al., 2022).

However, challenges in yield, stability, extraction, and regulatory approval must be addressed to enable their widespread industrial adoption. Wild-type strains often produce pigments in small quantities, limiting industrial feasibility (Ramesh et al., 2019). Furthermore, many microbial pigments are sensitive to pH, temperature, and light, reducing their shelf life and dye fastness (Khattab et al., 2020).

Intracellular pigments require solvent-intensive recovery methods, increasing costs and environmental burden (Rifna et al., 2023). Approval for use in food and cosmetics also require extensive safety testing, delaying commercialization (Agarwal et al., 2023). Limited awareness and uncertainty about microbial pigments compared to synthetic dyes may slow consumer acceptance and adoption (Gemelli et al., 2024).

2.4.4 Global Market of Bacterial Pigments

The global bacterial pigment market is driven by sustainability, regulation, and consumer demand with strong growth projected in textiles, food, cosmetics, and pharmaceutical sectors despite the critical hurdles in production costs, scalability, and regulatory approval to unlock full industrial potential. Regulatory bodies like the European food safety authority have

restricted synthetic dyes such as Allura Red AC (E129) and Tartrazine (E102) in food applications with studies linking them to hyperactivity in children, accelerating demand for natural alternatives. Moreover, the rising interest in clean-label, eco-friendly, and non-toxic products has boosted adoption of microbial pigments in food, cosmetics, and textile industries (Barreto et al., 2023).

With regards to market size and growth, the global microbial fermentation pigments market is projected to grow significantly driven by applications in textile, pharmaceutical, food, and cosmetic industries. The market demand is expected to expand as industries transition toward sustainable practices. Reports indicate double digit growth rates for bio-based pigments due to strict environmental regulations (Anshi et al., 2024).

With growing consumer awareness and stricter environmental regulations bacterial pigments are positioned to become mainstream alternatives to synthetic dyes across multiple sectors aligning with sustainability goals, thereby expanding their market relevance. Though the high production costs, scalability, and regulatory approval remain big bottlenecks, advancements in fermentation technology, strain improvements, and agro-waste utilization are expected to reduce costs and expand industrial feasibility of microbial pigments as sustainable alternatives to synthetic dyes (Lyu et al., 2022).

2.5 Synthesis and Research Positioning

2.5.1 Gaps in the Literature

Despite notable advances in microbial pigment research, several critical gaps remain that limit industrial adoption. A major challenge lies in scaling production from laboratory experiments to industrial systems where yield variability, process optimization, and economic feasibility present significant obstacles (Ramesh et al., 2019). Pigment output is highly dependent on bacterial strain, substrate type, and environmental parameters. Moreover, precise control of factors such as pH, temperature, and nutrient composition remains complex and time-consuming (Musa & Yusof, 2019). Although agro-waste substrates offer cost-effective alternatives, their long-term economic viability, downstream processing, and purification efficiency are not well established (Grewal et al., 2022).

While bacterial pigments show promise as natural dye alternatives, gaps exist in understanding their functional attributes, including antioxidant, antimicrobial, and UV-protective properties which might add value to dyed fabrics and thermal stability (Khattab et al., 2020). Regulatory hurdles also persist with concerns about safety, standardization, and intellectual property rights slowing commercialization in textiles, food, and cosmetics. Consumer acceptance remains uncertain as doubts about efficacy and safety compared to synthetic dyes continue to hinder widespread adoption.

Environmental sustainability presents another underexplored area. While microbial pigments are biodegradable, large-scale production raises questions about managing microbial by-products, and comparative studies on their ecological impacts versus synthetic dyes are limited. Furthermore, most studies address pigment production and waste valorization separately with few integrated approaches combining bacterial isolation, agro-waste optimization, and textile dyeing applications.

Addressing these gaps require research focused on novel agro-waste substrates, genetic engineering for improved pigment yield and stability, and holistic studies that integrate microbial cultivation, substrate valorization, and textile dyeing performance. Such efforts are essential to advance microbial pigments from laboratory feasibility to scalable and environmentally responsible industrial solutions.

This study explored the dyeing potential of pigments extracted from bacterial isolates cultured on agro-waste extracts; a low-cost and eco-friendly substrate, marking significant progress in industrial dyeing practices. By evaluating fabric dyeing applications under laboratory scale conditions, this research tried to identify key challenges affecting pigment stability and its dyeing performance, paving the way for scalable and environmentally responsible dyeing solutions.

2.5.2 Theoretical Framework

This theoretical framework provides the foundation for understanding microbial pigment production within established scientific paradigms. The shift from synthetic dyes to bio-origin pigments in textile dyeing is gaining momentum guided by several models (Figure 1). Eco-

physiological, bioprocess engineering, life cycle assessment, functionalization, colorfastness and compatibility, and economic feasibility models are among key models for substituting synthetic dyes with bacterial pigments (GOMES et al., 2023; Kramar & Kostic, 2022). The models help industries transition to eco-friendly dyeing methods, reduce reliance on toxic chemicals and water-intensive processes, and enable innovation in sustainable way and functionalize textile materials with additional therapeutic properties.

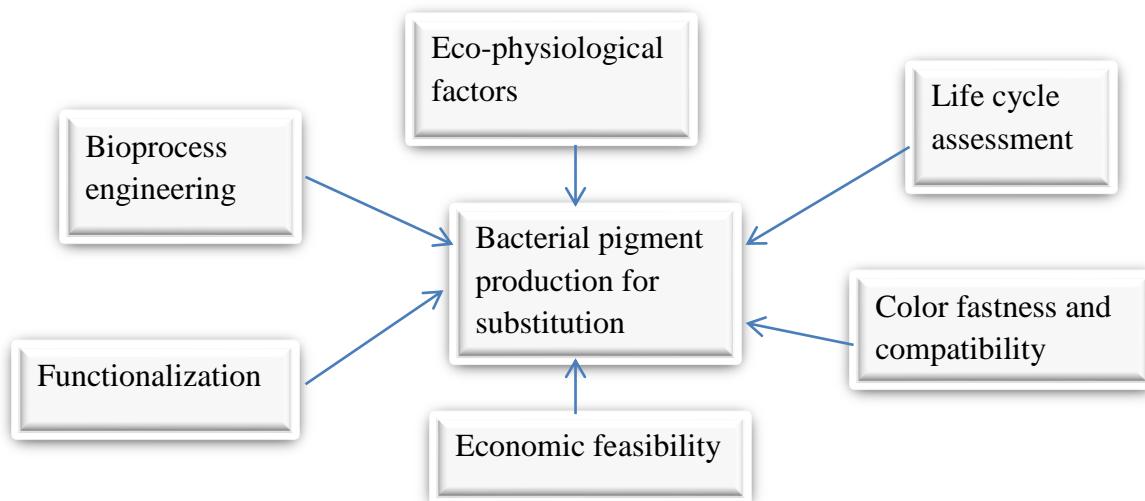


Figure 1 Schematic representation of how key models interconnect in the transition from synthetic dyes to pigments derived from bacterial sources, highlighting integration points

2.5.3 Conceptual Framework Overview

This framework integrates comprehensive research activities into a coherent model. Figure 2 illustrates the conceptual framework flowchart that maps the flow of activities, shown by arrows representing investigative links between variables. The activities were begun with the collection of environmental samples to identify potential pigment-producing bacterial isolates.

These isolates undergo detection, purification, species identification, and eco-physiological tolerance testing. Selected strains were then inoculated into agro-waste extracts serving as growth substrates followed by cultivation aiming to reduce production costs and environmental impact. Pigments produced were extracted and characterized. The final stage involved applying the pigments in textile dyeing and assessing their performance.

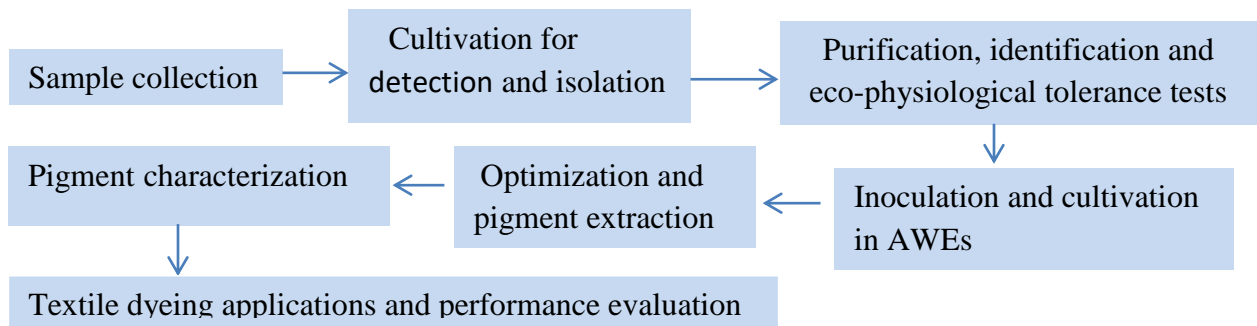


Figure 2 Conceptual frameworks illustrating the interconnections between core activities, guiding the research approach

CHAPTER THREE

MATERIALS AND METHODS

3.1 Research Design

A multi-phase experimental laboratory based research design was adopted. The experimental approach was chosen due to its suitability for testing hypotheses under controlled conditions, allowing for the systematic manipulation of variables such as temperature, pH, agitation rate, culture volume and age, incubation time, and substrate concentration. Through this design, the study sought optimization of pigment production, characterized the extracted pigments, and assessed their dyeing performance on cotton and polyester fabrics.

The first phase was collection of environmental samples from diverse agro-industrial and natural sites to ensure broad representation of potential pigment-producing microorganisms. These samples served as the foundation for subsequent microbiological investigations. In the second phase, isolation and screening of pigment-producing bacteria were carried out by subjecting the collected samples to serial dilution, culturing on standard nutrient media, and observing for pigment production. Data on the number of pigment-producing isolates, pigment color, and intensity were recorded.

The third phase focused on agro-waste media preparation and evaluation of their growth support capability compared to conventional synthetic media, nutrient broth. Selected pigment-producing isolates were cultivated under identical conditions on both media types, and culture growth was quantified using optical density (OD_{600}) measurements, followed by statistical comparison to assess performance differences.

The fourth phase focused on optimization of culture conditions using factorial designs to test main and combined effect of environmental conditions on culture growth and pigment yield. Pigment yield under each condition were evaluated via OD_{600} value measurements and surface

response analyses data were generated to identify optimal conditions. Phase five was about stability and application testing with the objective of assessing pigment stability and their applications on fabrics dyeing after exposing pigments to varying environmental conditions and applying pigments to fabric samples. Color retention, and degradation rate score data were generated.

3.2 Study Area and Sampling Sites

Environmental samples comprising of soil, water, and, air were collected from various sites in Ethiopia, ranging from the Dallol depression area, Sulfure lake to the highlands of Showa plateau with altitudes spanning from -89 m to 2,375 m above sea level (Table 2). Each site was documented with GPS coordinates and basic environmental parameters such as temperature and pH were recorded at the point of sampling to provide context for the microbial isolates recovered.

Table 2 Sample data sources, types, characteristics, and geographical coordinates

Sample collection site	Sample type	Sample characteristics at the time of collection		Geographical location of sample collection area	
		Temperature (°C)	pH	Elevation (meter)	Coordinate
Sodere hot spring	Water	46.9	6.9	1368	8°23'51.93" N, 39°23'47.21" E
Boku hot spring	Water & soil	42.7	8.1	1734	82°9'18.57" N, 39°16'16.65" E
Ziway lake	Water	26	7.4	1638	7°56'41.79" N, 38°43'54.04" E
Awash river	Water	24	7.2	1595	8°21'46.74" N, 39°00'08.78" E
Solid waste disposal site	Soil	21	8.2	1685	8°31'41.78" N, 39°13'21.60" E
Garage	Soil	21.5	7.3	1610	8°31'32.46" N, 39°15'34.59" E
Gas station	Soil	23		1618	8°32'26.50" N, 39°15'51.70" E
Horticulture plantation site	Water and soil	24	6.8	1597	8°23'34.91" N, 39°01'13.91" E
Sulfur lake (Dallol depression)	Sulfur soil	42		-93	14°14'14.42" N, 40°17'59.44" E
	Red soil	42		-100	14°28'74.02" N, 40°19'85.14" E
	Gray soil	44		-89	14°23'74.02" N, 40°29'89.51" E
	Volcanic ash	41.5		-102	14°13'43.94" N, 40°30'17.58" E
Abattoir	Effluent	24	7.4	1594	8°30'30.04" N, 39°14'36.63" E

Spinning factory	Effluent	25	6.5	1628	8°32'51.49" N, 39°15'21.34" E
Lake Beseka	Water, soil sediment and volcanic ash	29.2	8.4	960	8°54'06.06" N, 39°54'29.73" E
Quarry site	Soil	28		1428	8°22'55.49" N, 39°23'51.11" E
Wastewater treatment plant	Effluent	26	6.8	1663	8°33'38.59" N, 39°17'16.63" E
Nursery site	Soil	26		1709	8°34'21.99" N, 39°17'24.09" E
Green garden	Soil	24	7.2	1661	8°33'35.81" N, 39°17'08.82" E
Laboratory	Air			1663	8°33'41.89" N, 39°17'03.76" E
Open ditch	Effluent	24	4.5	1696	8°34'35.21" N, 39°16'08.59" E
Lake Langanano	Water	26	7.5	1587	7°33'08.10" N, 38°40'59.28" E
Sugar factory	Effluent	27	6.5	1575	8°22'25.37" N, 39°19'13.29" E
Brewery	Effluent	23	6.4	2375	9°00'53.76" N, 39°44'45.06" E

Samples were collected from those diverse natural and agro-industrial sites such as hot springs, volcanic ash sediments, quarry site soil, fresh and alkaline water lakes, river estuaries with irrigation activities, municipal solid waste dumping sites, garages and gas stations, wastewater treatment plants, rhizosphere and rhizoplane root zones of trees, stagnant water-sediment interfaces, and ambient air, aiming to increase the likelihood of isolating diversity of pigment-producing isolates. These environments shaped by stress and nutrient variability serve as prime reservoirs for microbial pigments.

The physico-chemical characteristic of these areas vary greatly, characterized by extreme temperature, salinity, acidity and alkalinity, and rugged terrains. Biologically, both normal and extreme environments support microbial communities that thrive under different conditions (Rothschild & Mancinelli, 2001). Human activities in these regions range from mining around sulfure lake in the Dallol depression to agriculture and settlement in the highlands, influencing the natural ecosystems of microorganisms, provides distinctive habitats where microorganisms demonstrate remarkable adaptability.

Extreme environments such as high heat, salinity, acidity, alkalinity, and rugged terrains create distinctive ecological niches where microorganisms including pigment-producing ones evolve protective adaptations (Wani et al., 2022). Pigmentation often serves as survival mechanism, shielding cells from UV radiation, oxidative stress, high salinity, desiccation, and temperature

fluctuations, while also aiding in energy capture and signaling (Parrilli et al., 2022; Sajjad et al., 2020). Microorganisms also demonstrate remarkable adaptability through specialized metabolic pathways, stress-response proteins, and genetic flexibility that allow them to thrive under harsh conditions (Wani et al., 2022).

Samples were collected from hot springs, volcanic ash sediments, and alkaline water lakes to target extremophilic microorganisms as these habitats expose microbes to high temperature, salinity, and pH fluctuations. Such stress conditions often drive pigment biosynthesis as protective mechanisms against oxidative and thermal stress (Mendes-Silva et al., 2020). Quarry soils and general soil ecosystems were included because they are rich in actinomycetes and other pigment-producing bacteria such as *Streptomyces* and *Micrococcus*. Mineral-rich substrates in quarry sites select for microbes with unique metabolic pathways, including pigment production (Kazi et al., 2022).

River estuaries with irrigation activities and stagnant water-sediment interfaces were sampled to capture microbes adapted to fluctuating oxygen levels, nutrient gradients, and pollutant exposure. These stressors are known to induce pigment biosynthesis, particularly carotenoids and melanins which function as antioxidant defenses (Losinska-Siçiūnienė et al., 2025). Samples from municipal solid waste dumping sites, garages, gas stations, and wastewater treatment plants were collected to isolate microbes exposed to hydrocarbons, heavy metals, and organic pollutants. Such environments select for pigment-producing strains with enhanced detoxification and stress tolerance capabilities (Akhtar et al., 2021).

Rhizosphere and rhizoplane root zones of trees were targeted because plant-associated microbes often produce pigments as signaling molecules or protective agents against UV radiation and reactive oxygen species (McPherson et al., 2018). Ambient air samples were included to capture airborne bacteria exposed to UV radiation and desiccation stress, conditions that favor pigment production such as carotenoids and melanins (Jufri, 2020).

3.3 Chemicals and Equipment Used in the Experiment

The materials used in this study included sterile sample collection containers, Petri dishes, test tubes, flasks, pipettes, and cotton swabs. Culture media such as nutrient agar and nutrient

broth (Oxoid) were prepared for initial bacterial cultivation. Agro-waste residues including potato, cabbage, tomato, orange, cannon ball cabbage, onion, watermelon, papaya, carrot, banana, and beetroot and leftover foods were collected, cleaned, dried and ground into fine particles for substrate preparation.

Laboratory equipment utilized included an incubator, autoclave, pH meter, and thermometer (Wagtech, UK), centrifuge (Hettick, Germany), microscope (Olympus, Japan), UV-Visible spectrophotometer (VWR P9, China), Palin Test photometer (Wagtech Potalab+ (C), UK), EXS3000 MALDI-TOF-MS (Bruker Daltonics, Germany) and analytical balance. Textile fabric samples (100% cotton) and Tetron 6000 were purchased for dyeing experiments.

Laboratory-grade ethanol, methanol, acetone, chloroform, and dimethyl sulfoxide (DMSO), all from Sigma-Aldrich, were used for pigment extraction and dissolution of pigment granules, ensuring precision and consistency in experimental procedures. Aluminum sulfate 10% (w/v) and potassium sulfate 5% (w/v) were utilized as mordants. As oxidizing and reducing agents, 3% H₂O₂ and glucose, respectively, were used and NaOH and HCl were utilized as pH adjusters.

3.4 Environmental sampling, microbial Isolation, and primary screening

Sampling was performed under aseptic conditions using sterile containers. A total of 30 samples comprising of soil, water, and air, were collected from designated sites (Table 2) with sterile Schott bottles, coded, and properly labeled at the point of collection. To ensure sample integrity, preservation techniques were applied immediately after collection. Soil and water samples were stored at 4 °C in ice boxes to minimize microbial activity and chemical changes, while air samples collected on nutrient agar plates were sealed with parafilm to prevent contamination and desiccation. All samples were transported to the laboratory on the same day under controlled temperature conditions.

Liquid and solid samples were collected according to methods previously described by Erickson et al. (2013) and McPherson et al. (2018), respectively. For solid samples, approximately 100 grams per sample were collected from a depth of 5-10 cm. For liquid samples, 100 mL were taken in sterile bottles from surface runoff or stagnant sources. Samples

were well mixed in Schott bottles before storage. Air samples were collected using the settle plate method as described by Napoli et al. (2012), by exposing Petri plates containing nutrient agar medium to ambient air for 15 minutes. After exposure, plates were sealed, stored at ambient temperature, and processed within 24 hours to preserve colony viability.

In the laboratory, isolation was carried out using the serial dilution technique followed by the streak plate methods on nutrient agar. For solid samples, 1 gram of each mixed sample was weighed, dissolved in 100 mL of 0.85% normal saline (w/v), and homogenized. For liquid samples, 1 mL of each well mixed sample was added to 9 mL of 0.85% normal saline (v/v). Finally, ten-fold serial dilutions were prepared for both solid and liquid samples.

From each test tube, 0.1 mL of diluted aliquots were poured into respective sterile Petri plates containing nutrient agar medium using the streak plate method. Air sample plates were directly incubated. All plates were prepared in duplicate and incubated at 37 °C and 44 °C with un-inoculated agar medium as negative control to ensure the recovery of both mesophiles and those adapted to warmer environments as these temperatures selectively favor the growth of different microbial groups. All plates were incubated for 24-48 hours after which distinct colonies exhibiting visible pigmentation were isolated and sub-cultured repeatedly to obtain pure culture.

Plates with confluent growth were further diluted for distinct colony detection and isolation. All distinct colonies were counted, providing a baseline for microbial diversity in the sample from which the most promising isolates were selected. Colony growth characteristics were screened based on their appearance, pigmentation, and growth pattern. Colony morphologies (cell shape, Gram reaction, and motility) were determined by light microscope (Olympus, Japan) at magnification power of X1000 using an oil immersion objective. Six potential pigment-producing isolates (PPPIs), designated PPPI₁–PPPI₆ were selected for presumptive screening based on the colony intensity and stability of colony coloration. These isolates were prioritized for subsequent biochemical and bio-molecular characterization to evaluate their pigment production potential.

3.5 Characterization of the potential pigment-producing isolates

3.5.1 Biochemical characterization

As conventional test for isolate differentiation, basic biochemical tests including enzyme based tests such as catalase, oxidase, urease, and coagulase tests were conducted to detect the presence of catalase enzyme which break down hydrogen peroxide (H_2O_2), cytochrome c oxidase enzyme to separate oxidase positive from oxidase negative ones, urease enzyme that break down urea, and coagulase enzyme that clots plasma, respectively. Hydrogen sulfide (H_2S) production test was performed to detect sulfide reducing enzymes using Sulfide-Indole-Motility (SIM) medium employing stab method. Moreover, to determine if an isolate utilizes nitrate as terminal electron acceptor in anaerobic respiration, nitrate reduction tests were also performed using nitrate broth (Cappuccino & Sherman, N., 2014).

To evaluate sugar fermentation by the isolates, carbohydrate fermentation test was performed to detect acid and/or gas production. IMViC (Indole, Methyl Red, Voges Proskaur, and Citrate utilization) tests were performed to detect tryptophanase enzyme, stable acid production from glucose fermentation, acetoin production, and ability to utilize citrate as sole carbon source, respectively. Biochemical characterization of the isolates was carried out following the procedures outlined in Bergey's Manual of Determinative Bacteriology (Whitman et al., 2015). For quality assurance, *Bacillus subtilis* and *Escherichia coli* obtained from the American Type Culture Collection (ATCC) and maintained at the Adama Public Health Research and Referral Laboratory Center were employed as reference controls representing Gram-positive and Gram-negative bacteria, respectively.

3.5.2 Biomolecular characterization

The pigment-producing isolates were accurately identified by analyzing their protein profiles via Matrix-Assisted Laser Desorption/Ionization Time-of-Flight Mass Spectrometry (MALDI-TOF) according to Haider et al.(2023). Using the formic acid extraction method, colonies of pigmented isolates were transferred to Eppendorf tubes containing 300 μ L of ultrapure water with sterile micropipette tip. Then 900 μ L of absolute ethanol was added and mixed thoroughly.

The mixtures were centrifuged at 12,000 rpm for 3 minutes, and the supernatants were discarded. After drying the precipitate at room temperature, 20 μ L of 70% formic acid and 20 μ L acetonitrile were added and thoroughly mixed. The mixtures were centrifuged at 5,000 rpm for 3 minutes, and the supernatants were transferred to new Eppendorf tubes. After air drying, a microliter of the extracted supernatants were added to the target plate and covered with one microliter of α -Cyano-4-hydroxycinnamic acid (CHCA) matrix solution for analysis.

Spectral fingerprints were generated using an EXS3000 MALDI-TOF-MS (Bruker Daltonics, Germany) according to its operating manual, with the laser frequency operating at 60 Hz, ion source voltage at 1.8 kV, and lens voltage at 6 kV. Spectra were generated in the 2000 to 20,000 mass-to-charge ratio (m/z) range. *E. coli* (ATCC25922) and α -CHCA were used as positive and negative quality controls, respectively. The spectra were compared with the EXS3000 database to determine the taxonomical species of the isolate.

For identification, the acquired mass spectra of the isolate were compared with the bacterial spectra in the MALDI Biotyper library (MBL) which contains a database of species-specific fingerprints for a wide variety of bacteria to define the taxonomical species to which the isolate belongs. Score values below 1.69 reported as non-reliable genus, scores of 1.70–1.99 were classified as probable genus, and scores above 2.00 were classified as probable species (Bruyne et al., 2011).

3.6 Eco-Physiological tolerance assessment of selected bacterial isolates

The purified bacterial isolates were screened for pigment production by inoculating each isolate onto fresh nutrient agar plates and incubating them at 30 °C for 24 -72 hours. Colonies were observed for distinct pigmentation among which red, yellow, orange and other visually detectable hues were identified. Pigment intensity and diffusion into the agar were recorded as preliminary indicators of production capacity. Isolates exhibiting strong and consistent pigmentation were selected for further analysis.

The one-variable-at-a-time (OVAT) approach was initially employed to establish tolerance ranges for key culture parameters, thereby ensuring reliable microbial growth. These baseline ranges served as the foundation for subsequent statistical optimization using Plackett-Burman

Design (PBD) to identify the most significant factors influencing pigment yield. Eco-physiological tolerance of pigment-producing isolates was systematically evaluated against variations in temperature, pH, agitation rate, salt concentration, and carbon and nitrogen levels in nutrient broth. Growth responses were quantified by measuring optical density at 600 nm (OD₆₀₀) with a UV-Visible spectrophotometer, providing a robust metric for assessing microbial performance under different environmental conditions.

All tests were conducted in triplicate with un-inoculated medium as a blank. Isolates were considered stress tolerant if a minimum OD value of 0.1 was recorded (McGoverin et al., 2021). The potent isolates were stored on slant at 4 °C for short term use, and in glycerol stocks at -20 °C for long term preservation.

The ranges of stressor conditions chosen to evaluate the eco-physiological tolerance of pigment-producing bacterial isolates were selected to reflect both ecological relevance and industrial applicability. Pigment biosynthesis in bacteria is often linked to stress adaptation and therefore, testing across realistic ranges of temperature, pH, salinity, agitation, and nutrient availability provides insight into survival capacity. Parameter ranges were elected to encompass ambient environmental conditions that reflect natural habitats, and tests metabolic flexibility and pigment biosynthesis of the isolates.

3.6.1 Temperature tolerance test

To assess temperature tolerance ability of the isolates, loop-full of one-day-old pure cultures were inoculated into freshly prepared nutrient broth containing 1 gram of 'Lab-Lemco' powder, 1 gram of yeast extract, 5 gram of peptone, and 5 gram of NaCl per liter (Oxoid), autoclaved at 121 °C for 15 minutes with pH adjusted to 7 for initial activation. Growth of chromogenic isolates in agro-waste extracts (AWEs) at different temperatures (20 °C, 25 °C, 28 °C, 32 °C, 37 °C, and 45 °C) were examined by adjusting pH to 7 using sterile 1 N NaOH and 1 N HCl as described by Deveikaite & Zvirdauskiene (2023).

3.6.2 pH tolerance test

The ability of chromogenic isolates to grow at different pH levels was tested in AWEs adjusted to pH 4.5, 6.0, 7.0, 8.0, and 10.0 using sterile 1N NaOH and 1N HCl, as described by

Fatima & Anuradha (2022). All isolates were incubated at 37 °C for 24-72 hours to assess growth at each pH level.

3.6.3 Salt tolerance test

Chromogenic isolates were tested for salinity tolerance in AWEs supplemented with NaCl at concentrations of 0.5%, 1.0%, 2.0%, 3.0%, 4.0%, and 5.0% (w/v). Growths were evaluated after 24-72 hours of incubation at 37 °C (Sharma et al., 2021).

3.6.4 Agitation tolerance test

Isolates were tested for agitation tolerance in AWEs at agitation rates of 30 rpm, 60 rpm, 90 rpm, and 120 rpm. Growths were evaluated after 24-72 hours of incubation at 37 °C Fatima & Anuradha (2022).

3.6.5 Carbon and Nitrogen utilization test

One-day-old culture broths of chromogenic isolates were inoculated into AWEs containing different carbon and nitrogen sources. Isolates were cultured in AWEs media supplemented with five carbon sources (glucose, fructose, lactose, maltose, and sucrose) at 1%, and nitrogen sources (yeast extract, peptone, tryptone, and urea) at 0.1%. Tests were conducted in triplicate per isolate, and growths were evaluated by measuring OD₆₀₀ after 24-72 hours of incubation at 37 °C as described by Fatima & Anuradha (2022).

3.7 Formulation of agro-waste based substrates for bacterial cultivation

Agro-waste materials including potato, cabbage, tomato, orange, cannon ball cabbage, onion, watermelon, papaya, carrot, banana and beetroot peels, and bread leftover were collected from local market sites and cafeteria. The wastes were segregated at the point of generation and washed thoroughly with tap water to remove dirt and surface contaminants, and then sun dried, ground into powder using a mechanical grinder and sieved using a stainless steel sieve with a mesh size of 1 mm to 2 mm.

The processed agro-waste residues underwent preliminary screening to ensure their suitability as experimental substrates. Particle size uniformity was verified through visual inspection and re-sieving to confirm homogeneity. The pH of each residue was determined by suspending

powdered residues in distilled water at a 1:10 (w/v) ratio and measuring with a calibrated pH meter to assess their acidity or alkalinity. Following screening, the powders were appropriately labeled, sealed in sterile Schott bottles, and stored at 4 °C to preserve substrate integrity and prevent contamination (Figure 3).



Figure 3 Media prepared from agro-waste residues to be used as alternative low-cost growth substrate

The decoction method as described by Hidayat & Patricia Wulandari (2021) was employed to extract nutrients from the powdered agro-waste preparations. Fifty grams of each powder were suspended in 1000 mL of distilled water within 2 L Erlenmeyer flasks and subjected to heat treatment by boiling to release active compounds. After reaching boiling point, the mixture was simmered for 45 minutes. The resulting decoctions were strained through gauze fabric and subsequently filtered using Whatman No. 1 filter paper.

Filtrates were transferred into clean appropriately labeled and sterilized stoppered Schott bottles by autoclaving at 121 °C for 15 minutes. Sterility was verified by incubating aliquots of each decoction overnight to confirm the absence of microbial contamination prior to inoculation. The sterile extracts were stored at 4 °C until use for successive trials aimed at evaluating their potential as low-cost substrate components to support the growth of chromogenic bacterial isolates for pigment production optimization.

With regards to experimental procedure, initially, potent isolates (*Micrococcus luteus*, *Exiguobacterium aurantiacum*, and *Kocuria* sp.) were activated using the shake-flask culture method by aseptically transferring a loopful of each isolate into nutrient broth and incubating

overnight at 30 °C to obtain actively growing cultures. From each overnight culture, 10 mL of suspension was inoculated into 150 mL of agro-waste extracts (AWEs) contained in sterile Erlenmeyer flasks as pre-culture development whereby cultures were incubated under shaking conditions to assess the effectiveness of AWEs in supporting the growth of respective isolates (Figure 4).



Figure 4 Fermentation initiation: inoculation of AWEs with potential chromogenic isolates

Growth was monitored spectrophotometrically at OD_{600} . At an hour time interval, 10 mL of culture broth was withdrawn and replaced with an equal volume of sterile AWE to maintain working volume. Growth curves were plotted by recording OD_{600} values against time. At the stationary growth phase, cultures were centrifuged to recover cell biomass and crude pigments were extracted from the harvested biomass using organic solvent extraction method. For data replication and reliability, all experiments were conducted in triplicate and average OD_{600} values were statistically analyzed to provide reliable estimates of the effects of the tested AWEs so as to identify the most nutritious extract that supported the growth of the isolates compared to nutrient broth, used as benchmark. Statistical models were used to predict optimal conditions for enhanced culture growth and pigment production using the most supportive AWE as a low-cost substrate alternative.

3.8 Optimization of growth conditions for enhanced pigment-production

3.8.1 Statistical screening of growth conditions

To enhance pigment yield, selected pigment-producing bacterial isolates were subjected to screening and optimization under varying culture conditions using factorial design analysis for interactive effects. Screening of culture conditions and nutrient concentrations were conducted using PBD, a fractional factorial design used to identify the most significant process variables affecting culture growth (Chaudhari & Shirkhedkar, 2020).

Parameters tested comprises incubation temperature, initial medium pH, culture agitation rate, culture incubation period, inoculum age, inoculum size, glucose concentration, yeast extract concentration, and salt concentration for their impact on culture growth. The selection of these parameters and their optimum ranges was guided by extensive literature review and laboratory trials. Each variable was represented at two levels, low (-) and high (+), in 12 randomized experimental runs (Table 3) as suggested by the Plackett-Burman experimental design and incorporated into the Design Expert Statistical Software (version 13).

Table 3 Key Independent Variables Identified for Screening Using PBD

S. No	Variable	Unit	Experimental level	
			Low (-1)	High (+1)
1	Incubation temperature	° C	23	37
2	pH		5	10
3	Culture agitation rate	rpm	60	180
4	Incubation period	hour	24	72
5	Inoculum size	%	1	2.5
6	Inoculum age	hour	12	36
7	Yeast extract	%	0.1	1
8	Glucose	%	0.5	1.5
9	Salt (NaCl)	%	5	10

Culture growth was monitored by measuring optical density at 600 nm (OD₆₀₀) using UV-Visible spectrophotometer. To help reduce the impact of variability and provide a more reliable estimate of the effects of the variables being studied, the average value of the response, represented by culture OD₆₀₀ values were measured. The main effects model and Pareto analysis were used to identify the most significant factors influencing the culture growth. Based on the magnitude of their effect from ANOVA, three most significant variables influencing culture growth were selected for further optimization study.

3.8.2 Statistical optimization of significant growth conditions

Response surface methodology with a face centered central composite design (CCD) was utilized using significant variables (Table 4) to fit a model for the response variables, estimating the first-order and second-order terms with three levels matrix, keeping the non-significant variables (incubation temperature, inoculum age, inoculum size, NaCl, and glucose) at average values according to Ghosh & Banerjee (2023) and Silva-Castro et al.(2019).

As maximum pigment production potential correlates with the stationary growth phase, the bacterial cultures were incubated until the growth reached stationary phase, which were monitored by measuring the OD₆₀₀ (Gondil et al., 2017). Model assumptions and fitness were checked to evaluate the goodness of fit of the statistical model.

Table 4 Experimental Design Matrix: Significant variables and their optimization levels

Variable name	Units	Low (-1)	High (+1)	- α	+ α
Culture agitation rate (X_1)	rpm	60	180	60	180
pH (X_2)		5	10	5	10
Yeast extract (X_3)	%	0.1	1.0	0.1	1.0

Graphical optimization, indicating the interactions between process variables were used to visually analyze the response surface and identify combinations of these variables that achieve the optimum response value using surface plots (Boateng, 2023). The numerical method using desirability functions were applied for simultaneous optimization of all the responses in the process to find the best operating conditions that provide the most desirable response values by setting a goal to find factor settings that maximize the overall desirability

(Marinkovic, 2020). The goals for optimization were set “in range” for the identified input variables to find the best optimal conditions for culture growth and “maximize” for output variables to achieve maximum pigment production.

3.8.3 Experimental validation of statistically optimized growth conditions

Prior to actual optimization experimentation, trial tests were conducted with the optimized parameters to compare results with statistical predictions to ensure that the selected parameters truly contribute to the desired outcomes. Cultivations were conducted in 150 mL of freshly prepared AWE broth that best supported the growth of pigment-producing isolates at the predicted optimal conditions of significant variables (culture agitation rate, initial culture pH and yeast extract) keeping other culture conditions at an average value (initial culture pH at 7.5, culture agitation rate at 120 rpm, incubation temperature at 30 °C, inoculum age at 24 hours, inoculum size at 2%, NaCl at 7.5%, glucose at 1%, and yeast extract at 0.55%).

The experiments were conducted in triplicates, and the average values of the responses were considered for reliable estimate of the effects of each factor being optimized. Statistical models were used to predict the best conditions for enhanced culture growth and pigment production using best AWE that support the culture growth as an alternative low-cost substrate.

3.9 Extraction and quantification of bacterial bio-pigments

Pigments were extracted by solvent extraction method according to (Padhan et al., 2021). After incubation under optimized conditions, bacterial cultures were centrifuged at 5,000 rpm for 20 minutes at 4 °C to separate the biomass from the culture supernatant at the respective stationary growth phase.

Following centrifugation, the supernatants were discarded, and the pellets were weighed and re-suspended in equal volumes of organic solvents (Figure 5), measured by assessing the solubility of pigments with different solvents such as methanol, ethanol, acetone, and chloroform.



Figure 5 Pigment extractions: centrifugation of biomass at stationary growth phase post-fermentation

The solvents were added in equal volume to the supernatant, followed by vortexing and heat and acid treatment at 60 °C in water bath and 3 N HCl, respectively for 20 minutes to ensure complete extraction. The mixture was then centrifuged again, and the supernatant was collected for analysis. After treatment, the broth cultures were centrifuged again at 5,000 rpm at 4 °C for 20 minutes repeatedly until the residues turned white. The residues were then discarded, and the colored supernatants were filtered through 0.45 µm filter paper and kept in biosafety cabinet (BSC) for a week to evaporate the solvent.

The weight of dry biomass and crude pigment extracts were determined using the gravimetric technique (Wechselberger et al., 2013). Briefly, the biomass was determined by computing the change in mass of the broth culture after discarding the supernatants following centrifugation and deducting tare weights of the Falcon tubes. The weight of the pigment was determined after evaporating the solvent.

3.10 Analytical characterization of extracted pigments

The extracted pigments were filtered and concentrated to remove impurities and enhance its detectability, respectively. Various analytical techniques were applied to characterize the pigment focusing on its chemical composition, spectroscopic properties, and chromatographic separation for identification and structural elucidation. After adjusting the absorbance values of each pigment between 0.1 and 1.0 absorbance ranges, the extracted pigments were characterized by scanning its absorbance in the wavelength region of 350-750 nm using a UV-Vis spectrophotometer to determine their absorbance maxima (λ_{max}), which provide insights into pigment type.

Liquid chromatography-mass spectrometry (LC-MS) was employed for separation and molecular identification of pigment compositions. Attenuated Total Reflectance Fourier Transform Infrared (ATR-FTIR) was also used to analyze the vibrational modes of chemical bonds, helping identify functional groups present in the pigments. Additional observations on pigment color, solubility, and stability under heat, acidic and alkaline conditions, oxidizing and reducing agents were recorded to assess their suitability for textile dyeing applications.

3.10.1 UV-visible Analysis

The pigments were characterized by scanning their OD values using P9 double beam UV-visible spectrophotometer (VWR®, China). Briefly, after adjusting the OD values of the methanolic extract between 0.1 and 1.0 through dilution, 10 mL of each extract were subjected to spectral scanning in the wavelength region of 350-750 nm to find the characteristic absorption peaks where they absorb light for the identification of each pigment based on their specific wavelengths. The instrument was blanked before all analyses and measurement readings were taken in triplicates to ensure consistency and accuracy.

3.10.2 LC-MS Analysis

An Agilent 1260 Infinity II LC-MS 6495 (Agilent 1260 Infinity II LC System, Germany) equipped with electrospray ionization (ESI) source and Triple Quadrupole mass analyzer was used to separate the pigment based on its chemical properties and identify individual components in the pigment by their mass-to-charge-ratio values (Gao et al., 2006). Briefly, each extract were first dissolved in 99.5% methanol and centrifuged at 10,000 rpm for 10 minutes at a temperature of 4 °C. The clear supernatant was poured into an autosampler vial from which 10 µL was injected into liquid chromatography (LC) system. Chromatographic separation of the pigment was conducted using a standard reversed-phase C18 column (10 cm x 4.6 mm, 3 µm) set at 35 °C before the mass spectra (MS) detection.

After separation, the sample entered the mass spectrometer where it undergoes ionization. Nitrogen gas was used to spray the sample for efficient ionization. The capillary voltage, the gas flow rate, gas temperature, and nebulizer pressure were set at 3000 V, 5 L/min, 300 °C, and 50 psi, respectively. For effective separation and ionization processes, 0.1% acetic acid in water

and methanol at a flow rate of 1 mL/minute were used as eluents at a 40 minutes gradient elution program.

The program started with 90% of water with acetic acid and 10% methanol, gradually increasing the proportion of methanol from 10% to 90% in the first 35 minutes and remaining at 90% methanol for the last 5 minutes before returning to the initial conditions. The MS operated in multiple reactions monitoring (MRM) mode and spectra were scanned in positive ionization mode between 50 and 1000 mass-to-charge (m/z) ratio. The generated spectra were compared with a database of known compounds to identify possible chromophoric compounds present in the pigmented extract.

3.10.3 ATR-FTIR Analysis

Attenuated Total Reflectance (ATR) measurements were carried out using an FTIR spectrometer (Thermo Scientific Nicolet iS50, USA) equipped with an ATR device for spectrum analysis. This technique determines the functional groups present in the pigment by passing infrared light through a crystal where it is partially absorbed by the sample pressed onto the crystal, then reflects back through the crystal again, and travels to the FTIR detector (Njuguna et al., 2022).

Two milligrams of finely ground solid pigment was placed on the ATR crystal and a pressure of 700 kg/cm² was applied to ensure better contact between the extract and the crystal. The infrared (IR) source of the spectrometer focused radiation onto a deuterated triglycine sulfate (DTGS) crystal detector coated with potassium bromide. Measurements were taken in the spectral range of 4000–400 cm⁻¹ with each spectrum collected by scanning the sample at an average of 32 scans with a resolution of 16 cm⁻¹. Finally, the ATR-FTIR spectra of the sample were collected and peaks corresponding to the functional groups present in the pigment were identified by comparing the spectra to a reference spectrum. The peaks were then assigned to the corresponding functional groups based on their wave number values.

3.10.4 Pigment stability test

Pigment degradation was examined by monitoring changes in absorbance peaks against its original peak in wavelength and intensity according to Ngamwonglumlert et al.(2017) and Szadkowski et al. (2022). The stability of the pigments were assessed after dissolving the

pigments in suitable solvents followed by exposing them to various environmental stressors such as pH, temperature, light, oxidizing and reducing agents

The pigment was then exposed to temperatures of 20 °C, 30 °C, 40 °C, 50 °C, 60 °C, 70 °C and 80 °C in water bath after adjusting the pH to neutral for heat stability. Similarly, to evaluate the stability of the pigment in acidic, neutral and alkaline conditions, the pH of the pigment was adjusted to 3, 4, 5, 6, 7, 8, 9, 10 and 11 using HCl and NaOH (Amorim et al., 2022; Su et al., 2023).

To assess the influence of oxidizing and reducing agents on the pigment stability, the pH was adjusted to neutral. H₂O₂ at concentrations of 0.1%, 0.5%, 1.0%, 1.5%, 2.0%, 2.5% and 3% (v/v), and glucose at concentrations of 0.25%, 0.5%, 0.75%, 1.0%, 1.25%, 1.5%, 1.75% and 2% (v/v) were added to the pigment solution to make a total volume of 10 mL to test the pigment's tolerance to oxidation-reduction reactions (Rao et al., 2021; Su et al., 2023; Wijesekara and Xu, 2024).

The exposure time for all variables were 2 hours to assess immediate pigment response to stressors fluctuation and detect rapid degradation, helping refine dyeing conditions. For all analyses, the UV-Visible spectrophotometer was blanked prior to scanning and absorbance tests were run in triplicates and mean values of the parameters were used for analysis. Moreover, the tests were supplemented with visual inspections for any physical changes such as color fading and precipitation that might not be immediately detected by instruments.

3.11 Application of bio-pigments in textile dyeing and performance evaluation

3.11.1 Pigment solution preparation and dyeing fabrics

Cotton and Tetron 6000 fabric samples, both white were cut into uniform pieces, washed with detergent, and rinsed thoroughly with tap water to remove surface impurities. The mordant bath was prepared by filling cooking pan with enough water to completely immerse the fabrics into which aluminum sulfate (10% of the fabric dry weight) and potassium sulfate (5% of the fabric dry weight) were added and stirred well to dissolve the mordant. The damp fabrics were then put into the mordant solution, heated gently to 60 °C in water bath for 40 minutes with intermittent stirring. Finally, the fabrics were removed, rinsed lightly, and let dry before dyeing.

Dye bath was prepared by filling a bowl with tap water into which the pigment granules dissolved in methanol at a concentration of 3% (w/v) was diluted at a liquor ratio of 1:20. The dye bath was maintained at a controlled temperature of 40 °C with constant stirring for an hour (Failisnur et al., 2018). Fabric dyeing was conducted using immersion method by which the mordanted fabrics were soaked into the dye bath with a fabric-to-dye liquor ratio of 1:20 for 40 minutes under continuous stirring to facilitate dye absorbance and ensure uniform color uptake.

The dyeing conditions were adjusted to match the absorption maxima of the pigment as determined from stability tests for optimal pigment binding by adjusting significant factors of the dye bath so as to enhance color fastness. After dyeing, the fabrics were removed and rinsed thoroughly in cold water until the excess dye is removed and air-dried away from direct sunlight to preserve the color.

3.11.2 Evaluation of dyeing performance

The effectiveness of the dyeing process was evaluated for colorfastness by measuring dye exhaustion and fixation (Xu et al., 2024). Tests included washing fastness and light fastness to assess the durability of the pigments on the fabrics.

The percentage of dye that transferred from the dye bath to the fabric was determined using UV-Vis spectrophotometer at λ_{max} . of dye solution after dyeing and calculated using Equation 1:

$$Dye\ exhaustion(\%) = \left(\frac{Initial\ absorbance - Final\ absorbance}{Initial\ absorbance} \right) 100 \quad (1).$$

Washing fastness was evaluated by subjecting the dyed samples to repeated washing cycles with detergent under controlled conditions, while light fastness was determined by exposing the fabrics to direct sunlight for 24 hours and observing for any color fading. The amount of dye washed was calculated using Equation 2:

$$Dye\ fixation(\%) = \left(\frac{Initial\ absorbance - absorbance\ of\ removed\ dye}{Initial\ absorbance} \right) 100 \quad (2).$$

Moreover, color changes were rated visually by comparing the differences against originally dyed cotton and Tetron 6000 fabrics to benchmark performance for any color change after exposure to environmental factors.

3.12 Data analysis

All experimental data were recorded in triplicate and statistically analyzed to ensure reliability and reproducibility of results. For optimization, Design-Expert (Version 13) statistical software was used for design of experiments in order to explore the effects of multiple factors on a response variable.

All input and the corresponding response data were entered into Microsoft Excel to perform descriptive, correlation, regression, and ANOVA analyses. Descriptive statistics were conducted to summarize central tendencies and variation (Das et al., 2023). Pearson correlation and regression analyses were performed to explore relationship between variables and predict outcome variable (OD_{600}) based on input variables, respectively.

The experimental data were analyzed using ANOVA for a second-order response surface regression model to compare means within and between groups. A Post-hoc (Bonferroni correction) test was used to figure out exactly where the differences lie within group means where ANOVA shows a significant difference between the means of two independent groups (Fahrmeir et al., 2021). Graphical representations such as bar graphs, heat map, and line graphs were generated to visualize trends in outcome variables as a function of input variables. A significance level of $p < 0.05$ was used throughout the analysis (Gillard, 2020; Nor et al., 2017).

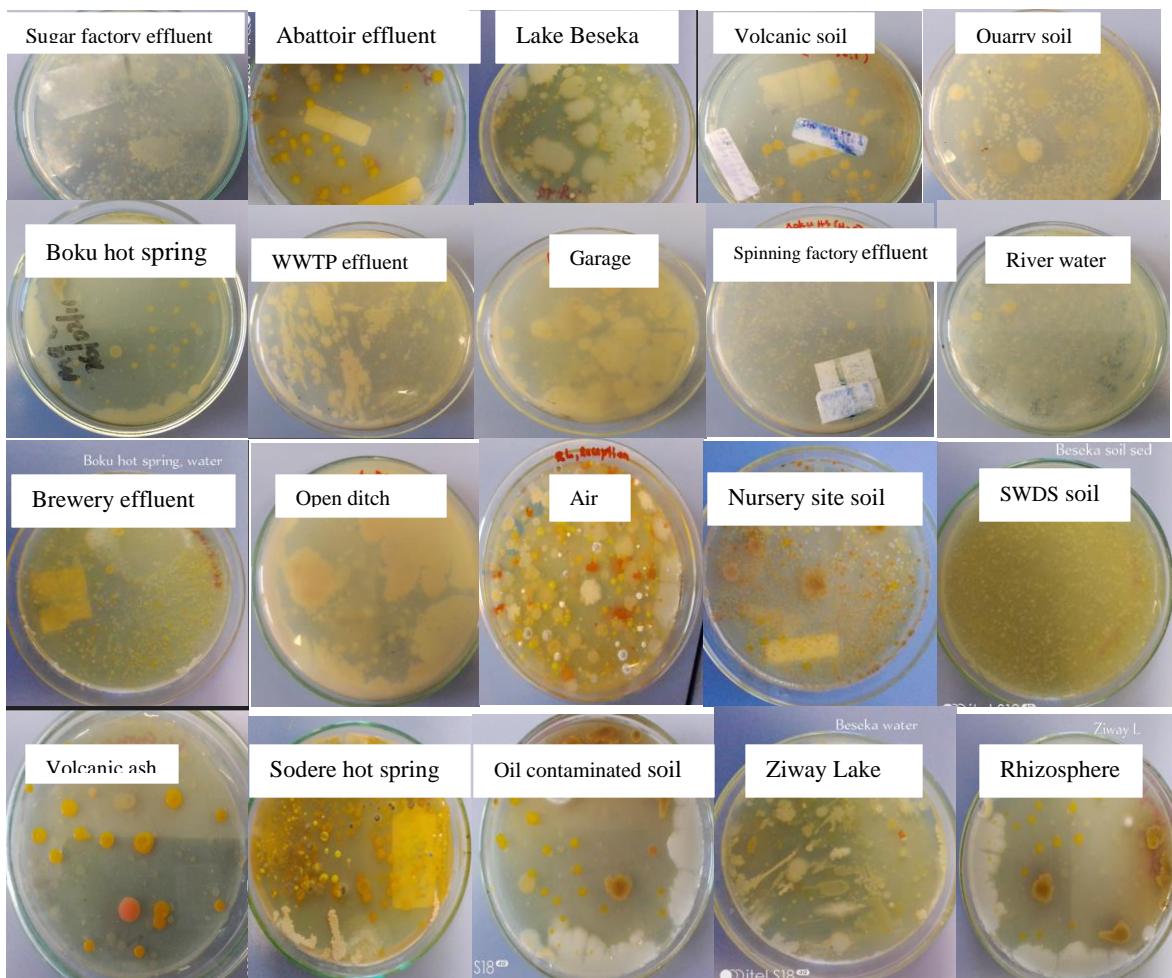
CHAPTER FOUR

RESULTS AND DISCUSSION

4.1 Screening and profiling of pigment-producing microbial isolates

Environmental samples gathered from various locations had temperatures ranging from 22 °C to 44 °C and pH values between 4.5 and 8.1 at the time of sample collection. After being cultured on nutrient agar, a total of 1,321 distinct colonies exhibiting variety of morphological characteristics were detected from all samples collected from the designated sampling sites after 48 hours of incubation at 30 °C (Figure 6). Among all, whitish-yellow and reddish-oranges colonies were the most prevalent.

The isolation process involved streaking the mixed colonies on an agar surface to obtain pure, single colonies each representing an identical strain derived from a single progenitor cell. Among these, 127 colonies exhibited visible pigmentation ranging from yellow and orange to red hues, suggesting the production of diverse bio-pigments. After further purification, 14 distinct isolates were presumptively recognized as pigment producers. The findings align with Agarwal et al. (2023) who explained that pigment-producing microorganisms are extensively dispersed and ubiquitous with various pigments being adaptive features across diverse environments.



Key: WWTP - wastewater treatment plant, and SWDS - solid waste disposal site

Figure 6 Representative colony morphologies of environmental isolates cultivated on nutrient agar for the recovery of pigment-producing strains. The printed labels on the culture plates denote the respective sources of the environmental samples.

Six potential pigment-producing isolates (PPPIs), designated PPPI1–PPPI6 (Figure 7) were selected for preliminary screening based on the intensity and stability of their colony coloration. The observation that only a limited proportion of isolates exhibited chromogenic potential indicates that pigment production is a genetically restricted and conditionally expressed trait rather than a universal characteristic among microbial populations. These selected isolates were subsequently prioritized for detailed evaluation, including stress tolerance assays, biochemical profiling and bio-molecular characterization to comprehensively assess their pigment production potential and industrial relevance.

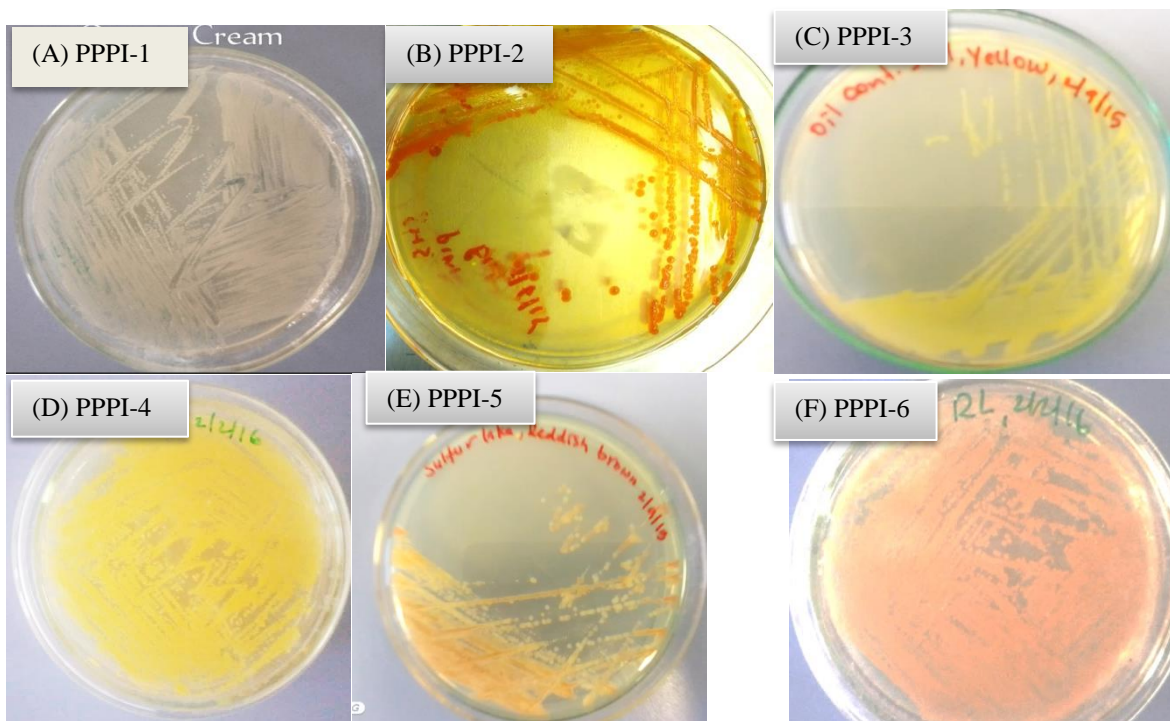


Figure 7 Pure colonies of pigment-producing bacterial isolates (PPPI-1 to PPPI-6) grown on nutrient agar. Panels (A)–(F) show isolates obtained from quarry soil (PPPI-1), hot spring (PPPI-2), oil-contaminated soil (PPPI-3), volcanic ash sediments (PPPI-4 and PPPI-5), and air sample (PPPI-6), respectively

As accurate classification of colony colors in pigment-producing bacterial isolates is essential for reproducibility and comparative analysis, Munsell color system was employed to group the pigments in order to avoid subjectivity (Munsell, 2010). The distinct colony color shows successful isolation, enabling further analysis. Morphological characterization revealed variations in colony shape, elevation, margin, surface texture and opacity (Table 5), providing preliminary insights into diversity of pigment-producing isolates. The Gram staining tests showed that four of the isolates were Gram-positive. From colony color versus Gram reaction, Gram-positive cocci (GPC) isolates (PPPI-1, PPPI-4, PPPI-5) produced creamy to bright yellow and reddish pink pigments. Whereas, Gram-negative bacilli (GNB) isolates (PPPI-2, PPPI-3) showed reddish brown and yellow pigmentation and Gram-positive bacillus (GPB) isolate (PPPI-6) produced reddish orange pigment, suggests that pigment production is not exclusive to a single Gram type, but certain colors may be more prevalent among specific groups.

Circular colonies were mostly associated with moist or sticky textures, especially among GPCs. Irregular colonies (PPPI-2 and PPPI-6) showed sticky or moist textures, possibly indicating extracellular matrix or pigment diffusion. Colony shape and texture may reflect species-specific growth traits and pigment secretion behavior. All isolates except PPPI-6 were non-motile, and most showed convex or raised elevation. The only motile isolate (PPPI-6) has an irregular shape and convex elevation, possibly linked to active spreading or swarming behavior, suggesting motility may influence colony irregularity and elevation due to dynamic surface movement. On the other hand, margin and opacity result indicated that entire margins dominated across isolates, except for PPPI-5 (lobate) which also has a sticky texture. Opaque colonies were common except for PPPI-1 (translucent), which may indicate lower pigment concentration or thinner biomass which may correlate with pigment density and colony compactness.

Table 5 Morphological characteristics of pigment-producing potential isolates (PPPI)

No	Isolate code	Pigment color	colony shape	Texture	Margin	Motility	Gram reaction	Opacity	Elevation
1	PPPI-1	Creamy	Circular	Moist	Entire	Non-motile	GPC	Translucent	Convex
2	PPPI-2	Reddish brown	Irregular	Sticky	Entire	Non-motile	GNB	Opaque	Raised
3	PPPI-3	Yellow	Circular	Moist	Entire	Non-motile	GNB	Opaque	Convex
4	PPPI-4	Bright yellow	Circular	Moist	Entire	Non-motile	GPC	Opaque	Convex
5	PPPI-5	Reddish Pink	Circular	Sticky	Lobate	Non-motile	GPC	Opaque	Raised
6	PPPI-6	Reddish orange	Irregular	Moist	Entire	Motile	GPB	Opaque	Convex

Key: PPPI-Potential Pigment-Producing Isolate, GPC- Gram Positive cocci, and GPB and GNB- Gram Positive and Gram Negative Bacilli, respectively.

The overall profile of biochemical test results showed that all six isolates were indole and methyl red (MR) negative, catalase-positive, and H₂S-negative. Citrate utilization was positive in three isolates (PPPI-3, PPPI-4, PPPI-6, while oxidase was positive in PPPI-1, PPPI-2, PPPI-4, and PPPI-5. Urease was positive only in PPPI-4 and PPPI-6 and nitrate reduction was positive in PPPI-1, PPPI-2, and PPPI-5. But, lactose fermentation was observed in PPPI-6 only and coagulase was positive in PPPI-4 (Table 6). Most of proposed genera align with prior colony and Gram reactions. For example GPC for *Micrococcus/Kocuria*, GNB non-fermenters for *Pseudomonas/Acinetobacter*, and GPB motile for *Bacillus/Exiguobacterium*. However, final identification requires further test such as endospore staining and molecular analysis for confirmation.

Table 6 Biochemical characteristics of pigment-producing potential isolates (PPPI)

No	Isolate code	Indole	MR	VP	Citrate reduction	Oxidase	Urease	Catalase	Nitrate reduction	Lactose fermentation	H ₂ S production	Coagulase	Possible proposed Genera
1	PPPI-1	-	-	+	-	+	-	+	+	-	-	-	<i>Micrococcus/Kocria</i>
2	PPPI-2	-	-	-	-	+	-	+	+	-	-	-	<i>Pseudomonas</i>
3	PPPI-3	-	-	-	+	-	-	+	-	-	-	-	<i>Acinetobacter</i>
4	PPPI-4	-	-	-	+	+	+	+	-	-	-	+	<i>Staphylococcus</i>
5	PPPI-5	-	-	+	-	+	-	+	+	-	-	-	<i>Micrococcus/Kocria</i>
6	PPPI-6	-	-	-	+	-	+	+	-	+	-	-	<i>Bacillus/Exiguobacterium</i>

Key: (+) test reaction is present, (-) test reaction is absent, MR- methyl red and VP-Voges Proskauer

Catalase positivity suggests the presence of catalase enzyme decomposing H₂O₂ into water and oxygen, allowing isolates survive oxidative stress. Likewise, Oxidase positivity indicates the presence of cytochrome c oxidase which helps separate oxidase-positive non-fermenters from oxidase-negative ones. Citrate utilization indicates the ability of an isolate to utilize citrate as sole carbon source which is common in environmental Gram-negative rods and some Gram-positive rods. The ability to use nitrate as terminal electron acceptor supports facultative

anaerobic respiration and environmental versatility. The absence of hydrogen sulfide (H₂S) production also suggests that these isolates do not engage in sulfur metabolism, reducing the risk of undesirable odors and unwanted reactions with fabric substrates if used for dyeing applications.

The morphological and biochemical findings suggested that the isolates are predominantly Gram-positive, aerobic, and non-motile with strong ability to resist oxidative damage. The catalase-positive reaction implies that these isolates thrive in oxygenated environments, while the lack of H₂S production further indicates that the isolates do not rely on anaerobic sulfur metabolism. Overall, the oxidase/catalase positivity and non-fermentative metabolism of the isolates suggest resilience in oxidative environments, potentially correlating with stable pigment pathways. In addition, citrate and urease profile of an isolate indicates diverse carbon/nitrogen utilization capacity; tailoring agro-waste extracts to these metabolic traits may enhance pigment yields.

MALDI-TOF mass spectrometry analysis identified five isolates as bacteria, three isolates to the genus and two isolates to the species level (Table 7). One isolate (PPPI-2) remained unidentified. Two isolates (PPPI-1 and PPPI-5) were identified homologous isolates despite being collected from different environments, suggesting potential environmental adaptation of the isolates.

Table 7 Bio-molecular characteristics of pigment-producing potential isolates (PPPI)

No	Isolate code	Identified isolate	Score	Identification level
1	PPPI-1	<i>Kocuria</i> sp.	1.70	Genus
2	PPPI-2	Unidentified	1.68	Unreliable
3	PPPI-3	<i>Acinetobacter</i> sp.	1.82	Genus
4	PPPI-4	<i>Micrococcus luteus</i>	2.19	Species
5	PPPI-5	<i>Kocuria</i> sp.	1.74	Genus
6	PPPI-6	<i>Exiguobacterium aurantiacum</i>	2.25	Species

Scoring criteria: < 1.7 unreliable, 1.7-2.0 probable genus and >2.0 probable species

MALDI-TOF mass spectrometry is a powerful tool for rapid microbial identification through the analysis of protein profiles of the isolates. The technique generates characteristic marker ion peaks, which were compared with a reference database to classify the isolates at the genus and species levels. Zhang et al. (2022) described that the characteristic peaks of different bacteria could be used as marker ion peaks for identification and successfully identified *Bacillus cereus*, *Listeria monocytogenes*, and *Micrococcus luteus* based on their protein profiles using MALDI-TOF technique.

The identification of three bacterial isolates at the genus level suggests that their protein spectra matched known genera but lacked sufficient specificity for species-level classification which could be due to limited database entries or variations within the isolates. While, identifying two isolates at the species level indicates a more precise match in the database, confirming their identity with high confidence. On the other hand, the failure to identify one isolate (PPPI-2) suggests either the isolate is a novel strain or an insufficient reference in the database, requiring further molecular analysis for confirmation.

MALDI-TOF analysis identified two of the isolates as *Kocuria* sp. The other isolate was identified as *Acinetobacter* sp. which is an opportunistic pathogen group (Chiu et al., 2015), and hence rejected from the subsequent screening for pigment production due to safety reason. Hence, pigments were extracted from three isolates, identified as *Micrococcus luteus* (*M. luteus*), *Exiguobacterium aurantiacum* (*E. aurantiacum*) and *Kocuria* sp. because of their non-pathogenicity and rapid growth in the employed agro-waste extract under various environmental conditions in repeated laboratory trials.

While most published works focused on engineered strains or marine isolates, this study highlighted that environmental isolates offer natural, non-genetically modified alternatives to engineered strains with potential for eco-safe industrial use; avoids genetic modification, and aligning with eco-safety goals but may give less pigment yield compared to engineered strains unless further optimized (López-Mora et al., 2025; Ramos et al., 2021).

Genus-level identification of *Kocuria* matches the earlier inference of *Micrococcus/Kocuria* from Gram-positive *cocci* morphology and oxidase/catalase positivity. Similarly, the genus level identification of *Acinetobacter* is congruent with oxidase-negative, citrate-positive, non-

fermenting GNB traits. The species level identification of *M. luteus* and *E. aurantiacum* fits the biochemical pattern observed, while the unreliable score for PPPI-2 indicates insufficient spectral match (Table 8).

Table 8 Summary table of match quality: MALDI-TOF consistency with morphological and biochemical test results

Isolate	MALDI-TOF identification	Score	Identification level	Consistency with morphological and biochemical data	Remark
PPPI-1	<i>Kocuria</i> sp.	1.70	Genus	High	Gram-positive cocci; oxidase/catalase positive profiles are consistent with <i>Micrococcus/Kocuria</i> .
PPPI-2	Unidentified	1.68	Unreliable	Indeterminate	Low score; retain as “GNB non-fermenter” needs reanalysis.
PPPI-3	<i>Acinetobacter</i> sp.	1.82	Genus	High	Oxidase-negative, catalase-positive GNB with citrate use fits <i>Acinetobacter</i> like traits.
PPPI-4	<i>M. luteus</i>	2.19	Species	High	Strong species level match; aligns with Gram-positive cocci and pigmenting morphology.
PPPI-5	<i>Kocuria</i> sp.	1.74	Genus	High	Similar to PPPI-1; biochemical pattern (oxidase/catalase+, VP+) supports <i>Micrococcaceae</i> .
PPPI-6	<i>E. aurantiacum</i>	2.25	Species	Moderate	Species level match; <i>Exiguobacterium</i> are Gram-positive short rods, often motile, catalase+, urease variable consistent with isolate's profile.

Key: **High** consistency-morphological traits closely align with the expected species characteristics, and biochemical reactions show strong agreement with reference profiles, **Intermediate** consistency-broader morphology traits matches at the genus level but differ in finer details, and only partial agreement in biochemical traits, and **Moderate** consistency-colony morphology is ambiguous or inconsistent with reference descriptions, and biochemical reactions exhibit limited or conflicting overlap with expected traits.

4.2. Stress tolerance profiling of pigment-producing bacteria

4.2.1 Temperature tolerance and growth pattern analysis

The stress tolerance tests demonstrated that the pigment-producing bacterial isolates (PPPI-1 to PPPI-6) cultured across thermal gradient from 20 °C to 45 °C (Figure 8), demonstrated mesophilic growth characteristics, assessed via OD₆₀₀ absorbance measurements. The thermal tolerance suggested that these isolates possess mechanisms to withstand environmental fluctuations.

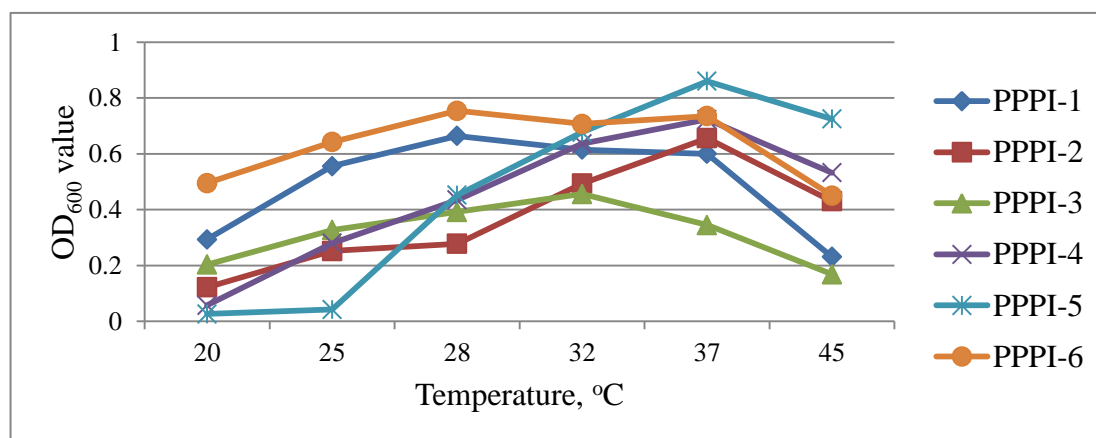


Figure 8 Line chart illustrating the effect of incubation temperature variations on culture growth of pigment-producing isolates (PPPI-1 to PPPI-6), evaluated via OD₆₀₀ measurement

All six isolates demonstrated the ability to grow across moderate temperature range with varying degrees of tolerance and stability. Isolates PPPI-1 and PPPI-6 showed optimal growth between 25 °C and 37 °C, indicating they thrive in mesospheric environments. While PPPI-4 and PPPI-5 exhibited progressive growth up to 37 °C which indicates adaptation to moderate environments and potential suitability for applications requiring stability under typical ambient and physiological conditions. The findings align with previous reports by Fatima & Anuradha (2022), who observed peak pigment production at 37 °C and emphasized that no universal temperature suits all pigment-producing bacteria.

Descriptive statistical analysis (Table 9) revealed that PPPI-6 had the highest mean OD₆₀₀ value of 0.63 ± 0.13 and the lowest coefficient of variation (CV = 20.45%), indicating high growth with low variability. Conversely, PPPI-5 displayed high growth variability (CV = 77.18%) with poor performance at lower temperatures and marked improvement from 32 °C onward. Other isolates, such as PPPI-2 and PPPI-4 showed moderate mean OD₆₀₀ values but higher variability, suggesting less stable thermal responses.

Table 9 Summary statistics (Mean, SD, CV%) of OD₆₀₀ for potential pigment-producing bacterial isolates across culture temperature conditions

Isolate	Mean OD ₆₀₀ value	Standard deviation (SD)	Coefficient of variation (CV %)
PPPI-1	0.4932	0.1834	37.19
PPPI-2	0.3718	0.1920	51.65
PPPI-3	0.3152	0.1105	35.05
PPPI-4	0.4438	0.2446	55.12
PPPI-5	0.4637	0.3579	77.18
PPPI-6	0.6305	0.1289	20.45

The ANOVA (Table 10) confirmed statistically significant differences in mean OD₆₀₀ values among the isolates ($F = 5.21$, $p < 0.002$), indicating that temperature had a differential impact on bacterial growth across isolates, supports the observation that thermal tolerance was isolate specific. Post hoc analysis with Bonferroni correction revealed that only *Acinetobacter* sp. differed significantly from *E. aurantiacum* in its response to temperature variation, whereas no significant differences were detected among the other isolates.

Table 10 ANOVA summary for differences in mean OD₆₀₀ values among six potential pigment-producing bacterial isolates in relation to temperature

Source of Variation	SS	df	MS	F	P-value	F crit
Between Groups	0.831862	5	0.166372	5.210982	0.001469	2.533555
Within Groups	0.957819	30	0.031927	-	-	-
Total	1.789681	35	-	-	-	-

Key: SS-sum of squares, df-degree of freedom, MS-mean Square, F-F-statistic, and F crit-F-critical

Pearson's correlation analysis (Table 11) further demonstrated the relationship between temperature and growths. Isolates PPPI-2, PPPI-4, and PPPI-5 exhibited strong positive correlations ($r = 0.745, 0.766, \text{ and } 0.853$, respectively), suggesting that their growth increased reliably with rising temperature. In contrast, PPPI-1, PPPI-3, and PPPI-6 showed weak to negligible negative correlations, signifying that while temperature influences growth, the relationship is not uniformly linear across all strains.

Table 11 Pearson's correlation between temperature and OD_{600} for potential pigment-producing isolates

Isolation	r(correlation) value	Strength of correlation	Interpretation
PPPI-1	-0.195	Weak negative	Slight tendency but not very reliable
PPPI-2	0.745	Strong positive	Strong and consistent correlation
PPPI-3	-0.164	Very weak negative	Almost no linear relationship
PPPI-4	0.766	Strong positive	Strong and consistent correlation
PPPI-5	0.853	Very strong positive	Highly predictive linear relationship
PPPI-6	-0.134	Negligible negative	Almost no linear relationship

These results highlighted that PPPI-6 is the most thermally stable and consistently productive isolate, while PPPI-5 stands out for its strong temperature responsiveness despite variability. The statistical evidence reinforced the isolate-specific nature of thermal tolerance, validating the assumption that no universal temperature suits all pigment-producing bacteria.

4.2.2 pH tolerance and growth pattern analysis

All bacterial isolates demonstrated the ability to grow within a pH range of 6 to 10 (Figure 9) with optimal growth observed near neutral pH (7–8), suggesting that these bacteria thrive best in neutral environment. This pattern supports findings by Deveikaite & Zvirdauskiene (2023), who emphasized that neutral pH enhances nutrient uptake and pigment production in bacteria, while extreme acidity or alkalinity impairs growth. In our study, growth generally increased with rising pH, peaking around pH 7, followed by a decline beyond pH 8.

Neutral pH supports efficient nutrient uptake, a common trait among chromogenic bacteria as their pigment production may be linked to stable metabolic processes at neutral pH conditions. Though the isolates tolerated increasing pH levels their growth started declining beyond pH 8, implies that further alkaline conditions may hinder bacterial metabolism possibly affecting enzyme functionality or nutrient absorption.

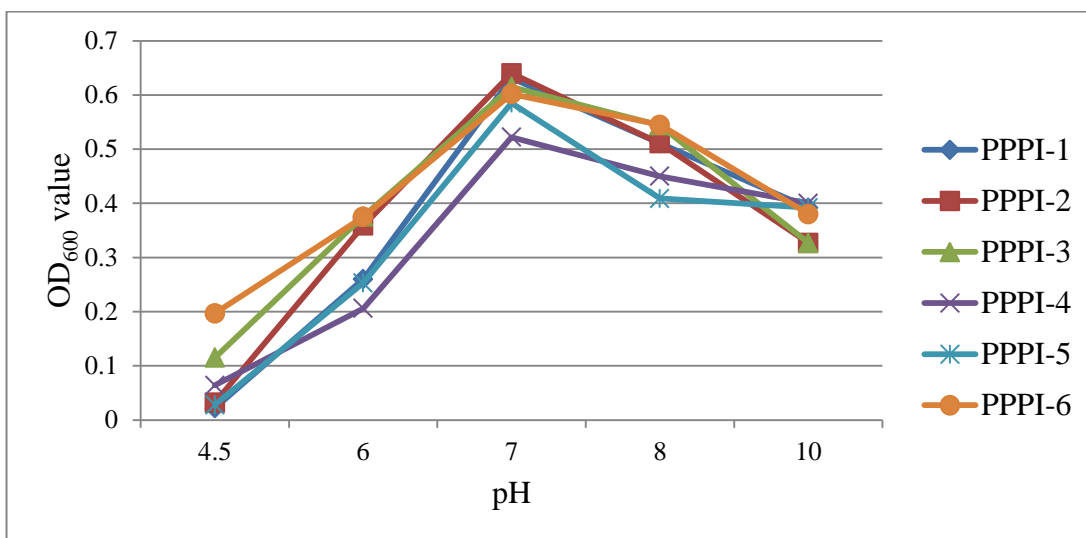


Figure 9 Line chart demonstrating the effect of the variation in culture medium pH on culture growth of pigment-producing isolates (PPPI-1 to PPPI-6), evaluated via OD₆₀₀ measurement

The results highlighted that the isolates prefer near neutral environments but struggle with excessively acidic or highly alkaline conditions. Their ability to tolerate a broad pH range (6–10) could indicate adaptability to different environment, making them suitable for applications where pH fluctuations are common.

Descriptive statistics (Table 12) revealed that PPPI-6 had the highest mean OD₆₀₀ value (0.4198±0.16) and the lowest coefficient of variation (CV = 38.06%), indicating consistent growth and better pH tolerance compared to other isolates. Conversely, PPPI-4 showed the lowest mean OD₆₀₀ (0.3284±0.19) and high variability (CV = 57.43%), suggesting inconsistent adaptation to pH shifts. Other isolates, such as PPPI-1 and PPPI-5, exhibited moderate growth but with high variability, indicating fluctuating responses across the pH range.

Table 12 Summary statistics (Mean, SD, CV%) of OD₆₀₀ for potential pigment-producing bacterial isolates across different culture medium pH conditions

Isolate	Mean OD ₆₀₀ value	Standard deviation (SD)	Coefficient of variation (CV %)
PPPI-1	0.3632	0.2353	64.78
PPPI-2	0.3738	0.2285	61.14
PPPI-3	0.3954	0.1962	49.62
PPPI-4	0.3284	0.1886	57.43
PPPI-5	0.3334	0.2075	62.23
PPPI-6	0.4198	0.1598	38.06

The ANOVA (Table 13) confirmed significant differences in mean OD₆₀₀ values among the isolates ($F = 84.85$, $p < 0.001$), reinforcing that pH sensitivity varies remarkably between strains. This statistical evidence underscores the importance of pH optimization tailored to each isolate for pigment production. Post hoc analysis with Bonferroni correction showed that *M. luteus* differed significantly from both *E. aurantiacum* and *Kocuria* sp. in its response to medium pH, whereas no significant differences were detected among the remaining isolates.

Table 13 ANOVA summary for differences in mean OD₆₀₀ values among six potential pigment-producing bacterial isolates in relation to variation in pH

Source of Variation	SS	df	MS	F	P-value	F crit
Between Groups	0.951742	3	0.317247	84.85161	1.50434E-11	3.098391
Within Groups	0.074777	20	0.003739	-	-	-
Total	1.026519	23	-	-	-	-

Key: SS-sum of squares, df-degree of freedom, MS-mean Square, F-F-statistic, and F crit-F-critical

Table 14 summarizes the Pearson's correlation coefficients between OD₆₀₀ values and pH across the six isolates. The analysis showed positive correlations between pH and OD₆₀₀ across all isolates, indicating that growth generally improved with increasing pH level. Particularly, PPPI-4 ($r = 0.716$), PPPI-5 ($r = 0.636$), and PPPI-1 ($r = 0.610$) exhibited strong positive correlations, suggesting a strong and predictable growth response to pH elevation. Isolates PPPI-2, PPPI-3, and PPPI-6 showed moderate correlations, indicating a less pronounced but still favorable relationship. Overall, the data suggested that while all isolates

tolerate a broad pH range, PPPI-6 stands out for its consistent performance, and PPPI-4 and PPPI-5 for their strong responsiveness to pH changes.

Table 14 Pearson's correlation between medium pH and OD₆₀₀ for potential pigment-producing isolates

Isolate	r(Correlation) value	Strength of correlation	Interpretation
PPPI-1	0.610	Strong positive	Strong and consistent correlation
PPPI-2	0.457	Moderate positive	Noticeable linear relationship
PPPI-3	0.408	Moderate positive	Noticeable linear relationship
PPPI-4	0.716	Strong positive	Strong and consistent correlation
PPPI-5	0.636	Strong positive	Strong and consistent correlation
PPPI-6	0.458	Moderate positive	Noticeable linear relationship

4.2.3 Salt tolerance and growth pattern analysis

Figure 10 demonstrates growth response of chromogenic bacterial isolates (PPPI-1 to PPPI-6) cultured in AWE medium supplemented with varying NaCl concentrations (0.5%–5%), assessed via OD₆₀₀ absorbance measurements. The isolates displayed differential growth responses when cultured in nutrient broth supplemented with varying concentrations of sodium chloride.

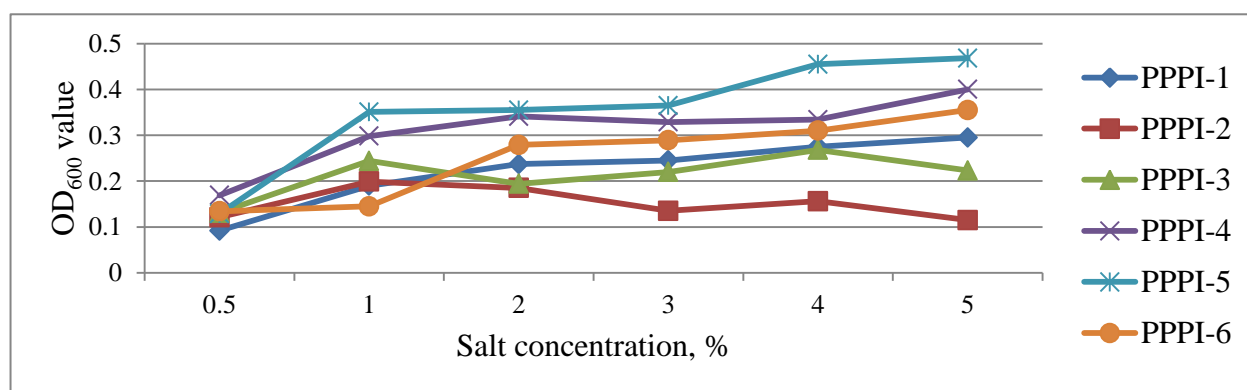


Figure 10 Line chart illustrating the effect of the variation in salt concentration on culture growth of pigment-producing isolates (PPPI-1 to PPPI-6), evaluated via OD₆₀₀ measurement

All isolates demonstrated the ability to grow under saline conditions ranging from 0.5% to 5% NaCl with varying degrees of tolerance and stability. Most isolates exhibited progressive

growth with increasing salinity, consistent with findings by Deveikaite and Zvirdauskiene's (2023) who reported optimal pigment production at 4% NaCl (w/v). However, isolate PPPI-2 showed peak growth at 1-2% NaCl (w/v), aligning with Yang et al. (2020) who noted that elevated salt concentration can inhibit bacterial growth due to osmotic stress which forces cells to work harder to balance internal and external solute levels.

Differences in growth patterns among isolates suggest that some strains may be more resilient to salinity fluctuations, potentially influencing their pigment stability and production efficiency in textile dyeing processes. Halophilic species thrive under saline conditions and produce pigments with enhanced stability and solubility which can be beneficial for textile dyeing (Silva-Castro et al., 2019). The observed salinity tolerance ranges among the isolates highlighted their potential for industrial pigment production especially in environments where salt exposure is a factor such as textile dyeing baths.

Descriptive statistics (Table 15) demonstrated that PPPI-5 had the highest mean OD₆₀₀ value (0.3538±0.12) followed by PPPI-4 (0.3118±0.08), suggesting relatively better growth under saline conditions. However, both PPPI-5 and PPPI-6 exhibited high coefficients of variation (CV = 34.37% and 36.13%, respectively), indicating inconsistent growth responses across the salt gradient. In contrast, PPPI-2 and PPPI-3 had lower mean OD₆₀₀ values and lower CVs (22.69% and 22.20%, respectively), suggesting weaker but more stable growth patterns.

Table 15 Summary statistics (Mean, SD, CV %) of OD₆₀₀ for potential pigment-producing bacterial isolates across culture medium salt concentration (% NaCl)

Isolate	Mean OD ₆₀₀ value	Standard deviation (SD)	Coefficient of variation (CV %)
PPPI-1	0.2223	0.0732	32.94
PPPI-2	0.1518	0.0344	22.69
PPPI-3	0.2133	0.0474	22.20
PPPI-4	0.3118	0.0775	24.84
PPPI-5	0.3538	0.1216	34.37
PPPI-6	0.2520	0.0910	36.13

Table 16 presents results from ANOVA, evaluating whether mean OD₆₀₀ value significantly differs across the isolates. The analysis confirmed statistically significant differences in mean OD₆₀₀ values among the isolates ($F = 3.44$, $p < 0.05$), indicating that salinity tolerance varies

notably between strains. This supports the assumption that salt concentration exerts a differential impact on bacterial growth, necessitating isolate-specific optimization. Post hoc analysis with Bonferroni correction revealed significant differences in salt concentration tolerance between the unidentified isolate, designated as PPPI-2 and *Kocuria* sp. as well as between PPPI-2 and *M. luteus*. No significant differences were detected among the remaining isolates.

Table 16 ANOVA summary for differences in mean OD₆₀₀ values among six potential pigment-producing bacterial isolates in relation to variation in salt concentration

<i>Source of Variation</i>	<i>SS</i>	<i>df</i>	<i>MS</i>	<i>F</i>	<i>P-value</i>	<i>F crit</i>
Between Groups	0.126676	5	0.025335	3.442332	0.014124	2.533555
Within Groups	0.220797	30	0.00736			
Total	0.347472	35				

Key: *SS*-sum of squares, *df*-degree of freedom, *MS*-mean Square, *F*-*F*-statistic, and *F crit*-*F*-critical

Pearson's correlation analysis (Table 17) revealed that five out of six isolates exhibited positive correlations between OD₆₀₀ and salt concentration, indicating that growth generally increased with salinity. Particularly, PPPI-6 ($r = 0.940$), PPPI-1 ($r = 0.899$), PPPI-5 ($r = 0.845$), and PPPI-4 ($r = 0.820$) showed very strong positive correlations, suggesting highly predictive and strong growth responses to increasing salt levels. PPPI-3 showed moderate positive correlation ($r = 0.576$), while PPPI-2 exhibited weak negative correlation ($r = -0.399$), reinforcing its unique sensitivity to elevated salinity.

Table 17 Pearson's correlation between salt concentration and OD₆₀₀ for potential pigment-producing isolates

Isolate	r(correlation) value	Strength of correlation	Interpretation
PPPI-1	0.899	Very strong positive	Highly predictive linear relationship
PPPI-2	-0.399	Weak negative	Slight tendency, but not very reliable
PPPI-3	0.576	Moderate positive	Noticeable linear relationship
PPPI-4	0.820	Very strong positive	Highly predictive linear relationship
PPPI-5	0.845	Very strong positive	Highly predictive linear relationship
PPPI-6	0.940	Very strong positive	Highly predictive linear relationship

Overall, these results highlighted PPPI-5 and PPPI-6 as promising candidates for pigment production under saline conditions despite their growth variability. The strong correlation patterns observed in most isolates suggested that salinity can be strategically manipulated to enhance bacterial pigment yield, provided strain specific tolerances are considered.

4.2.4 Agitation tolerance and growth pattern analysis

All isolates were capable of growth under agitation rates ranging from 30 to 150 rpm with maximum OD₆₀₀ values observed at 90 rpm (Figure 11) which is slightly lower than the optimal agitation range of 90–120 rpm reported by Fatima & Anuradha (2022). The difference could result from variability in bacterial species with different isolates responding differently to mechanical agitation which affects pigment biosynthesis and metabolic activity and environmental conditions such as temperature, pH, and oxygen diffusion which can influence growth patterns.

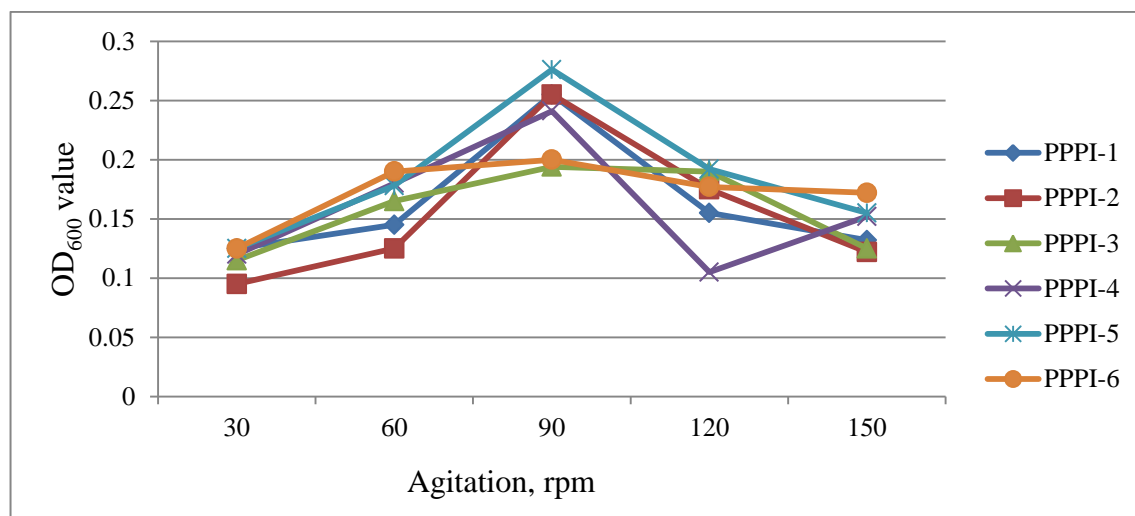


Figure 11 Line chart showing the effect of the variation in culture agitation rate on culture growth of pigment-producing isolates (PPPI-1 to PPPI-6), evaluated via OD₆₀₀ measurement

Descriptive statistics (Table 18) indicated that overall OD₆₀₀ values were low across agitation conditions, suggesting limited biomass accumulation. Among the isolates, PPPI-6 exhibited the most consistent growth with the lowest coefficient of variation (CV = 16.72%) and a

relatively higher mean OD₆₀₀ (0.1728±0.03) followed by PPPI-5 (mean=0.1852±0.06, CV = 30.64%). Other isolates showed greater variability with CVs ranging from 23.08% to 40.95%, indicating inconsistent responses to mechanical agitation.

Table 18 Summary statistics (Mean, SD, CV %) of OD₆₀₀ for potential pigment-producing bacterial isolates across culture medium agitation rate (rpm)

Isolate	Mean OD ₆₀₀ value	Standard deviation (SD)	Coefficient of variation (CV %)
PPPI-1	0.1624	0.0530	32.66
PPPI-2	0.1544	0.0632	40.95
PPPI-3	0.1578	0.0364	23.08
PPPI-4	0.1596	0.0540	33.81
PPPI-5	0.1852	0.0567	30.64
PPPI-6	0.1728	0.0289	16.72

The ANOVA (Table 19) revealed statistically significant differences in mean OD₆₀₀ values among the isolates ($F = 18.12$, $p < 0.001$), confirming that agitation rate had a differential impact on growth performance. The findings support the need for isolate-specific optimization of agitation conditions to enhance pigment production.

Pairwise mean difference analyses among the isolates for agitation rate tolerance conducted with Bonferroni correction showed that none of the comparisons yielded adjusted p -values below 0.05 despite the overall ANOVA being significant. This outcome reflects the conservative nature of post hoc testing, where the overall variation is statistically detectable but no individual pairwise difference was sufficiently strong to remain significant after correction.

Table 19 ANOVA summary for differences in mean OD₆₀₀ values among six potential pigment-producing bacterial isolates in relation to variation in culture agitation rate

Source of Variation	SS	df	MS	F	P-value	F crit
Between Groups	0.047408	4	0.011852	18.12417	4.21E-07	2.75871
Within Groups	0.016349	25	0.000654	-	-	-
Total	0.063757	29	-	-	-	-

Key: SS-sum of squares, df-degree of freedom, MS-mean Square, F-F-statistic, and F crit-F-critical

Table 18 summarizes the Pearson's correlation coefficients between OD₆₀₀ values at varying agitation rates across the six potential pigment-producing isolates. The analysis showed that most isolates had weak or negligible correlations between OD₆₀₀ and agitation rate, suggesting minimal linear responsiveness. However, PPPI-6 stood out with moderate positive correlation ($r=0.443$), indicating a noticeable and consistent growth trend with increasing agitation. Other isolates such as PPPI-2, PPPI-3, and PPPI-5 showed weak positive correlations, while PPPI-4 exhibited a negligible negative correlation ($r=-0.032$), reinforcing its insensitivity to agitation changes.

Table 20 Pearson's correlation between culture agitation and OD₆₀₀ for potential pigment-producing isolates

Isolate	Correlation (r) value	Strength of correlation	Interpretation
PPPI-1	0.072	Negligible positive	Almost no linear relationship
PPPI-2	0.260	Weak positive	Slight tendency, but not very reliable
PPPI-3	0.195	Weak positive	Slight tendency, but not very reliable
PPPI-4	-0.032	Negligible negative	Almost no linear relationship
PPPI-5	0.206	Weak positive	Slight tendency, but not very reliable
PPPI-6	0.443	Moderate positive	Noticeable linear relationship

4.2.5 Nutrient utilization and growth pattern analysis

Figure 12, Panels (A) and (B) show growth performance of chromogenic bacterial isolates (PPPI-1 to PPPI-6) cultured in AWE medium supplemented with various carbon (1%) and nitrogen (0.1%) sources, measured via OD₆₀₀ absorbance. All isolates demonstrated enhanced growth on glucose and sucrose (carbon sources) and yeast extract (nitrogen source), suggesting preferential utilization of simple sugars and organic nitrogen.

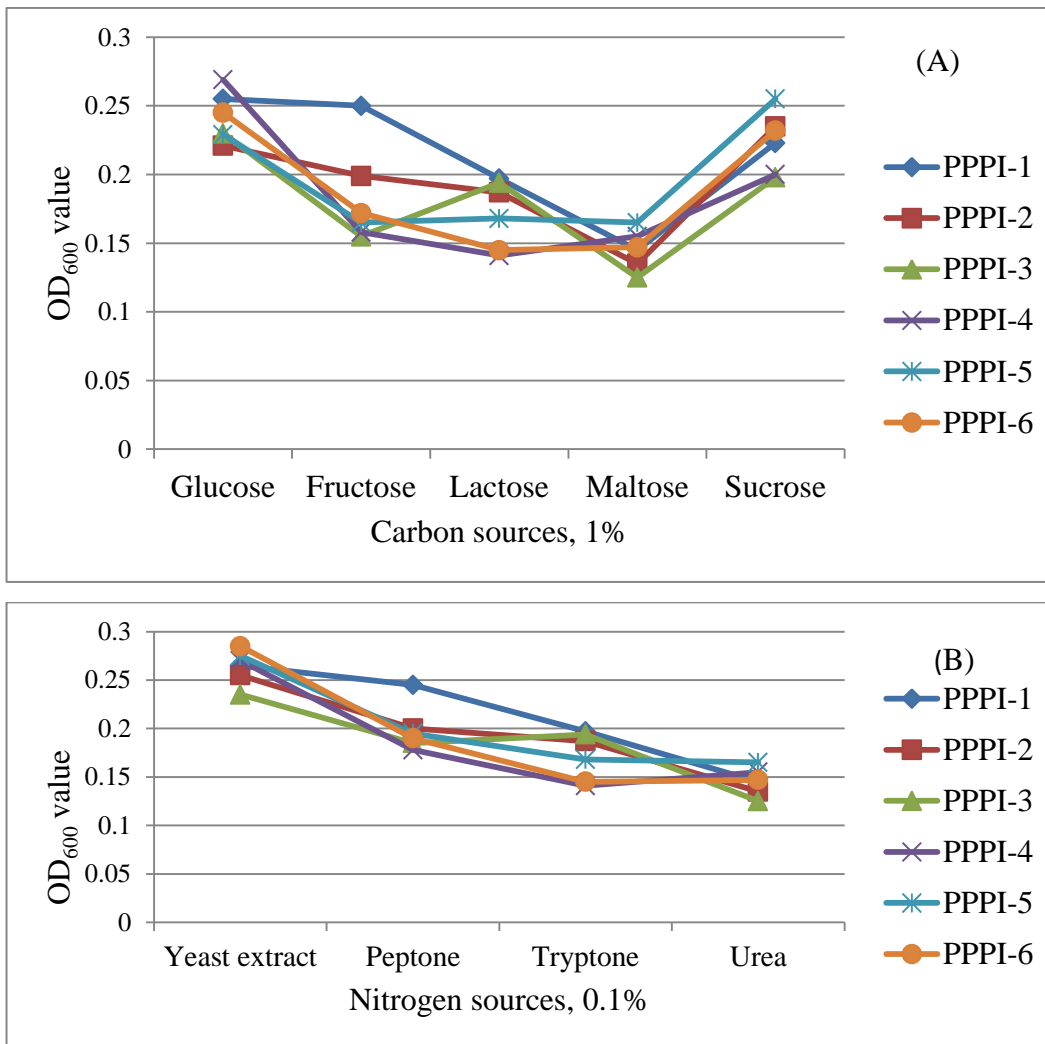


Figure 12 Line chart depicting the effect of carbon and nitrogen sources on growth of pigment-producing isolates (PPPI-1 to PPPI-6) evaluated via OD₆₀₀ measurement. Panel (A) shows culture response to various carbon sources supplied at 1%, while Panel (B) illustrates growth under different nitrogen sources provided at 0.1%

The observed nutrient utilization trends highlighted optimal metabolic conditions for bacterial pigment production, paving the way for efficient bio-pigment extraction in textile dyeing applications. These isolates likely possess enzymes such as amylase, sucrase, or glucokinase to break down simple sugars effectively and switching efficiently between different energy sources, supporting pigment biosynthesis and cellular processes (Nasha Musa & Zulaikha Yusof, 2019). Yeast extract supported the highest growth, suggesting that it provides a rich

nitrogen supply essential for protein synthesis and enzymatic activity. The ability to use broader range of nutrient sources can affect pigment type and yield, providing a selection advantage for exploiting bacteria for pigment production with diverse carbon and nitrogen sources (Pisareva & Kujumdzieva, 2010).

Descriptive statistics revealed generally low OD₆₀₀ values across all nutrient conditions, indicating modest biomass accumulation. With carbon sources (Table 21), PPPI-1 showed the highest mean OD₆₀₀ (0.2140±0.05) with a CV of 21.04%, while PPPI-2 and PPPI-5 followed closely. For nitrogen sources (Table 22), PPPI-1 again led with mean OD₆₀₀ of 0.2130±0.054, and PPPI-3 showed the most stable growth (CV = 24.57%). PPPI-6 exhibited the highest variability in nitrogen utilization (CV = 34.18%), suggesting less consistent growth across nitrogen sources.

Table 21 Summary statistics (Mean, SD, CV %) of OD₆₀₀ for potential pigment-producing bacterial isolates across culture medium carbon sources (1% each)

Isolate	Mean OD ₆₀₀ value	Standard deviation (SD)	Coefficient of variation (CV %)
PPPI-1	0.2140	0.0450	21.04
PPPI-2	0.1954	0.0386	19.75
PPPI-3	0.1804	0.0408	22.63
PPPI-4	0.1846	0.0521	28.21
PPPI-5	0.1964	0.0426	21.71
PPPI-6	0.1882	0.0474	25.16

Table 22 Summary statistics (Mean, SD, CV %) of OD₆₀₀ for potential pigment-producing bacterial isolates across culture medium nitrogen sources (0.1 % each)

Isolate	Mean OD ₆₀₀ value	Standard deviation (SD)	Coefficient of variation (CV %)
PPPI-1	0.2130	0.0536	25.15
PPPI-2	0.1943	0.0493	25.37
PPPI-3	0.1848	0.0454	24.57
PPPI-4	0.1860	0.0580	31.20
PPPI-5	0.2008	0.0513	25.56
PPPI-6	0.1918	0.0655	34.18

The ANOVA results (Table 23 and 24) confirmed statistically significant differences in mean OD₆₀₀ values among isolates for both carbon ($F = 15.59$, $p < 0.001$) and nitrogen ($F = 37.05$, $p < 0.001$) sources, indicating isolate-specific nutrient preferences and metabolic capabilities. Pairwise post hoc analysis with Bonferroni correction for both carbon and nitrogen sources among the potent pigment-producing isolates revealed that none of the comparisons yielded adjusted p -values below 0.05 despite the overall ANOVA being significant for both nutrient sources. This indicates that while overall variation was statistically detectable no individual pairwise differences were sufficiently strong to remain significant after correction.

Table 23 ANOVA summary for differences in mean OD₆₀₀ values among six potential pigment-producing bacterial isolates grown on different carbon sources

<i>Source of Variation</i>	<i>SS</i>	<i>df</i>	<i>MS</i>	<i>F</i>	<i>P-value</i>	<i>F crit</i>
Between Groups	0.036675667	4	0.009169	15.59287	1.6E-06	2.75871
Within Groups	0.0147005	25	0.000588			
Total	0.051376167	29				

Key: *SS*-sum of squares, *df*-degree of freedom, *MS*-mean Square, *F*-*F*-statistic, and *F crit*-*F*-critical

Table 24 ANOVA summary for differences in mean OD₆₀₀ values among six potential pigment-producing bacterial isolates grown on different nitrogen sources

<i>Source of Variation</i>	<i>SS</i>	<i>df</i>	<i>MS</i>	<i>F</i>	<i>P-value</i>	<i>F crit</i>
Between Groups	0.046767	3	0.015589	37.05037	2.34E-08	3.098391
Within Groups	0.008415	20	0.000421			
Total	0.055182	23				

Key: *SS*-sum of squares, *df*-degree of freedom, *MS*-mean Square, *F*-*F*-statistic, and *F crit*-*F*-critical

Pearson's correlation matrices revealed strong positive relationships in nutrient utilization patterns among isolates. For carbon sources (Table 25), correlation coefficients ranged from moderate (e.g., PPPI-1 vs. PPPI-5, $r = 0.440$) to very strong (e.g., PPPI-5 vs. PPPI-6, $r = 0.922$), suggesting shared metabolic traits. Nitrogen source correlations (Table 26), were uniformly strong to very strong (e.g., PPPI-4 vs. PPPI-5, $r = 0.992$; PPPI-5 vs. PPPI-6, $r = 0.998$), indicating consistent nitrogen assimilation patterns across isolates.

Table 25 Pearson's correlation between carbon sources and OD₆₀₀ for potential pigment-producing isolates

Correlation	PPPI-1	PPPI-2	PPPI-3	PPPI-4	PPPI-5	PPPI-6
PPPI-1	1	0.841	0.662	0.579	0.440	0.670
PPPI-2	0.841	1	0.810	0.601	0.787	0.818
PPPI-3	0.662	0.810	1	0.727	0.689	0.736
PPPI-4	0.579	0.601	0.727	1	0.749	0.913
PPPI-5	0.440	0.787	0.689	0.749	1	0.922
PPPI-6	0.670	0.818	0.736	0.913	0.922	1

Table 26 Pearson's correlation between nitrogen sources and OD₆₀₀ for potential pigment-producing isolates

Correlation	PPPI-1	PPPI-2	PPPI-3	PPPI-4	PPPI-5	PPPI-6
PPPI-1	1	0.945	0.896	0.744	0.804	0.815
PPPI-2	0.945	1	0.973	0.841	0.901	0.892
PPPI-3	0.896	0.973	1	0.716	0.796	0.776
PPPI-4	0.744	0.841	0.716	1	0.992	0.994
PPPI-5	0.804	0.901	0.796	0.992	1	0.998
PPPI-6	0.815	0.892	0.776	0.994	0.998	1

These findings underscored the metabolic adaptability of the isolates, particularly PPPI-1 and PPPI-5, which demonstrated strong and stable growth across diverse nutrient conditions. Such adaptability enhances their suitability for pigment production under variable industrial fermentation setups.

Heat map analysis (Figure 13) depicts growth intensity of these isolates across different environmental conditions in a color-coded visual matrix, highlighting which conditions each isolate tolerates best and worst. Among the environmental factors, culture incubation temperature between 25 °C-45 °C and pH of the culture medium near neutral had the strongest impact on the growth of the isolates followed by salt concentration, expressed in terms of OD₆₀₀ readings (red highlight). The rest environmental conditions showed weak to moderate influences on the growth of the isolates.

Condition		PPPI-1	PPPI-2	PPPI-3	PPPI-4	PPPI-5	PPPI-6
Temperature (°C)	20	0.293	0.122	0.203	0.057	0.026	0.495
	25	0.556	0.252	0.327	0.28	0.042	0.642
	28	0.664	0.278	0.392	0.435	0.452	0.754
	32	0.615	0.493	0.456	0.636	0.677	0.707
	37	0.6	0.656	0.345	0.723	0.86	0.735
	45	0.231	0.43	0.168	0.532	0.725	0.45
	pH	4.5	0.022	0.032	0.115	0.064	0.028
6		0.26	0.359	0.376	0.206	0.253	0.375
7		0.631	0.64	0.615	0.522	0.585	0.602
8		0.511	0.511	0.544	0.45	0.409	0.545
10		0.392	0.327	0.327	0.4	0.392	0.38
Salt concentration (%)		0.5	0.092	0.121	0.131	0.169	0.129
	1	0.19	0.199	0.244	0.298	0.351	0.145
	2	0.237	0.185	0.194	0.341	0.355	0.279
	3	0.245	0.135	0.22	0.329	0.365	0.289
	4	0.275	0.156	0.268	0.334	0.455	0.31
	5	0.295	0.115	0.223	0.4	0.468	0.355
Agitation (rpm)	30	0.125	0.095	0.115	0.12	0.125	0.125
	60	0.145	0.125	0.165	0.18	0.178	0.19
	90	0.255	0.255	0.194	0.241	0.276	0.2
	120	0.155	0.175	0.19	0.105	0.192	0.177
	150	0.132	0.122	0.125	0.152	0.155	0.172
	Carbon sources (1%)	Glucose	0.255	0.221	0.23	0.269	0.229
Fructose		0.25	0.199	0.155	0.158	0.165	0.172
Lactose		0.197	0.187	0.194	0.141	0.168	0.145
Maltose		0.145	0.135	0.125	0.155	0.165	0.147
Sucrose		0.223	0.235	0.198	0.2	0.255	0.232
Nitrogen sources (0.1%)		Yeast extract	0.265	0.255	0.235	0.27	0.275
	Peptone	0.245	0.2	0.185	0.178	0.195	0.19
	Tryptone	0.197	0.187	0.194	0.141	0.168	0.145
	Urea	0.145	0.135	0.125	0.155	0.165	0.147

Figure 13 Heat maps of OD₆₀₀ readings illustrating isolates' tolerance across diverse environmental conditions; rows represent test conditions, columns indicate bacterial isolates. Colors reflect OD values: Green-weak growth, Yellow- medium growth, and Red-high growth

4.3. Growth performance of pigment-producing bacterial isolates on agro-waste extracts

The selected potential pigment-producing bacterial isolates were cultured in respective agro-waste extracts (AWEs) along with key culture conditions, initially optimized via one-variable at-a-time (OVAT) and statistical methods using nutrient broth as cultivation medium. The process helped identify AWEs that effectively support culture growth and enhanced pigment production. The OD₆₀₀ values (Figure 14) show the growth performance of different isolate-AWE combinations. Two AWEs (banana and beetroot peels), and bread leftover showed minimal bacterial growth (OD₆₀₀ < 0.1) and were excluded, while nine AWEs successfully supported fermentation with nutrient broth serving as benchmark.

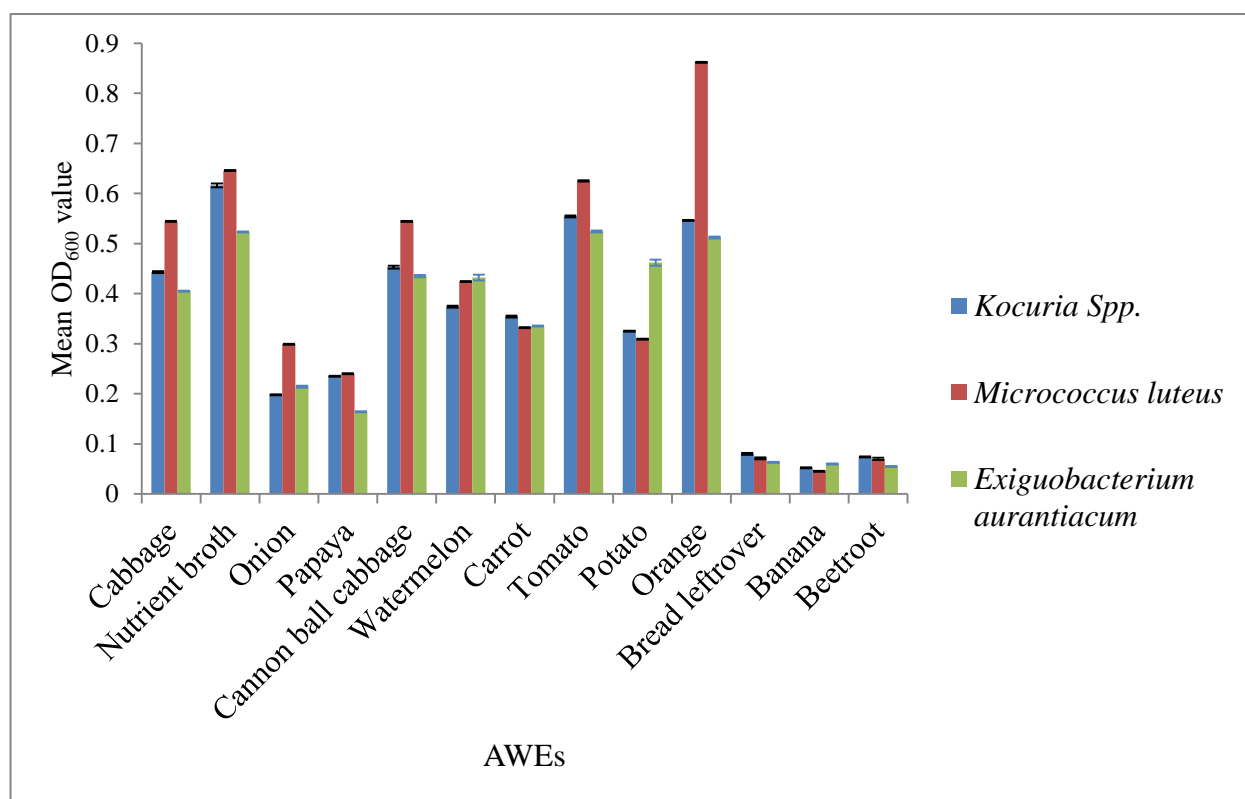


Figure 14 Clustered bar charts depicting the impact of AWEs as growth substrate on the selected potent pigment-producing bacterial isolates. Bar height shows mean and standard deviations of triplicate OD₆₀₀ measurements and error bars show standard deviations

Among the tested bacterial isolates, *M. luteus* exhibited the highest growth when cultivated in orange-waste extract (OWE) whereas, both *Kocuria sp.* and *E. aurantiacum* proliferate well in

tomato-waste extract (TME) and OWE as well (Figure 14) in conjunction with nutrient broth as the basal cultivation medium, evaluated via OD₆₀₀ measurements.

The ANOVA test yielded highly significant differences in mean OD₆₀₀ values among various AWEs for all the isolates, highlighted at least one AWE affects the growth of these isolates differently. The very large *F*-statistic of mean OD₆₀₀ values for *M. luteus* cultured in different AWEs (Table 27) confirmed that at least two AWEs differ in their effects on the growth of the isolate. The remarkably low *p*-value indicated strong evidence supporting the null hypotheses; specific agro-waste extracts significantly enhance bacterial pigment production.

Table 27 ANOVA depicting average OD₆₀₀ values of *M. luteus* cultured in different AWEs

Groups	Count	Sum	Average	Variance		
Cabbage	3	1.631	0.544	3.33E-07		
Nutrient broth	3	1.937	0.646	3.33E-07		
Onion	3	0.896	0.299	3.33E-07		
Papaya	3	0.721	0.240	3.33E-07		
Cannon ball cabbage	3	1.632	0.544	0.000001		
Watermelon	3	1.271	0.424	3.33E-07		
Carrot	3	0.997	0.332	3.33E-07		
Tomato	3	1.874	0.625	3.33E-07		
Potato	3	0.926	0.309	3.33E-07		
Orange	3	2.586	0.862	0.000001		
ANOVA						
Source of Variation	SS	df	MS	<i>F</i>	<i>P</i> -value	<i>F</i> crit
Between Groups	1.041141633	9	0.115682	247890.9	1.83E-48	2.392814
Within Groups	9.33333E-06	20	4.67E-07			
Total	1.041150967	29				

Key: *SS*-sum of squares, *df*-degree of freedom, *MS*-mean Square, *F*-*F*-statistic, and *F* crit-*F*-critical

The analysis revealed that different substrates exerted varying effects on isolate growth with orange waste extract (OWE) emerging as the most effective substrate. OWE produced the highest mean OD₆₀₀ value among all tested substrates, thereby demonstrating its superior competence to enhance the growth of *Micrococcus luteus*. The linear regression model provided further insight into the relationship between incubation temperature and pH of the culture medium on the growth of the isolate in OWE (Figure 15). The strong positive correlation ($r = 0.85$) between incubation temperature and culture growth indicated that temperature was a primary determinant for the proliferation of the isolate compared to pH of the culture medium with lower correlation value ($r = 0.64$).

The analysis indicated that optimal thermal conditions are crucial for maximizing biomass yield, 73% of growth variability explained by temperature. The remaining 27% could be influenced by additional factors such as nutrient composition, pH, aeration, or light exposure. These variables may interact synergistically or independently with temperature to impact overall microbial metabolism.

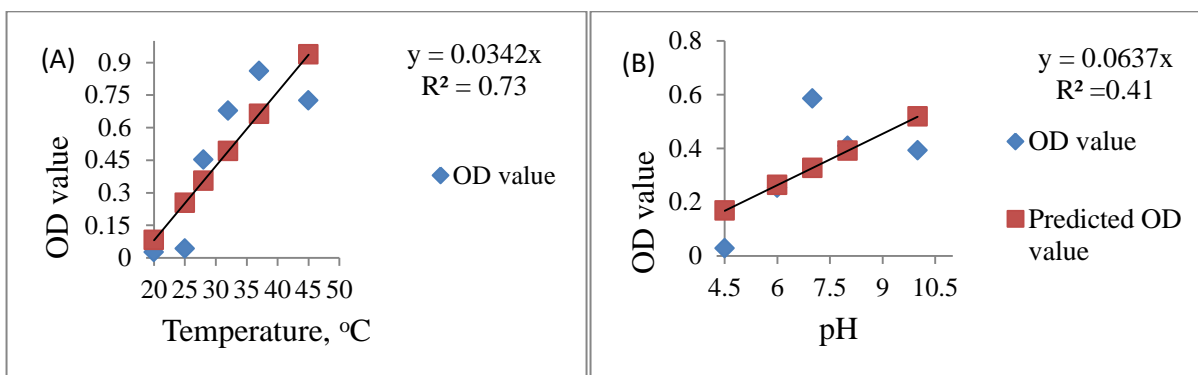


Figure 15 Regression analyses of incubation temperature and pH effects on OD₆₀₀ based measurements of *M. luteus* growth cultured in orange waste extract. Panel (A) presents the growth trend across temperature gradients, while Panel (B) depicts the growth response to varying pH levels

The linear regression analysis also highlighted the significant role of salt concentration on the growth of *M. luteus* (Figure 16), showing a strong correlation ($r = 0.85$). The result suggested that salinity plays essential role in cellular metabolism and adaptation, potentially influencing

nutrient uptake, osmotic balance, and stress response mechanisms. Whereas, culture agitation exhibited weak correlation ($r = 0.21$), signifying a minimal impact on growth dynamics.

The results demonstrated *M. luteus* does not strongly rely on pH of the culture medium and mechanical mixing for optimal proliferation, suggesting that other environmental factors such as nutrient availability or temperature play more dominant role on the isolate's growth efficiency. The regression analyses pinpointed the importance of precise variable analysis and regulation in designing microbial cultivation strategy for practical application.

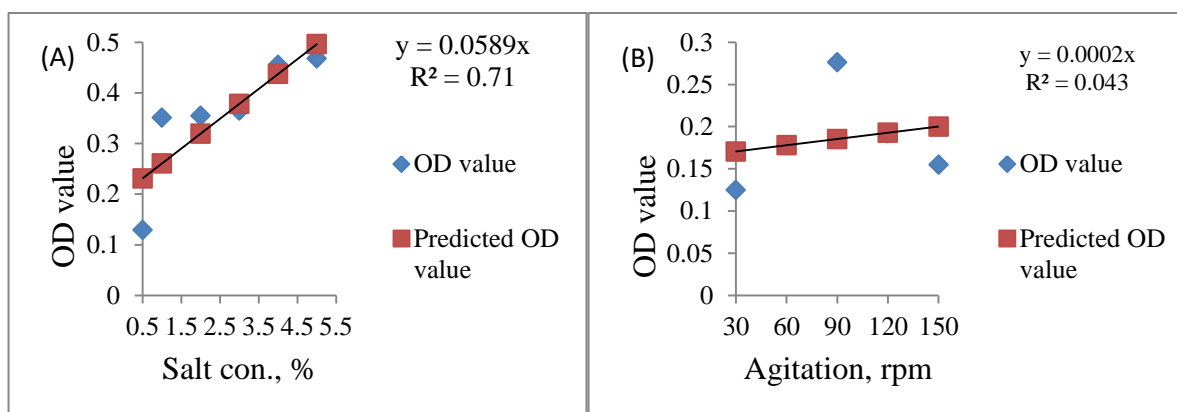


Figure 16 Regression analyses of salt concentration and agitation effects on OD_{600} based growth of *M. luteus* cultured in orange waste extract. Panel (A) presents the growth trend across different salt concentrations, and Panel (B) illustrates the growth response to varying culture agitation rates

Similarly, Table 28 presents the ANOVA analysis for *E. aurantiacum* cultured on diverse agro-waste extracts (AWEs). The results demonstrated that substrate type significantly influenced the growth of the isolate with tomato waste extract (TWE) yielding the highest mean OD_{600} value among all tested substrates. Accordingly, TWE was identified as the most effective substrate and selected as the optimal medium to support the growth of *E. aurantiacum*.

Table 28 Group-wise OD₆₀₀ measurements of *E. aurantiacum* broth culture and ANOVA summary

<i>Groups</i>	<i>Count</i>	<i>Sum</i>	<i>Average</i>	<i>Variance</i>		
Cabbage	3	1.214	0.405	3.33E-07		
Nutrient broth	3	1.57	0.523	0.003508		
Onion	3	0.641	0.214	2.33E-06		
Papaya	3	0.493	0.164	1.33E-06		
Cannon ball cabbage	3	1.304	0.435	2.33E-06		
Watermelon	3	1.295	0.432	3.33E-05		
Carrot	3	1.004	0.335	3.33E-07		
Tomato	3	1.573	0.524	4.33E-06		
Potato	3	1.385	0.462	3.33E-05		
Orange	3	1.536	0.512	4E-06		
ANOVA						
<i>Source of Variation</i>	<i>SS</i>	<i>df</i>	<i>MS</i>	<i>F</i>	<i>P-value</i>	<i>F crit</i>
Between Groups	0.4313035	9	0.047923	133.49	7.19E-16	2.392814
Within Groups	0.00718	20	0.000359			
Total	0.4384835	29				

Key: *SS*-sum of squares, *df*-degree of freedom, *MS*-mean Square, *F*-*F*-statistic, and *F crit*-*F*-critical

The ANOVA result ($F = 133.49$, $p < 0.05$) indicated at least one AWE source has considerable impact on the isolate's growth. This variability in culture biomass is likely due to differences in essential nutrient composition as reported in previous research work by (Chua et al., 2021). The pairwise comparisons (post-hoc test) revealed that most AWEs exhibited

significant differences in OD₆₀₀ values, suggesting the variability in nutrient availability across different AWEs and emphasizes the importance of screening potential substrates before large-scale application in microbial culture cultivation. However, tomato vs. orange, watermelon vs. cannon ball cabbage, watermelon vs. cabbage, watermelon vs. potato, and cannon ball cabbage vs. potato waste showed no statistically significant differences, suggesting similar impacts on bacterial growth.

The differences in the growth of the isolates under controlled culture conditions suggest that the composition of the AWEs significantly influences microbial adaptation and metabolism, highlighting the importance of substrate composition and microbial adaptability, reinforcing the idea that microorganisms respond dynamically to available resources (Pacciani-Mori et al., 2020).

Orange and tomato waste extracts contribute to pigment biosynthesis by supplying carbon substrates, micronutrients, and signaling molecules. Nevertheless, seasonal and geographic variability in their composition can compromise reproducibility of pigment yield and quality. Inhibitory compounds such as phenolics, pesticide residues, and organic acids may further suppress microbial growth, underscoring the need for analytical profiling to detect and manage these factors. To ensure stable pigment production, mitigation strategies should include waste pretreatment, microbial adaptation, and targeted nutrient supplementation, thereby enhancing process consistency and supporting industrial scalability.

Bacteria from different environments may have evolved distinct metabolic pathways to utilize nutrients in the agro-waste extract differently. Their prior environmental conditions may also shape their efficiency in breaking down complex organic materials. Variations in genetic makeup can also influence enzyme production, stress tolerance, and nutrient uptake efficiency, leading to differences in growth rates among isolates. Even under controlled conditions, microbial interactions such as competition or synergy might occur, influencing how isolates grow and consume resources. Furthermore, some bacteria may be better equipped to extract and metabolize key compounds in agro-waste extract due to prior adaptation in environments rich in similar organic materials.

4.4. Enhanced pigment yield through growth conditions optimization

A follow-up study on pigment-production enhancement evaluated via OD₆₀₀ measurements further explored the performance of one potential isolate; *E. aurantiacum* cultivated in TWE under optimized culture conditions. While *M. luteus* exhibited relatively higher pigment yield under un-optimized conditions, optimization experiment was deliberately conducted on *E. aurantiacum* with initially lower baseline yield to unlock its latent potential as this isolate also demonstrated stable growth with consistent pigmentation, thereby positioning it as a promising candidate for sustainable pigment production.

4.4.1 Evaluation of growth parameters

The optimization analysis employed PBD, a statistical tool used for screening multiple variables to identify those with the most significant impact on the culture growth. By evaluating nine variables, the influence of each factor on the growth of the isolate was determined, measured via OD₆₀₀ values (Table 29). PBD effectively distinguished influential factors from less significant ones, streamlining the optimization process.

Table 29 PBD experimental run matrix with the corresponding response, mean values of triplicate OD₆₀₀ for *E. aurantiacum* cultured in TWE

Std order	Run	Assigned variables									Average OD
		Incubation temperature, °C	pH	Incubation period, hr	Inoculum size, %	Inoculum Age, hr	Agitation, rpm	Yeast extract, %	Glucose, %	Salt, %	
10	1	23	10	24	1.0	36	60	0.1	1.5	10	0.54
6	2	23	5	72	2.5	12	180	0.1	1.5	5	1.38
9	3	37	10	72	2.5	12	60	0.1	0.5	10	0.52
4	4	23	10	72	2.5	36	60	1.0	1.5	5	0.58
12	5	23	5	24	1.0	12	60	0.1	0.5	5	0.78
3	6	37	5	72	1.0	36	180	0.1	1.5	10	1.04
8	7	37	10	24	2.5	36	180	0.1	0.5	5	0.98
7	8	37	5	72	1.0	26	60	1.0	0.5	5	0.62
11	9	37	5	24	2.5	12	60	1.0	1.5	10	0.64
2	10	23	10	72	1.0	12	180	1.0	0.5	10	0.5
1	11	37	10	24	1.0	12	180	1.0	1.5	5	0.8
5	12	23	5	24	2.5	36	180	1.0	0.5	10	0.88

The analysis of the half-normal plot (Figure 17) and Pareto chart (Figure 18) revealed that culture agitation rate, initial culture medium pH, yeast extract, salt concentration, glucose, and inoculum size exhibited significantly larger effects on the response, OD₆₀₀ value, compared to background noise. These variables were thus identified as the most influential factors affecting the growth of *E. aurantiacum*. The impacts of these variables highlighted the necessity of condition-specific optimization to maximize bacterial culture development for pigment-production.

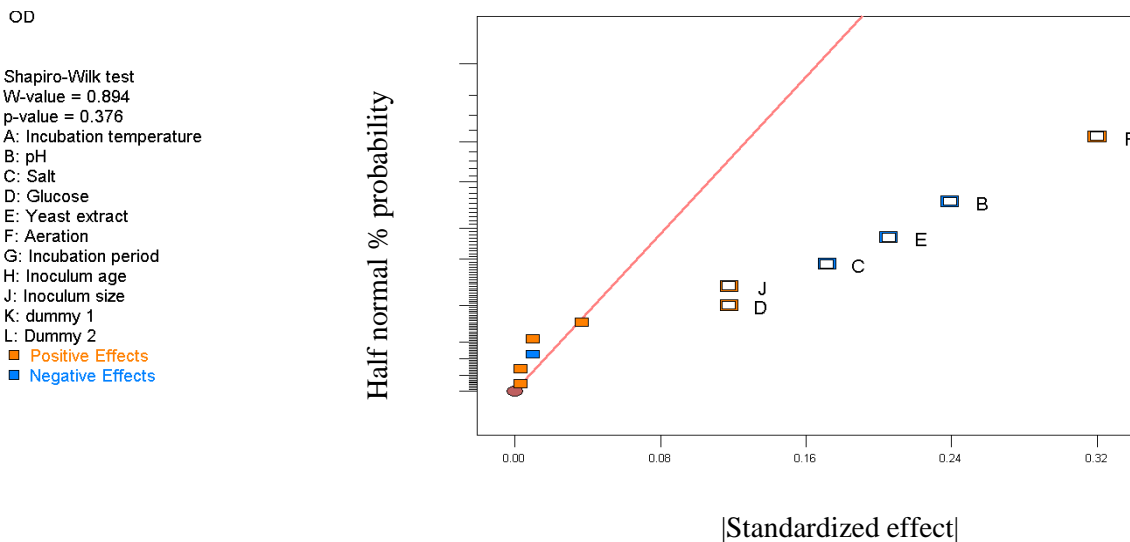


Figure 17 Half-normal plot for the standardized effects of process variables on OD₆₀₀ value highlighting critical factors for optimization. The absolute values of the estimated effects were plotted against the expected normal order statistics, gives half-normal distribution.

The half-normal plot provides a standardized visualization of process variable effects on OD₆₀₀ value where each point represents a variable, and its deviation from the straight line indicates its significance. Variables that deviate significantly from the straight line are identified as having substantial impacts on culture growth, highlighting critical factors for optimization and points that lie close the straight line are likely due to random noise. Hence, this half-normal plot helped visually separate important factors for further optimization.

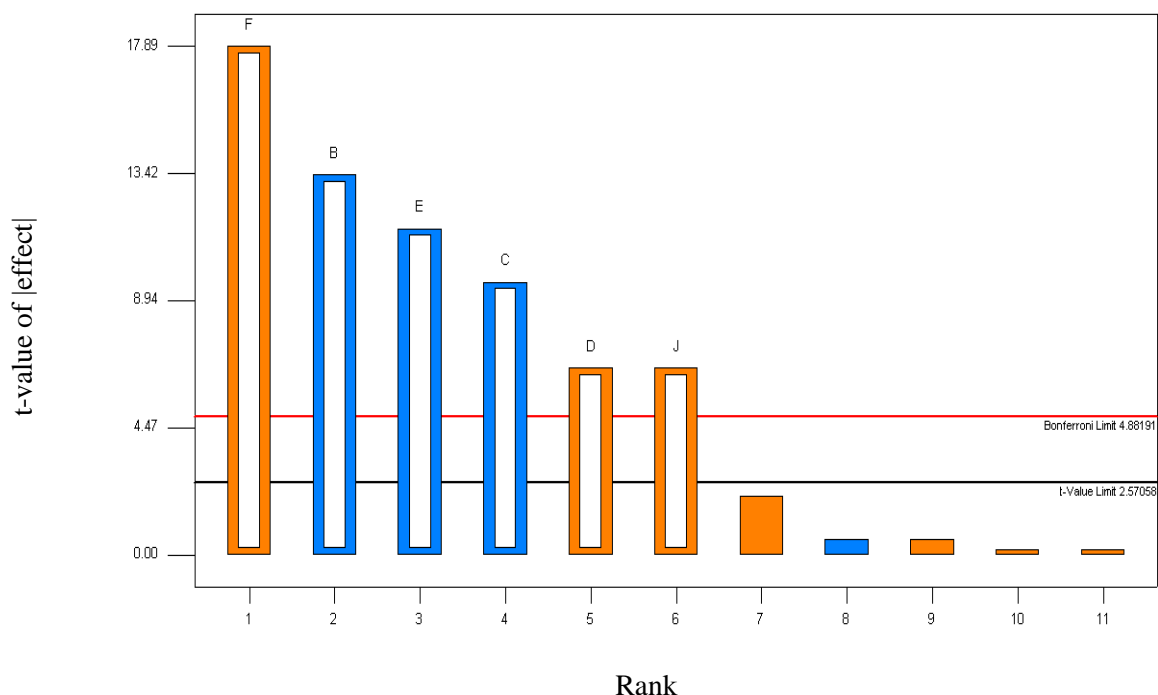


Figure 18 Pareto chart depicting the influence of process variables on OD₆₀₀ value in descending order, bars representing each variable's contribution to the overall effect

Meanwhile, the Pareto chart ranks process variables by their influence on OD₆₀₀ value in descending order with bars representing each variable's contribution to the overall effect. This graphical representation also helped prioritize key factors, enabling precise adjustments to optimize bacterial growth and pigment production. Together, these tools facilitated data driven decision-making in refining cultivation conditions.

Statistical analysis using ANOVA confirmed the model's significance with an F -value of 134.98 and a corresponding P -value of < 0.001 (Table 30). The coefficient of determination (R^2) of 0.9939 (Table 31) suggests that the selected model terms can explain nearly all variability in culture growth. Additionally, the Adjusted R^2 value of 0.9865 accounts for the number of model terms, further reinforcing model reliability. The Predicted R^2 value of 0.9647 indicated strong predictive accuracy for future observations under identical conditions with good agreement between adjusted and predicted R^2 values, confirming a well-fitting model.

Table 30 ANOVA table for selected factorial model: Statistical significance assessment

Source	SS	df	Mean square	F-value	P-value
Model	0.76	6	0.13	134.98	< 0.0001 significant
B-pH	0.17	1	0.17	178.76	< 0.0001
C-Salt	0.087	1	0.087	92.23	0.0002
D-Glucose	0.041	1	0.041	43.44	0.0012
E-Yeast extract	0.12	1	0.12	131.95	< 0.0001
F-Culture agitation	0.30	1	0.30	320.04	< 0.0001
J-Inoculum size	0.041	1	0.041	43.44	0.0012
Residual	4.700E-003	5	9.400E-004		
Cor Total	0.77	11			

Key: df - degree of freedom, SS-sum of squares

Table 31 Fit Statistics Table: Model evaluation and Goodness-of-Fit Metrics

Std. Dev.	0.031	R ²	0.9939
Mean	0.77	Adj R ²	0.9865
C.V. %	3.97	Predicted R ²	0.9647
PRESS	0.027	Adeq Precision	36.014

The first-order polynomial model equation was derived from ANOVA data using the coefficients presented in Table 30 as shown in Equation 3:

$$Y = 0.77 + 0.16X_1 - 0.12X_2 - 0.1X_3 \quad (3)$$

Where Y is the OD₆₀₀ value, X₁ is the culture agitation rate, X₂ is the initial culture pH and X₃ is the concentration of yeast extract. This equation served as a predictive tool for estimating culture biomass, expressed in terms of OD₆₀₀ value based on significant process variables. The generated model provided mathematical framework for optimizing bacterial growth conditions and enhancing pigment production efficiency.

The selection of variables for further optimization was guided by their statistical significance as determined by the *F* statistic and *p*-value from the ANOVA test (Table 32). Variables with the strongest impact on the growth of the isolate and pigment production were prioritized for refinement (Table 33), ensuring that the optimization process focuses on the most influential factors.

Table 32 Regression coefficients expressed in terms of factors

Factor	Coefficient Estimate	df	Standard Error	95% CI, low	95% CI, high	VIF
Intercept	0.77	1	8.851E-003	0.75	0.79	1.00
B-pH	- 0.12	1	8.851E-003	- 0.14	- 0.096	1.00
C-Salt	- 0.085	1	8.851E-003	- 0.11	- 0.062	1.00
D-Glucose	0.058	1	8.851E-003	0.036	0.081	1.00
E-Yeast extraction	- 0.10	1	8.851E-003	- 0.12	- 0.079	1.00
F-Culture agitation	0.16	1	8.851E-003	0.14	0.18	1.00
J-Inoculum size	0.058	1	8.851E-003	0.036	0.081	1.00

Key: CI - Confidence interval, df-degree of freedom, and VIF - Variance Inflation Factor

4.4.2 Optimization of selected growth parameters

The face-centered central composite design (FCCCD) experiment investigated how agitation speed (rpm), pH of the culture medium, and yeast extract concentration influenced bacterial growth and pigment production. The response variables, OD₆₀₀ value (Y₁), culture biomass (Y₂), and pigment yield (Y₃) were measured at the stationary growth phase.

Each experimental run in Table 33 represents the mean response values for OD₆₀₀, biomass and pigment yield under different combinations of significant factors, allowing the interaction effects of these factors to be assessed, influencing the OD value as a measure of bacterial growth. OD₆₀₀ values (Y₁) were used to measure bacterial growth, reflecting cell density under different experimental conditions. Cell biomass was collected at the stationary growth phase where maximum cell density is reached to extract the pigment.

Table 33 Face-Centered Central Composite Design (FCCCD): Experimental matrix and response values

Std	Run	Factors			Responses		
		Agitation (rpm)	pH	Yeast extract (%)	Mean OD ₆₀₀ value (Y ₁)	Mean culture biomass (g/L) (Y ₂)	Mean pigment yield (g/L) (Y ₃)
11	1	60	7.5	0.55	0.65	3.6	0.82
13	2	120	7.5	0.1	0.8	4.7	0.84
2	3	60	10	0.1	0.71	4.1	0.85
9	4	120	5	0.55	0.78	4.3	0.8
12	5	180	7.5	0.55	0.6	3.4	0.76
7	6	180	5	1	0.58	3.68	0.74
16	7	120	7.5	0.55	0.74	4.12	0.8
5	8	60	5	1	0.77	4.12	0.74
8	9	180	10	1	0.89	4.2	0.88
1	10	60	5	0.1	0.88	4.62	1.06
19	11	120	7.5	0.55	0.74	4.12	0.8
4	12	180	10	0.1	0.83	4.0	0.73
18	13	120	7.5	0.55	0.74	4.2	0.8
14	14	120	7.5	1	0.78	4.5	0.76
3	15	180	5	0.1	0.71	3.82	0.72
17	16	120	7.5	0.55	0.74	4.2	0.82
20	17	120	7.5	0.55	0.72	4.1	0.78
6	18	60	10	1	0.78	3.92	0.65
10	19	120	10	0.55	0.84	4.2	0.78
15	20	120	7.5	0.55	0.72	4.12	0.8

The results indicated that moderate agitation (120 rpm), a balanced pH (around 7.5), and optimized yeast extract concentration contributed to improved bacterial density and pigment synthesis. The highest pigment yield of 1.06 g/L was recovered at 60 rpm, pH 5, and 0.1% yeast extract, suggesting nutrient availability and environmental conditions strongly influence microbial performance.

Table 34 summarizes the ANOVA result for OD₆₀₀ value, culture biomass, and pigment yield emphasizing the impact of key independent factors: pH (X₁), agitation speed (X₂), and yeast extract concentration (X₃). These variables were found significantly influenced bacterial growth and pigment production, guiding optimization strategies to enhance overall efficiency.

Table 34 ANOVA Results for Responses: Statistical Significance and Model Evaluation

Factor	Mean OD ₆₀₀ value (Y ₁)	Mean culture biomass (g/L) (Y ₂)	Mean pigment yield (g/L) (Y ₃)
Intercept	0.7318	4.14	0.7965
X ₁ -pH	0.0330	-0.0120	-0.0170
X ₂ -Agitation	-0.0180	-0.1260	-0.0290
X ₃ -Yeast extract	-0.0130	-0.0820	-0.0430
X ₁ X ₂	0.0738	0.1775	0.0562
X ₁ X ₃	0.0463	0.0825	0.0312
X ₂ X ₃	-0.0037	0.0925	0.0862
X ₁ ²	0.0805	0.1045	
X ₂ ²	-0.1045	-0.6455	
X ₃ ²	0.0605	0.4545	
Model F-value	179.14	130.58	216.10
Model P-value	< 0.0001	< 0.0001	< 0.0001
Lack of Fit P-value	0.8145	0.6927	0.9185
R ²	0.9938	0.9916	0.9901
Adjusted R ²	0.9883	0.9840	0.9855
Predicted R ²	0.9799	0.9678	0.9841

The polynomial equation coefficients derived from the ANOVA (Table 34) were used to predict response variables, including OD₆₀₀ value (Y₁), culture biomass (Y₂), and pigment yield (Y₃). The regression equations below (Equations 4-6) represent the mathematical relationships between the independent factors and the predicted outcomes, allowing for precise modeling of the growth of the isolate and pigment production under optimized conditions.

$$Y_1 = 0.7318 + 0.033X_1 - 0.018X_2 - 0.013X_3 + 0.0738X_1X_2 + 0.0463X_1X_3 - 0.0037X_2X_3 + 0.0805X_1^2 - 0.1045X_2^2 + 0.0605X_3^2 \quad (4)$$

$$Y_2 = 4.14 - 0.012X_1 - 0.126X_2 - 0.082X_3 + 0.1775X_1X_2 + 0.0825X_1X_3 + 0.0925X_2X_3 + 0.1045X_1^2 - 0.6455X_2^2 + 0.4545X_3^2 \quad (5)$$

$$Y_3 = 0.7965 - 0.017X_1 - 0.029X_2 - 0.043X_3 + 0.0562X_1X_2 + 0.0312X_1X_3 \quad (6)$$

The Intercept Values for OD₆₀₀, culture biomass, and pigment yield were 0.7318, 4.14, and 0.7965, respectively; representing the models' predicted baseline values of response variables when all predictor variables are zero (Table 34). Analysis of main effects showed pH (X₁) has

a positive effect on OD₆₀₀ but showed negative effect on biomass and pigment yield. Whereas, Agitation (X₂) and yeast extract (X₃) showed negative impact across all responses, suggesting higher agitation may reduce biomass and pigment-production and excessive yeast extract concentration also may limit growth and pigment yield (Table 34).

combined effects revealed that X₁X₂ (pH × agitation), and X₁X₃ (pH × yeast extract) exhibited positive interaction effects, suggesting that these factor combinations contribute to improved bacterial growth and pigment synthesis as well (Table 34). On the other hand, quadratic effects, pH (X₁²) and yeast extract (X₃²) positively influenced responses, suggesting an optimal level improves OD₆₀₀ and therefore, improves biomass production. On the contrary, Agitation (X₂²) showed a strong negative effect, particularly on biomass (-0.6455; Table 34), predicting excessive agitation negatively impacts bacterial density.

Model Significance analysis indicated strong statistical significance, showing that the model reliably predicts responses. *P*-values (< 0.001) confirmed high significance of the model, and R² values (~0.99) indicated that the model explains nearly all variability in the data and adjusted R² and predicted R² values confirmed a strong correlation between experimental data and model predictions. The lack of fit *p*-values were also not significant (*p*>0.05) relative to the pure error, suggesting that the models were statistically accurate.

The results highlighted the influence of pH, agitation speed, and yeast extract concentration on bacterial growth and pigment yield. Moderate agitation, balanced pH, and optimized yeast extract levels improved microbial performance. Additionally, interaction effects between factors had vital role in maximizing yield, offering valuable insights for industrial applications.

4.5. Analysis of the effects of significant predictors on outcome variables

In this section how the most influential growth parameters identified during screening and optimization affected key outcome variables; OD₆₀₀ value, biomass yield and pigment production using ANOVA, regression analysis, and interaction plots to quantify the impact of

each variable. Model predictions were validated with laboratory level experimental work to ensure reliability.

4.5.1 Effect on OD value

The OD₆₀₀ value measurements revealed that the *E. aurantiacum* cell concentration cultured in the nutritious agro-waste medium, tomato waste extract (TWE) was significantly affected by initial pH of culture medium, displaying linear, quadratic, and interaction effects with both culture agitation rate and concentration of yeast extract ($p < 0.001$) (Table 35). However, interaction effects between culture agitation rate and yeast extract did not show a statistically significant effect ($p > 0.05$) on OD value of the culture medium, highlighting that the effect of agitation rate did not depend on the amount of the concentration of yeast extract or vice versa. On the other hand, the quadratic term of each variable shows the curvilinear effect of the variable non-linearly on OD value of the culture medium. These findings underscored the importance of optimizing agitation rate and medium pH to enhance bacterial growth while highlighting that the combined effect of culture agitation and yeast extract may not have critical influence on the growth of cell biomass.

Table 35 ANOVA results for quadratic model: Evaluating OD₆₀₀ response

Source	Sum of Squares	df	Mean Square	F-value	p-value	
Model	0.1226	9	0.0136	179.14	< 0.0001	significant
X ₁ -pH	0.0109	1	0.0109	143.16	< 0.0001	
X ₂ -Agitation	0.0032	1	0.0032	42.59	< 0.0001	
X ₃ -Yeast extract	0.0017	1	0.0017	22.22	0.0008	
X ₁ X ₂	0.0435	1	0.0435	572.02	< 0.0001	
X ₁ X ₃	0.0171	1	0.0171	224.96	< 0.0001	
X ₂ X ₃	0.0001	1	0.0001	1.48	0.2519	
X ₁ ²	0.0178	1	0.0178	234.01	< 0.0001	
X ₂ ²	0.0301	1	0.0301	395.13	< 0.0001	
X ₃ ²	0.0101	1	0.0101	132.13	< 0.0001	
Residual	0.0008	10	0.0001			
Lack of Fit	0.0002	5	0.0000	0.4263	0.8145	not significant
Pure Error	0.0005	5	0.0001			
Corrected Total	0.1234	19				

df- degree of freedom

Culture agitation rate play vital role in enhancing oxygen transfer, ensuring uniform nutrient distribution (McDonough, 1997). Another critical factor influencing culture growth was pH which exerted significant linear, quadratic, and interaction effects with both agitation and yeast extract concentration ($p < 0.001$; Table 35). Maintaining optimal pH levels is essential for promoting enzymatic activity, maximizing bacterial growth, and enhancing fermentation efficiency (Musa & Yusof, 2019). These findings highlighted the importance of carefully adjusting culture agitation speed and pH conditions to achieve optimal bacterial development and pigment-production.

The response surface graph (Figure 19) demonstrates the interaction effects among culture agitation rate, yeast extract concentration, and initial culture pH on bacterial growth. This graphical representation helps identify optimal conditions by highlighting how variations in these factors impact biomass development. The response surfaces provide insights into the best combinations to maximize bacterial growth and pigment production.

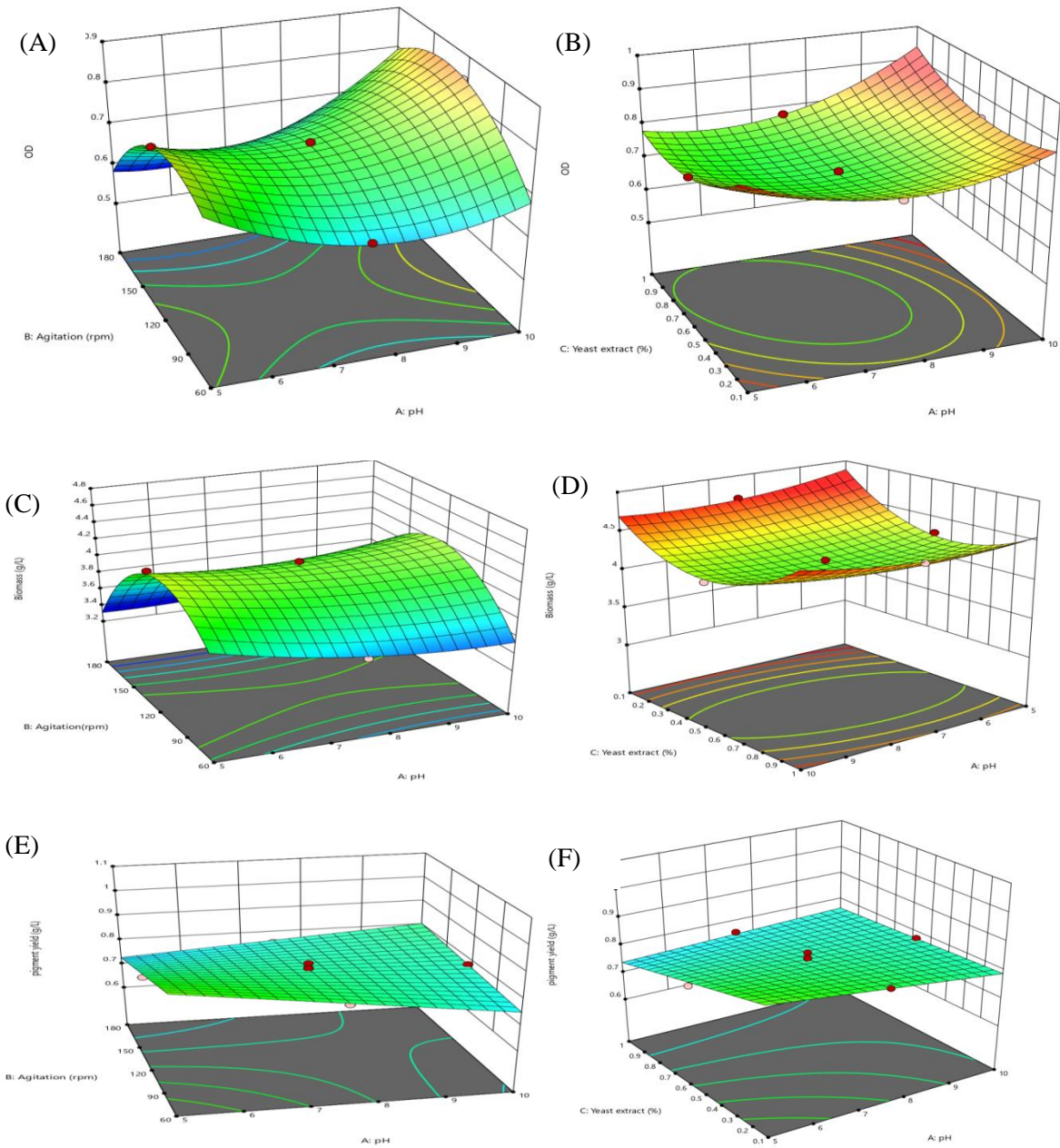


Figure 19 Response surface optimization graphs generated by Design Expert Statistical software, version 13. Panels (A)-(F) depicting how changes in independent variables affect output variables. Panel (A) shows the relationship between agitation speed (rpm) and pH on OD value. Panel (B) illustrates effects of yeast extract concentration and initial medium pH on OD value. Panels (C) and (D) elucidate the combined effects of agitation versus pH and yeast extract versus pH on culture biomass yield, and Panels (E) and (F) demonstrates how pigment yield was influenced by agitation rate, pH, and yeast extract concentration

These graphs illustrate how culture agitation rate, yeast extract concentration, and pH interact influence these output variables. By adjusting two independent factors within experimental ranges while holding the third constant at the center point the response patterns became clearer. Figure 19, panel (A) highlights the relationship between agitation speed (rpm) and pH on OD value, revealing an optimal OD value of 0.85 at an agitation rate of around 140 rpm and a pH of 10. This result is in harmony with previous reports that *E. aurantiacum* thrives within pH range of 5-11 (White et al., 2019). Furthermore, the optimal agitation rate identified was in consistent with the recommended culture agitation rate range (130-150 rpm) for bacterial cultures.

The response surface graph, Figure 19, panel (B) illustrates the linear, quadratic, and interaction effects of yeast extract concentration and initial medium pH on OD value. The convex curvature suggests OD is lowest at moderate yeast extract and pH levels. The highest OD values were recorded at both highest yeast extract and pH levels, highlighting more nutrients and favorable pH promotes growth. Likewise, highest OD values were again recorded at low nutrient levels and pH values which could be possibly due to stress induced adaptation or nonlinear effects, suggesting that there is no one optimal zone, hence multiple combinations can yield high OD value, might be helpful in reducing yeast extract costs if extreme pH conditions support good culture growth.

4.5.2 Effect on cell biomass

Culture agitation demonstrated a significant impact on bacterial growth at linear, quadratic, and interaction levels with both pH and yeast extract concentration (Table 36). Other key contributors to the growth of culture biomass included the linear and quadratic terms of yeast extract ($p < 0.001$), the quadratic term of medium pH ($p < 0.001$), and the interaction between concentration of yeast extract and medium pH ($p < 0.002$). However, the linear effect of initial medium pH was not statistically significant ($p > 0.05$). Bacterial growth rate and final biomass influence pigment production. Hence, optimizing these factors can enhance overall yield. Studies suggest that fine-tuning agitation, pH, and nutrient concentrations can substantially improve biomass accumulation, ultimately leading to efficient pigment production (Poddar et al., 2021; Shahin et al., 2022).

Table 36 ANOVA results for quadratic model: Statistical evaluation of biomass response

Source	Sum of Squares	df	Mean Square	F-value	p-value	
Model	1.89	9	0.2103	130.58	< 0.0001	significant
X ₁ -pH	0.0014	1	0.0014	0.8940	0.3667	
X ₂ -Agitation	0.1588	1	0.1588	98.56	< 0.0001	
X ₃ -Yeast extract	0.0672	1	0.0672	41.74	< 0.0001	
X ₁ X ₂	0.2520	1	0.2520	156.47	< 0.0001	
X ₁ X ₃	0.0545	1	0.0545	33.80	0.0002	
X ₂ X ₃	0.0684	1	0.0684	42.49	< 0.0001	
X ₁ ²	0.0301	1	0.0301	18.66	0.0015	
X ₂ ²	1.15	1	1.15	711.24	< 0.0001	
X ₃ ²	0.5682	1	0.5682	352.73	< 0.0001	
Residual	0.0161	10	0.0016			
Lack of Fit	0.0062	5	0.0012	0.6216	0.6927	not significant
Pure Error	0.0099	5	0.0020			
Corrected Total	1.91	19				

df - degree of freedom

Ensuring an optimal balance of nutrient availability, pH stability, and proper agitation rates are fundamental for maximizing bacterial biomass production (Agudelo-Escobar et al., 2017). Since microbial growth is highly sensitive to nutrient composition and environmental conditions, adjusting these parameters can significantly enhance biomass yield and pigment production efficiency (Musa & Yusof, 2019). Optimizing bacterial cultivation involves tailoring significant factors to species specific requirements so as to create an environment that promotes rapid growth while supporting metabolic activity crucial for pigment biosynthesis.

The response surface optimization graph (Figure 19, panels C and D) illustrated the combined effects of agitation versus pH and yeast extract versus pH on culture biomass yield. The graph indicated that biomass production increased with rising pH levels, while both excessively high and low agitation rates resulted in reduced biomass yield (Figure 19, panel C). Moreover, the concave response surface plot indicates a maximum point on the surface, implying that the center combination of the independent variables (agitation versus pH) yields the highest cell mass having synergistic interaction. However, the convex surface of the graph, Figure 19, panel D suggests that culture growth decreases toward the center of the surface which indicates the interaction of yeast extract and medium pH at the center yields lowest cell

biomass. Overall, both shapes of the response surface plots reveal interaction effects of the independent variables and help identify optimal conditions for maximum culture growth.

Excessive agitation can induce shear stress, potentially damage cells and lower biomass output (Agudelo-Escobar et al., 2017). Conversely, insufficient agitation also reduces oxygen transfer rates, creates nutrient gradients, and promotes cellular clumping, slowing metabolic activity and ultimately decreasing biomass production (Agudelo-Escobar et al., 2017; Maiorano et al., 2020; Peerhossaini, 2022). These insights emphasize the need for precise regulation of agitation speed and pH to optimize bacterial growth and pigment synthesis efficiency.

Lower nitrogen source concentrations help prevent nitrogen toxicity which can hinder microbial growth, thereby fostering a balanced environment that enables efficient nutrient utilization for biomass production (Vishnivetskaya et al., 2009). The adaptability of *E. aurantiacum* to a broad pH spectrum (5-11) allows the bacterium to sustain metabolic activity and growth under varying conditions, enhancing its biomass yield (Ontman et al., 2023). These findings reinforce the importance of optimizing nutrient composition and pH conditions to maximize bacterial productivity.

4.5.3 Effect on pigment yield

Table 37 reveals that pigment yield was significantly affected by initial culture pH, agitation rate, and yeast extract concentration at both linear and two-factor interaction (2FI) levels ($p < 0.001$). These results underscored the importance of fine-tuning these variables to maximize pigment-production efficiency.

Table 37 ANOVA results for 2FI Model: Statistical evaluation of pigment yield response

Source	Sum of Squares	df	Mean Square	F-value	p-value	
Model	0.1224	6	0.0204	216.10	< 0.0001	significant
X ₁ -pH	0.0029	1	0.0029	30.61	< 0.0001	
X ₂ -Agitation	0.0084	1	0.0084	89.07	< 0.0001	
X ₃ -Yeast extract	0.0185	1	0.0185	195.82	< 0.0001	
X ₁ X ₂	0.0253	1	0.0253	268.08	< 0.0001	
X ₁ X ₃	0.0078	1	0.0078	82.74	< 0.0001	
X ₂ X ₃	0.0595	1	0.0595	630.27	< 0.0001	
Residual	0.0012	13	0.0001			
Lack of Fit	0.0004	8	0.0001	0.3340	0.9185	not significant
Pure Error	0.0008	5	0.0002			
Corrected Total	0.1237	19				

df- degree of freedom

The response surface optimization graph (Figure 19, panels E and F) demonstrated that there is direct effect of each independent variable on the pigment yield. A significant linear term ($p < 0.001$) indicates as the respective independent variable increases, the pigment yield increases consistently. The 2FI also suggests the effect of one variable depends on the level of the other. But the visual flatness of the response surface plot may indicate that the interaction effect is very minimal.

At lower agitation and yeast extract levels, slight pigment-production increment has been seen noticed as pH decreases. This trend may be linked to a stress-induced metabolic response, where reduced pH and nutrient availability trigger enhanced secondary metabolite synthesis, improving pigment yield. Additionally lower agitation minimizes shear stress on bacterial cells, creating a more stable environment conducive to pigment biosynthesis (Fatima & Anuradha, 2022; Pitt et al., 2007).

4.6 Yield and efficiency of pigment recovery

The extraction process was carried out at the stationary growth phase, a critical point where maximum pigment accumulation typically occurs. Among different organic solvents used for pigment extraction, methanol (99.5%) offered the highest pigment yield, proving to be the most efficient solvent for pigment extraction from all the three isolates compared to other utilized organic solvents. Most studies used similar solvent systems like methanol and acetone and also recent studies employ solvent mixtures for better extraction, suggesting this organic

solvent extraction method is efficient as it is simpler and more effective than multi-step chromatographic extraction methods (Ramos et al., 2021).

The ANOVA test confirmed significant differences in OD₆₀₀ values ($F = 81204.88$, $p < 0.001$) and pigment yields ($F=122067$, $p < 0.001$) among the utilized organic solvents (Table 38 and 39). These extremely low p -values (< 0.05) indicate that at least two solvents differ significantly in their extraction efficiency.

Table 38 ANOVA summary table illustrating measured average OD values using different organic solvents for pigment extraction from *M. luteus*

Groups	Count	Sum	Average	Variance		
Methanol	3	2.586	0.862	0.000001		
Ethanol	3	1.958	0.652	4.33E-06		
Acetone	3	0.492	0.164	0.000001		
Chloroform	3	1.598	0.532	6.33E-06		
ANOVA						
Source of Variation	SS	df	MS	F	P-value	F crit
Between Groups	0.771446333	3	0.257149	81204.88	2.86E-18	4.066181
Within Groups	2.53333E-05	8	3.17E-06			
Total	0.771471667	11				

Key: *SS*-sum of squares, *df*-degree of freedom, *MS*-mean Square, *F*-*F*-statistic, and *F crit*-*F*-critical

Table 39 ANOVA summary table depicting average pigment yield recovered from *M. luteus* using different organic solvents

Groups	Count	Sum	Average	Variance		
Methanol	3	4.397	1.466	1.33E-06		
Ethanol	3	1.03	0.343	3.33E-05		
Acetone	3	0.333	0.111	0.000001		
Chloroform	3	0.943	0.314	1.33E-06		
ANOVA						
Source of Variation	SS	df	MS	F	P-value	F crit
Between Groups	3.387364917	3	1.129122	122067.2	5.6E-19	4.066181
Within Groups	7.4E-05	8	9.25E-06			
Total	3.387438917	11				

Key: *SS*-sum of squares, *df*-degree of freedom, *MS*-mean Square, *F*-*F*-statistic, and *F crit*-*F*-critical

The results confirmed that methanol is the optimal solvent for pigment extraction, yielding high pigment recovery under controlled culture conditions. Figure 20, panels (A) to (F) illustrates the schematic overview of cultivating *M. luteus* in different AWEs as growth substrate and pigment extraction. The extracted pigment was subsequently dried in a biosafety cabinet to maintain purity and collected in granule form.

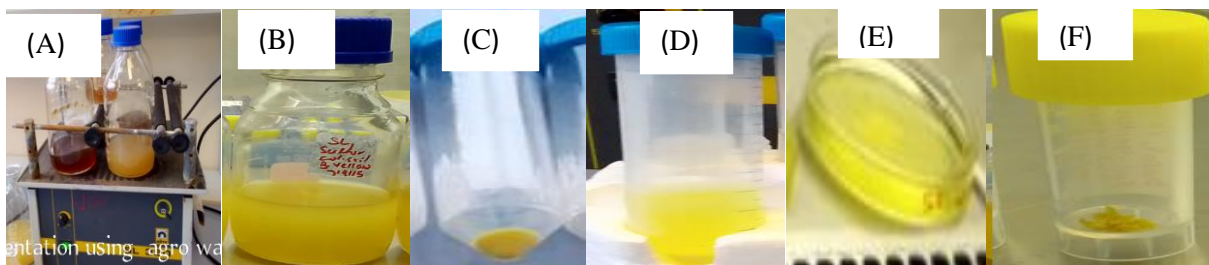


Figure 20 Cultivation and pigment extraction processes from *M. luteus*. (A) cultivation of an isolate in different AWEs at optimized culture conditions, (B) fermented culture in orange waste extract, (C) pigment pellet after centrifugation, (D) methanolic pigment extract, (E) concentration process in biosafety cabinet for solvent evaporation, and (F) solidified pigment

The downstream processing of microbial pigments represent critical determinant of economic feasibility and industrial scalability. In this study, pigment extraction from *M. luteus* cultivated on orange-waste extract achieved yield of 1.47 g/L, extracted using organic solvents. While this yield is promising compared to Hegazy et al. (2024), who recovered pigment yield of 2.19 g/L from the same isolate using synthetic media, the reliance on solvent extraction introduces significant cost and sustainability considerations. Organic solvents are effective for recovering carotenoid-like compounds but contribute to high operational expenses, solvent recovery requirements, and environmental burdens (Lu et al., 2023). Industrial translation therefore, necessitates the development of greener, cost-efficient alternatives such as supercritical CO₂ extraction.

Commercial synthetic dyes benefit from decades of process optimization, low raw material costs from petrochemical feed stocks, and highly efficient downstream processing. Production costs for synthetic dyes are typically lower, but they generate toxic effluents and face increasing regulatory restrictions. In contrast, microbial pigments offer biodegradability and sustainability nevertheless downstream costs remain high relative to yield. Microbial pigment yields often range between 0.5-1.0 g/L under laboratory conditions with higher yields achieved only under optimized fermentation conditions (Mohd Said, 2025). The yield of 1.47 g/L from *M. luteus* on orange-waste extract is therefore, competitive, particularly given the use of low-cost agro-waste substrates. However, scalability requires consistent yields at pilot and

industrial scales where downstream recovery efficiency and pigment stability under processing conditions become critical.

From a scalability perspective, the integration of agro-waste valorization into pigment production offers dual advantage; reduced substrate costs and alignment with circular bio-economy principles. However, downstream processing remains the bottleneck. Solvent extraction at industrial scale requires large volumes of solvent, energy-intensive recovery systems, and strict safety protocols, all of which inflate costs. To achieve industrial translation, process optimization strategies such as coupling fermentation with in situ extraction, or employing continuous solvent recovery must be adopted. Furthermore, benchmarking against synthetic dyes highlight those microbial pigments will initially occupy top markets in industries such as textiles, cosmetics, and food additives where sustainability credentials justify higher costs (Anshi et al., 2024).

The pre-optimization cultivation experiment of *E. aurantiacum* in TWE yielded an average of 0.65 g/L of crude pigment from culture biomass of 4.20 g/L with an OD₆₀₀ value of 0.60 at the stationary growth phase. For validation, forty-six different solutions were generated by the software, ranked according to their desirability values, which quantify how well each solution meets optimization criteria.

The highest-ranked solution with a desirability of 98.8% (Table 40) was chosen to test the predictive model. The selected optimal conditions were a pH of 5, an agitation rate of 65 rpm, and yeast extract concentration of 0.1%. These parameters offer a refined approach for maximizing pigment yield and bacterial growth.

Table 40 Software generated solutions for verification experiment

Number	pH	Aeration	Yeast extract	OD	Biomass	pigment yield	Desirability	
1	5.000	64.969	0.100	0.892	4.700	1.045	0.988	Selected
2	5.000	65.835	0.100	0.893	4.711	1.043	0.986	
3	5.027	65.474	0.100	0.890	4.702	1.043	0.986	
4	5.000	65.609	0.103	0.892	4.700	1.042	0.985	
5	5.000	62.375	0.100	0.887	4.665	1.052	0.982	

OD-optical density

To ensure the reliability and reproducibility of the predictive model, culture cultivation was conducted in triplicate under optimized conditions in 150 mL of TWE. During the experiment, culture growth dynamics was closely monitored by measuring OD₆₀₀ (Figure 21). These measurements provided valuable insights into growth trends, confirming whether the selected parameters effectively enhanced bacterial biomass and pigment production.

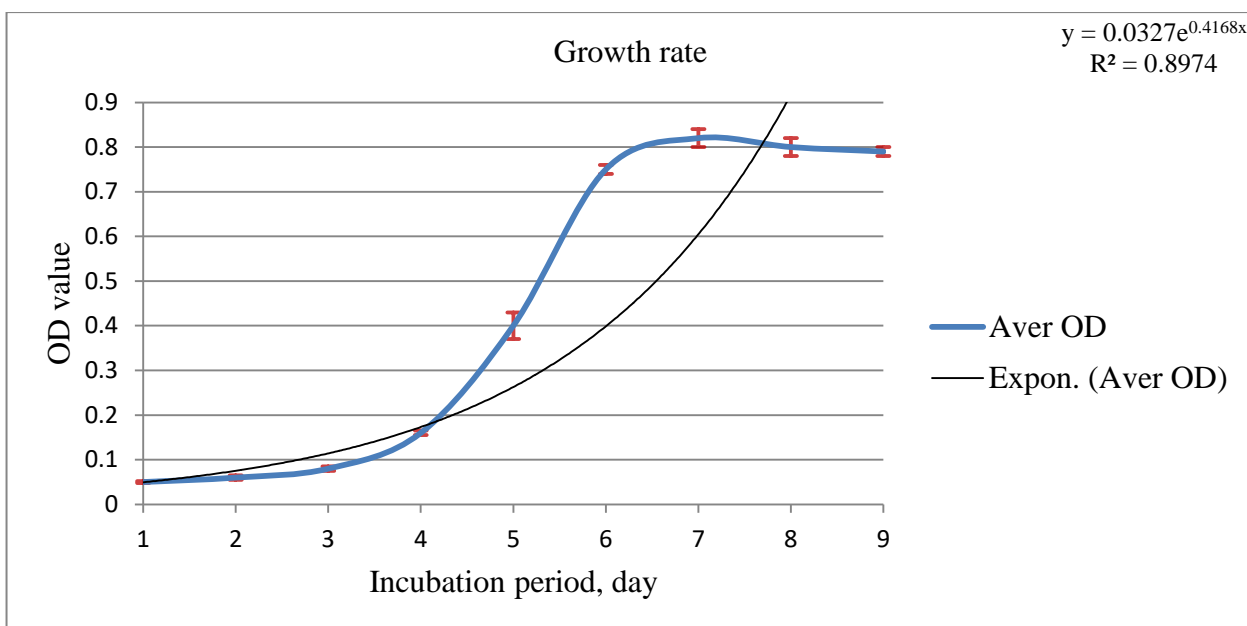


Figure 21 Smooth line graph showing OD₆₀₀ variation over time of *E. aurantiacum* at optimized process conditions using TWE as cultivation substrate with standard deviation represented as error bars around the line

The growth kinetics of *E. aurantiacum* under optimized conditions using TWE as the cultivation substrate demonstrated its effectiveness in promoting bacterial growth. The growth curve (OD₆₀₀ measurements over time) captured distinct bacterial phases, confirming TWE as sustainable medium. Optimal growth was observed on the 7th day when the culture reached the stationary phase, possibly due to environmental stress according to (Kato et al., 2018).

Biomass was harvested via centrifugation on the 8th day to recover the pigment, yielded 4.73 g/L of biomass and 0.96 g/L of crude pigment (Table 41). The experimental verification showed minor error, 0.63% in biomass concentration prediction likely due to slight model

noise and challenges in maintaining precise conditions. Overall, the validation confirmed strong alignment between the predicted and actual results, reinforcing the model's reliability.

Table 41 Predicted versus experimental response values from cultivating *E. aurantiacum* in TWE as substrate under optimized conditions

Optimum condition	Coded levels		Actual levels	
Culture agitation (rpm)	- 0.92		65	
Initial culture pH	-1.00		5.0	
Yeast extract (%)	-1.00		0.1	
Response	Un-optimized value	Predicted value	Optimized value	Optimization efficiency (%)
OD value	0.60	0.892	0.877 ± 0.025	31.6
Cell biomass (g/L)	4.20	4.700	4.733 ± 0.076	11.3
Pigment yield (g/L)	0.65	1.045	0.957 ± 0.060	32.1

The pigment yield from this study (0.96 g/L) surpasses the 180 µg per gram of biomass reported for *Chryseobacterium* sp. cultivated in feather meal (Gemelli et al., (2024). However, it remains lower than the yield achieved from *M. luteus* grown in orange waste extract as substrate, may due to differences in substrate nutrient composition (Ramesh et al., 2022).

When compared with pigments recovered from the two isolates examined in this study, as well as those reported in previous studies cultured on agro-industrial waste extracts, the dry weight of pigment obtained from *M. luteus* was significantly promising (Table 42). This enhanced yield may be attributed to the isolate's strong tolerance to oxidative and nutritional stress, coupled with its efficient substrate utilization capacity.

The isolate's pigment yield exceeds that of extracted from psychrotolerant *Paenibacillus* species using solvent extraction by a factor of 22 (Padhan et al., 2021). However, it remained lower than yields achieved in studies utilizing fruit waste substrates, such as pineapple, orange, and pomegranate from *Bacillus safensis* in shake flask fermentation, reported 6.96 g/L by (Rifna et al., 2023). While, *Kocuria* sp. showed lower yield, but still higher than the pigment yield of 0.0016 g/L recovered from *Kocuria sediminis*, reported by (López-Mora et al., 2025).

Table 42 Comparison of some recent studies on eco-friendly pigments derived from different microbial sources, highlighting the types of pigments produced and the substrates used to enhance pigment yield

Microorganism	Substrate	Pigment recovered	Yield	Reference
<i>Sporidiobolus pararoseus</i>	Glycerol, Corn steep liquor, parboiled rice water	Carotenoids(β -carotene)	0.000843 g/L total (0.000346 g /L β -carotene)	(Barreto et al., 2023)
<i>Serratia plymuthica</i>	Synthetic media	Prodigiosin	1.77 g/L	
<i>Rhodotorula mucilaginosa</i>	Food industry wastewater	Carotenoid	0.81 g/L	(Lau, W. X. et al., 2018)
<i>Pseudomonas</i> sp.	Vegetable waste	Melanin	0.00279 g/L	(Anshi et al., 2024)
<i>Bacillus safensis</i>	Agro-wastes		6.96 g/L	(Rifna et al., 2023)
<i>Rhodotorula rubra</i>	Sugarcane juice	Carotenoids	30.39 g/L	(Bonadio et al., 2018)
<i>Monascus purpureus</i>	Orange waste peels		0.58 Units/mL	(Kantifedaki et al., 2018)
<i>Paenibacillus</i> species			0.068 g/L	(Padhan et al., 2021)
<i>M. luteus</i>	Orange waste extract	Carotenoid	1.47 g/L	This study
<i>E. aurantiacum</i>	Tomato waste extract	Carotenoid	0.96 g/L	This study
<i>Kocuria</i> sp.	Tomato waste extract	Carotenoid	0.56 g/L	This study

These findings emphasize the critical role of substrate selection, isolate specificity, and environmental factors in maximizing pigment production efficiency, reinforcing the potential of AWEs as an effective low-cost substrate for microbial pigment-production potential from bacteria as eco-friendly alternatives to synthetic dyes, offering an alternative to synthetic dyes (Silva-Castro et al., 2019). Further optimization of cultivation conditions and extraction

techniques could enhance their commercial viability, making them a practical alternative to chemically synthesized dyes.

4.7 Characterization of extracted bio-pigments

M. luteus, *E. aurantiacum*, and *Kocuria* sp. produced yellowish pigments when cultured on different agro-waste extracts, exhibiting only minor variations in colony coloration (Figure 22). The similar yellow pigments likely arise from shared genetic pathways for carotenoid, flavin or other yellow pigments biosynthesis regardless of their origin combined with environmental stress signals provided by agro-waste substrates as they often contain sugars, amino acids, and minerals that can serve as precursors for pigment biosynthesis.

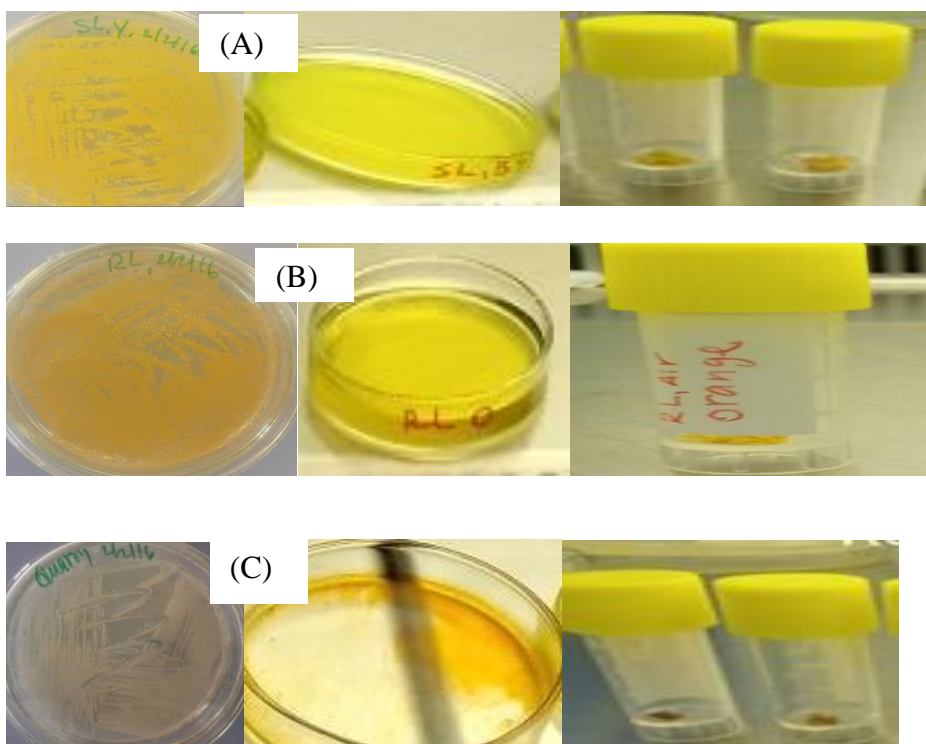


Figure 22 Pure cultures of three bacterial isolates alongside their respective extracted pigments: (A) *M. luteus*, producing a bright-yellow pigment, (B) *E. aurantiacum*, yielding an orange-yellow pigment, and (C) *Kocuria* sp., exhibiting a creamy light-yellow pigment

4.7.1 Spectral and Structural Characterization of Bio-Pigments Using UV-Vis, LC-MS, and ATR-FTIR

The spectral scanning of methanolic extract of the yellowish-orange pigments, conducted over wavelengths ranging from 350–750 nm provided crucial insights into its optical properties. By analyzing absorption peaks within this range, the study aimed to determine the characteristic absorbance profile of the pigments, aiding in its identification and potential application.

The spectral analysis revealed distinct absorption peaks corresponding to the extracted bacterial pigments. *M. luteus* exhibited a bright-yellow pigment with characteristic λ_{max} at 476 nm, *E. aurantiacum* produced an orange-yellow pigment with an absorption peak at λ_{max} 467 nm, and *Kocuria* sp. yielded a creamy light-yellow pigment with a λ_{max} at 527 nm (Figure 23).

The absorbance peak provides information about the chromophores present in the pigment (Mohammed, 2018). The UV-visible spectrophotometric analysis of the crude pigment extracted from the isolates revealed distinct absorption peaks, confirming the presence of chromophores within the pigments. These peaks provide valuable insights into the molecular structure and composition of the extracted compound (Marin et al., 2021; Shahin et al., 2022).

The pigments fell within the typical absorption range for carotenoids (400-550 nm) or their derivatives in the visible spectrum, characteristic of compounds with conjugated double bonds that absorb light in this range, leading to their yellowish appearances (Johra et al., 2020).

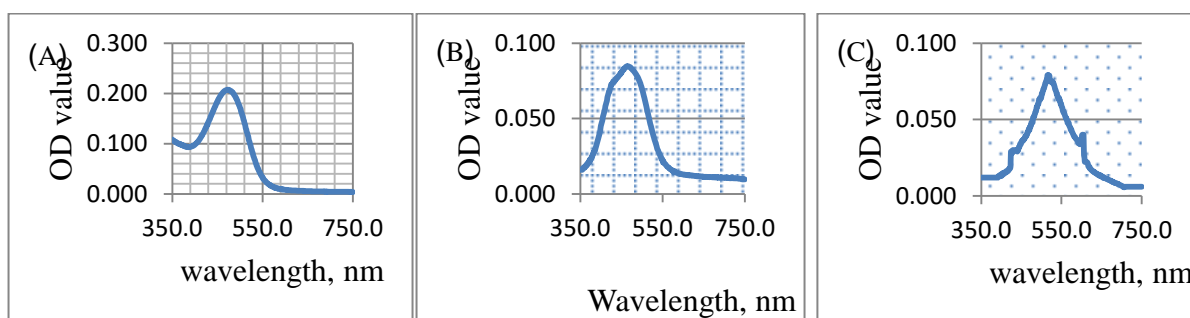


Figure 23 Absorption spectra of pigments extracted from three bacterial isolates from left to right: (A) *M. luteus*, (B) *E. aurantiacum*, and (C) *Kocuria* sp.

The characteristic absorbance peaks within the 400–550 nm range are typical of carotenoid compounds, crucial pigment group responsible for yellow to orange-red coloration (Machmudah & Goto, 2013; Neha et al., 2017). The pigments were classified as carotenoid-like compounds based on their absorption maxima in the visible range (400–500 nm), yellowish coloration, hydrophobic solubility, and characteristic C=C and C–H stretching vibrations. Tentative evidence from LC-MS profiles resembling known carotenoids and the biological origin of the isolates supports this categorization, though definitive structural confirmation requires advanced techniques such as NMR, LC-MS with authentic standards, or full elucidation.

Carotenoids exhibit strong absorption in this range due to π -electron delocalization within their conjugated system, allowing efficient light absorption in the UV-visible spectrum (Udensi et al., 2022). Since carotenoid biosynthesis is primarily regulated at the genetic level, substrate variations may not drastically alter the pigment color (Deng et al., 2025). Hence, while nutrient availability can influence growth rates and biomass, pigment biosynthesis in these isolates might be more constitutive rather than strongly regulated by specific substrates. Under stress conditions, carotenoid production functions as a multifunctional protective mechanism by mitigating oxidative damage, preserving membrane integrity, and enhancing overall stress tolerance and ecological fitness in pigment-producing bacterial isolates.

The variation in the absorbance of the pigments at their respective λ_{max} may be attributed to the specific carotenoid content and its degree of conjugation (Udensi et al., 2022) as revealed by the LC-MS analysis (Figure 24) of the respective pigmented extracts. The variable mass-to-charge (m/z) ratios observed in the LC-MS analysis highlights molecular diversity, yet the consistent yellowish pigment appearance suggests structural similarities among the carotenoids as witnessed from UV-visible and LC-MS analyses.

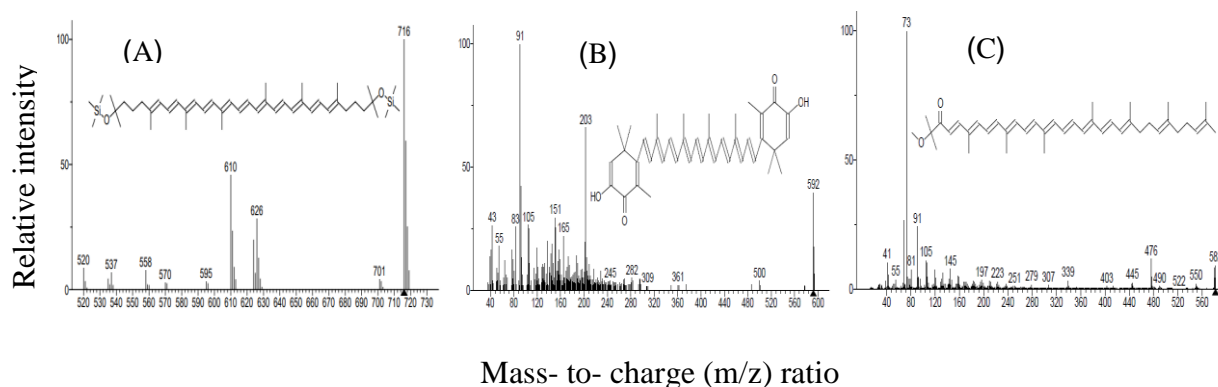
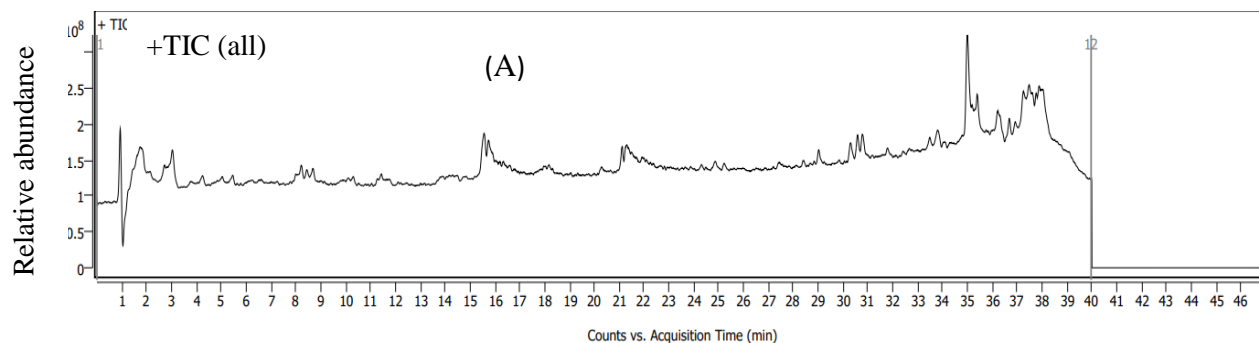


Figure 24 Mass spectra of pigmented compounds extracted from three bacterial isolates from left to right: (A) *M. luteus*, (B) *E. aurantiacum*, and (C) *Kocuria* sp.

The UV-Visible spectra and LC-MS analysis revealed that the yellowish pigments extracted from *M. luteus*, *E. aurantiacum* and *Kocuria* sp. have similar chromophoric structures but differ in their molecular weights and their specific substituents. The spectral data align well with published carotenoid profiles reported by (López-Mora et al., 2025) who identified 12 carotenoids in *M. luteus* with notable bioactivity using LC-MS analysis.

The examination of the pigment extracted from *M. luteus* using liquid chromatography (LC) paired with mass spectrometry provided structural details about the bioactive compounds responsible for pigmentation (Figure 25). The Total Ion Chromatogram (TIC) Fig 25, panel (A) and mass spectrum of psi, psi-Carotene,1,1',2,2'-tetrahydro-1,1'-bis[(trimethylsilyl)oxy]- Figure 25, panel (B) identified a compound as a carotenoid, aligning with the results from the UV-Visible spectrophotometer analysis.



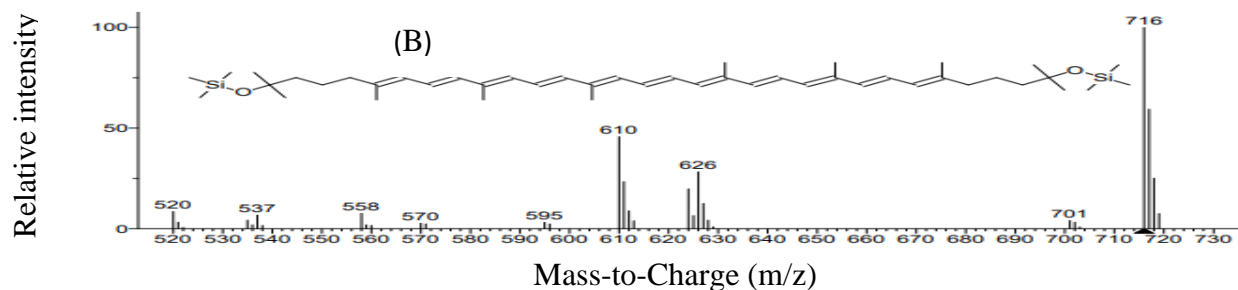
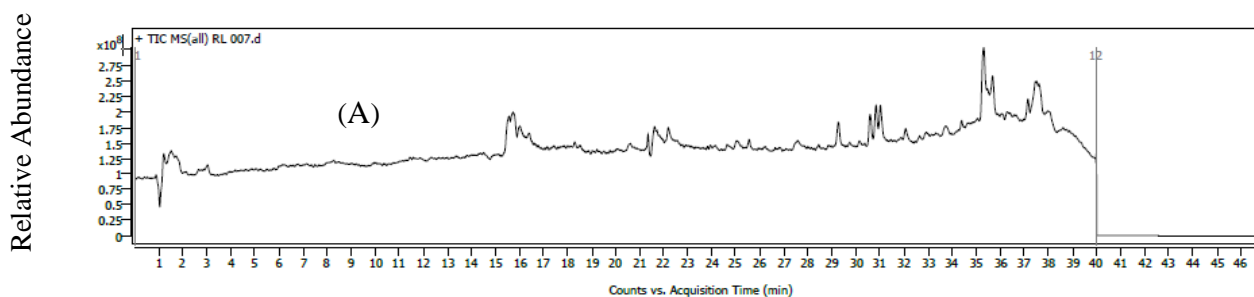


Figure 25 The structural information of bioactive compound responsible for pigmentation. (A) TIC of the pigmented compound extracted from *M. luteus* and (B) mass spectra of psi,psi.-carotene,1,1',2,2'-tetrahydro-1,1'-bis[(trimethylsilyl)oxy]-, having multiple peaks with the most abundant fragment ion at ($m/z=716$)

Multiple peaks were present in the mass spectrum, with the most abundant fragment ion ($m/z = 716$). The color-bearing property of psi, psi-Carotene, 1, 1', 2, 2'-tetrahydro-1, 1'-bis[(trimethylsilyl)oxy]- is influenced by its chemical structure and interactions with light. According to (Lopez Marin et al., 2021), the extended conjugated system allows carotenoids to absorb specific wavelengths of light in the blue and green regions, which is consistent with the UV-Visible spectroscopic analysis result.

The chromatogram (Figure 26) offers a detailed visual representation of the chromatographic separation and mass spectrometric detection of the pigment extracted from *E. aurantiacum*, showcasing distinct peaks corresponding to various carotenoid molecules. These peaks provide key insights into the composition, purity, and molecular identity of the pigment, helping to confirm its classification.



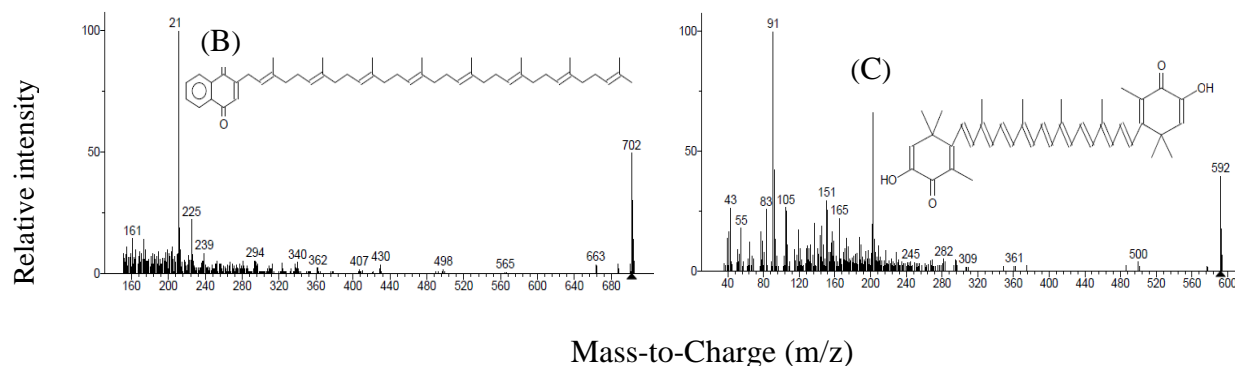


Figure 26 LC-MS analysis of carotenoid compounds extracted from *E. aurantiacum*: Panel (A) illustrates the ion intensity detected over time, Panels (B) and (C) reveal peaks corresponding to the mass-to-charge ratios (m/z) of the detected carotenoid molecules

The LC-MS analysis provided detailed characterization of carotenoid compounds extracted from *E. aurantiacum*. The Total Ion Chromatograph (TIC) plot (Figure 26, panel A) illustrates the ion intensity detected over time, highlighting distinct peaks corresponding to compounds eluting from the chromatography column at different intervals. These peaks represent the molecular components analyzed by the mass spectrometer.

The mass spectra (Figure 26, panels B and C) reveal peaks corresponding to the mass-to-charge ratios (m/z) of the detected carotenoid molecules, offering insights into their molecular weights and fragmentation patterns. The LC-MS investigation confirmed the presence of carotenoid compounds, specifically 1,4-Naphthalenedione, 2-(3,7,11,15,19,23,27,31-octamethyl-2,6,10,14,18,22,26,30-dotriacontaenyl)-(all-E) and 2,5-Cyclohexadien-1-one,3,3'-(3,7,11,15-tetramethyl-1,3,5,7,9,11,13,15,17-octadecanonaene-1,18-diyl)-bis[6-hydroxy-2,4,4-trimethyl].

These compounds belong to the naphthoquinone and polyene classes, known for their intense coloration due to conjugated double bonds that enable absorption of visible light. Their structural properties contribute to the yellowish-orange hue of the pigment extracted from *E. aurantiacum*, reinforcing their classification within the carotenoid group.

Pigments derived from biological sources are often complex mixtures rather than single molecules (Muthusamy et al., 2020). While UV-Vis spectroscopy can confirm the presence of conjugated systems, it cannot determine whether multiple structurally related compounds

contribute to the absorption profile. In cases where pigments are mixtures, their functional properties may vary with the relative proportions of individual components and hence, such mixtures can enhance stability through synergistic effects but may complicate reproducibility and standardization for industrial use. LC-MS provides molecular resolution by separating compounds chromatographically and identifying them based on mass-to-charge ratios. Unlike UV-Vis, LC-MS can reveal distinct peaks corresponding to different molecules, thereby confirming mixtures, quantifying relative abundances, and guiding purification strategies for targeted applications (Saha et al., 2020).

The infrared (IR) spectroscopy analysis showed bands of functional groups (Figure 27) with peaks at 3204.76, 2925.10, and 1621.18 cm^{-1} and fingerprint regions with different absorption bands, revealing the characteristics of the compound present in the pigment extracted from *M. luteus*.

The IR spectrum provides information about functional groups present in the compound. The weak and broad absorption band at 3204.76 cm^{-1} corresponds to the O-H stretching vibration in acids, suggesting the presence of hydrogen bonding. The second short peak at 2925.10 cm^{-1} is associated with C-H stretching vibrations, indicating the presence of aliphatic C-H bonds in alkane or alkene groups. The third absorption peak at 1621.18 cm^{-1} corresponds to the C=C stretching vibration in alkenes, matching the vibration of carbon-carbon double bonds in alkenes (Njuguna et al., 2022).

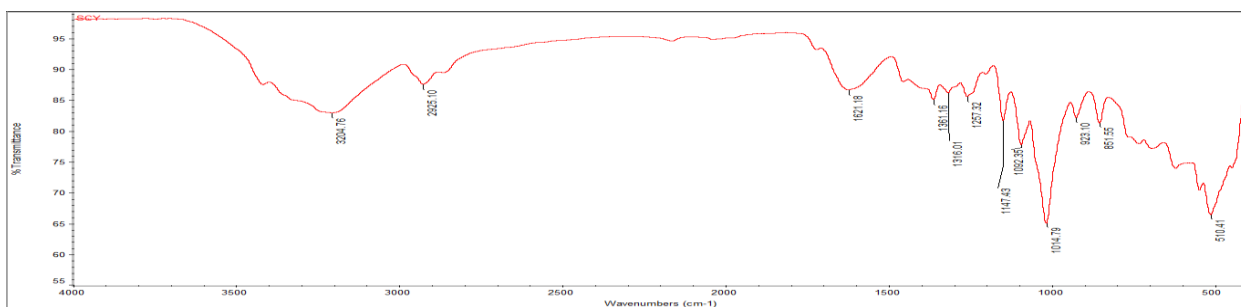


Figure 27 The IR spectrum of pigmented compound extracted from *M. luteus*. The IR spectrum corresponds to the O-H, C-H and C=C stretching vibrations showed the presence of hydroxyl, alkane and alkene groups

Based on common functional group frequencies, the IR spectrum of the bright yellow pigment extracted from *M. luteus* exhibited the presence of hydroxyl, alkane, and alkene groups. Additionally, the stretching of the double bond in an alkene may cause a shift in the energy levels of the electrons in the pi bond, leading to chromophore formation. The reduced peak intensity indicates typical conjugations with other double bond structures (Kantifedaki et al., 2018).

The spectroscopy analysis (Figure 28) presents the IR spectrum of the pigmented compound extracted from *E. aurantiacum*, providing insights into its functional groups and molecular structure. The IR spectroscopy detects specific bond vibrations, allowing the identification of characteristic absorption peaks associated with various functional groups within the pigment molecule.

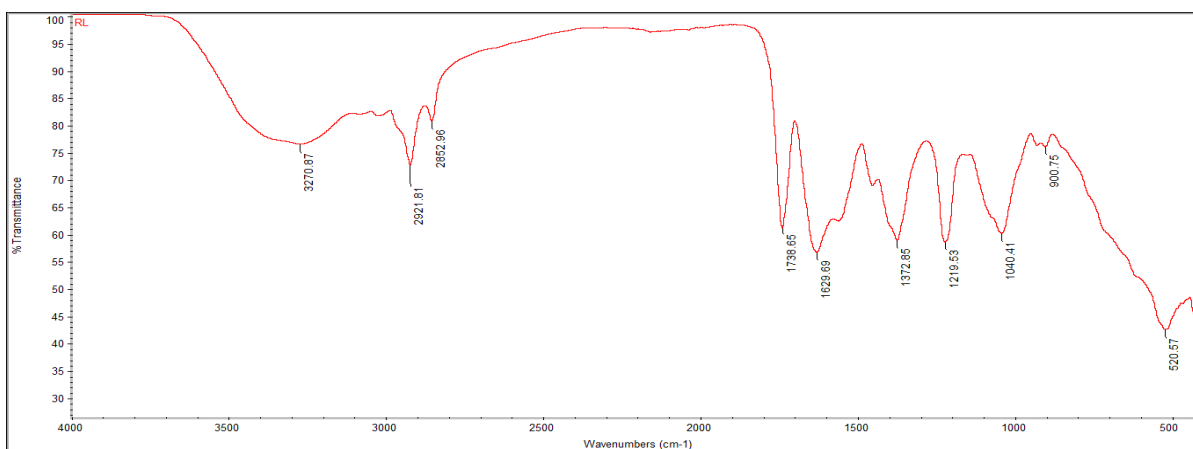


Figure 28 IR spectrum of pigmented compound extracted from *E. aurantiacum*, depicting characteristic absorption peaks corresponding to various functional groups present in the compound

The spectrum displays characteristic absorption peaks corresponding to various functional groups present in the compound. The IR spectrum showed bands of functional groups with peaks at 3270.86, 2921.81, 2852.96, 1738.65, and 1629.69 cm^{-1} . The fingerprint regions with different absorption bands provide information about the chemical composition of the pigment extracted from the isolate, *E. aurantiacum*.

The weak and broad absorption peak at $3270.87.76\text{ cm}^{-1}$ is associated with O-H stretching vibrations, characteristic of hydroxyl groups. The second and third short and narrow peaks at 2921.81 and 2852.96 cm^{-1} indicate C-H stretching vibrations commonly found in alkanes. The narrow peak at 1738.65 cm^{-1} is characteristic of C=O stretching vibrations, typically found in carbonyl groups, and the peak at 1629.69 cm^{-1} is associated with C=C stretching vibrations found in alkenes.

These Vibrations help identify different functional groups in molecules by their characteristic absorption bands. The functional group frequency analysis revealed that the IR spectrum of the yellowish-orange pigment extracted from *E. aurantiacum* indicates the presence of hydroxyl, hydrocarbon, olefinic, and carbonyl groups, which are among the functional groups present in carotenoid compounds (Maoka, 2020).

Pigment identification in this study remains putative (carotenoid-like) because the analytical techniques employed-UV-Vis spectroscopy, ATR-FTIR, and LC-MS primarily provide absorbance profiles, functional group signatures, molecular weights, and fragmentation patterns, respectively. However, they do not yield complete structural elucidation, particularly with respect to stereochemistry, isomeric variation, or precise molecular configuration. Full structural confirmation of natural pigments typically require nuclear magnetic resonance (NMR) spectroscopy or complementary techniques such as X-ray crystallography and can be applied once high-yield production and purification are achieved as these techniques are resource-intensive, and require purified pigment in sufficient quantity. Hence, they were beyond the scope of this laboratory-scale study which prioritized screening, optimization, and application feasibility.

4.7.2 Pigment stability analysis

Considering the similar color of carotenoid compounds along with the huge difference in pigment yield, the bright yellow pigment extracted from *M. luteus* was selected for final stability testing and fabrics dyeing activities. Hence, its stability was analyzed across varying environmental conditions.

The absorbance of the pigment increased as the pH approached neutrality (Figure 29 (A)). Specifically, the absorbance values increased from 0.127 to 0.196 in an acidic environment but

decreased from 0.196 to 0.118 in the alkaline pH range. A sharp decrease in absorbance was observed in both low and high pH ranges, correlating with a noticeable fading in color intensity (Figure 29 (B)).

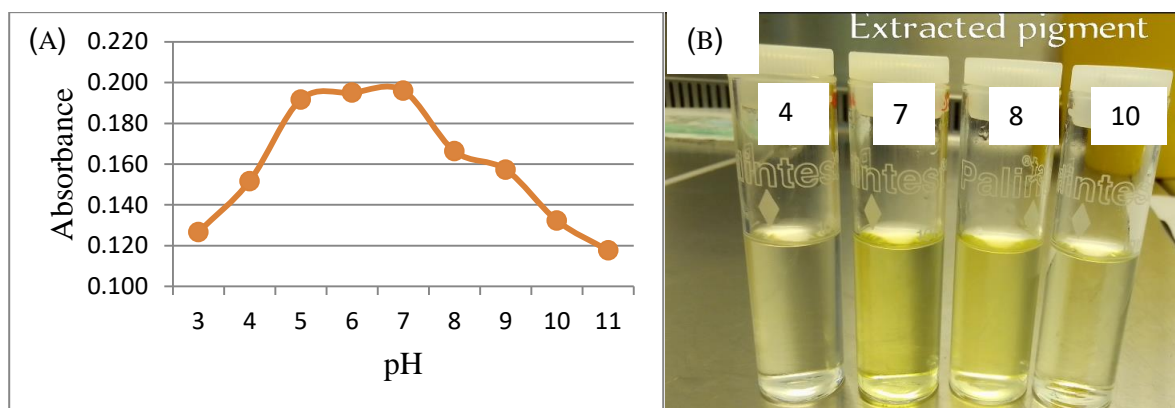


Figure 29 Influence of pH on the stability of the pigment extracted from *M. luteus*: (A) A line graph showing changes in absorbance of the pigment as a function of change in pH level, (B) Color intensity of the pigment across different pH levels, with labeled test tube vials indicating the respective pH values. The labels on each test tube vials indicate the pH value of the respective pigment solutions

Each absorbance value represents the average of three replications, ensuring accuracy in assessing the pigment's stability and color variation under different pH conditions. Exposure to both strong acidic and alkaline conditions degraded the pigments, signifying that the pigment is sensitive to pH changes and unstable under such extreme conditions. The statistically significant differences presented in ANOVA (Table 43) further validate the impact of pH variation on pigment stability.

Table 43 ANOVA summary table presenting the statistical analysis of variance results

Source of Variation	SS	df	MS	F	P-value	F crit
Between Groups	0.021918	8	0.00274	70.99	4.93E-12	2.510158
Within Groups	0.000695	18	3.86E-05			
Total	0.022613	26				

Key: SS-sum of squares, df-degree of freedom, MS-mean Square, F-F-statistic, and F crit-F-critical

The table shows parameters which assess the significance of differences among experimental groups; helped determine whether variations in the dataset are statistically significant. The ANOVA analysis result offered a strong case for pH as a critical factor influencing pigment absorbance. The Bonferroni adjusted post-hoc tests revealed that out of 36 pairwise comparisons, 47.22% showed significant differences in absorbance with a p value of 0.0014, reinforcing the ANOVA results. These significant differences across comparisons reinforce the importance of pH control in maintaining pigment stability (Wijesekara & Xu, 2024).

Interestingly, despite the statistical significance in group comparisons, the regression analysis (Table 44), evaluating the strength and significance of the relationship between independent and dependent variables suggested that pH does not reliably predict absorbance variations ($p = 0.44$).

Table 44 Summary of regression analysis presenting key statistical parameters

<i>Predictor</i>	<i>Coefficients</i>	<i>Standard Error</i>	<i>t Stat</i>	<i>P-value</i>
Intercept	0.1822	0.0297	6.13	0.0005
pH	-0.0033	0.0034	-0.82	0.44

From line fit plot analysis (Figure 30), the low R^2 value of 0.087 indicated weak explanatory power, reinforcing that pH alone does not reliably predict absorbance variation. While optimal absorbance was observed around slight acidic to neutral pH levels, the relationship between pH and absorbance is not linear.

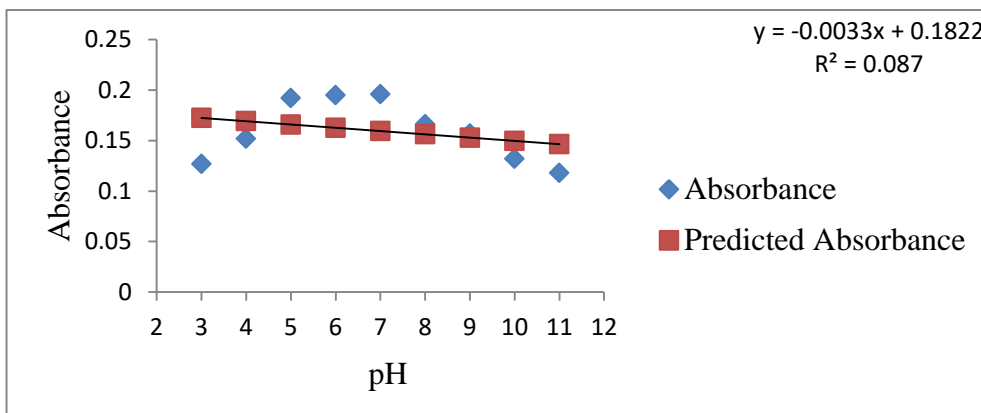


Figure 30 Line fit plot showing the relationship between pH and the pigment stability, illustrating how changes in pH influence absorbance. The fitted line represents the trend in pigment behavior across different pH levels, providing insights into its stability

The line fit plot analysis clearly highlighted the non-linear relationship between pH and absorbance; reinforcing the observation that pH affects pigment behavior but lacks strong predictive power in a linear model. This suggests that other interactive factors, such as buffering effects or molecular stability, might play a more dominant role in absorbance changes. Compared to broader pH tolerance range (2.5-9.5) reported in *Rhodotorula minuta* by Yadav & Prabha (2014), and yield focused study without absorbance analysis in *M. luteus* study by Hegazy et al. (2024), this study revealed narrow stability.

Upon exposing the pigment to different temperature, ranges from 20 °C to 80 °C under controlled conditions, the pigment solutions demonstrated significant decrease in absorbance as temperature increased (Figure 31 (A)). As temperature value rose, the absorbance started to decline progressively with a noticeable fading of the yellow color (Figure 31(B)), suggesting thermal degradation of the pigment molecules.

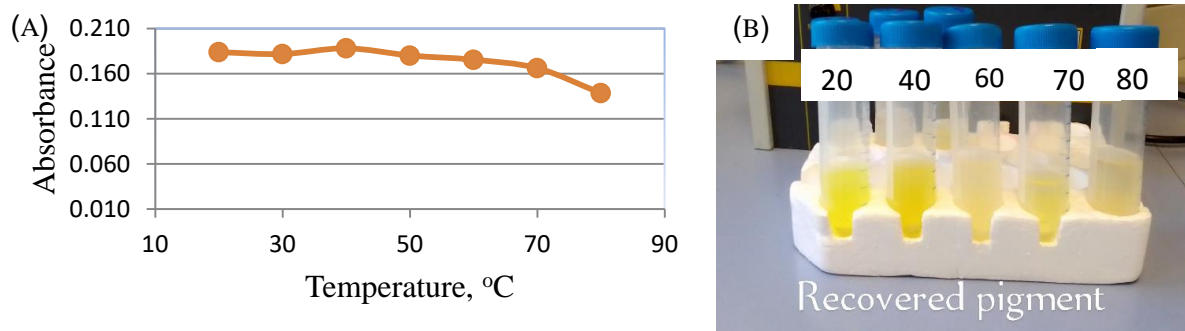


Figure 31 Influence of temperature on the stability of the pigment extracted from *M. luteus*: (A) A line graph illustrating changes in absorbance across different temperature levels, showing trends and variation patterns of the pigment as a function of temperature change, and (B) Visual representation of pigment color intensity at various temperatures. The labels on each test tube vials indicate the temperature of the respective pigment solutions

Each absorbance value represents the average of three replications, confirming accuracy in assessing the pigment's thermal stability and color variation under different temperature conditions. The results highlighted the thermal degradation of carotenoid pigments may be due to the breakdown of the conjugated double-bond system which is responsible for pigment color (Kardile et al., 2020). Hence, maintaining optimum temperatures during the application process is crucial to preserving the pigment's stability to ensure the desired color outcome in dyeing applications.

The ANOVA result (Table 45) confirmed statistically significant differences in absorbance values across different temperature ranges, validating the impact of heat exposure on pigment degradation.

Table 45 ANOVA summary table presenting the statistical analysis of variance results

Source of Variation	SS	df	MS	F	P-value	F crit
Between Groups	0.005157	6	0.000859	730.4483	1.19E-16	2.847726
Within Groups	1.65E-05	14	1.18E-06			
Total	0.005173	20				

Key: SS-sum of squares, df-degree of freedom, MS-mean Square, F-F-statistic, and F crit-F-critical

The result showed that temperature significantly impacted pigment absorbance, ($F=730.4483$, $p < 0.05$). Post-hoc Bonferroni analyses revealed that 81% of the 21 pairwise comparisons demonstrated statistically significant differences in absorbance values ($p < 0.002$) due to temperature variations. These findings pin-pointed specific temperature ranges where pigment stability is most affected, highlighting the critical role of temperature control in maintaining pigment integrity.

Furthermore, regression analysis (Table 46) indicated that temperature was a statistically significant predictor of absorbance ($p < 0.05$). The relatively high R^2 value (0.68) suggested strong relationship between temperature and absorbance fluctuations, indicating that temperature variations account for a considerable proportion of pigment behavior, indicating the need to optimize thermal conditions during dyeing applications.

Table 46 Regression results table summarizing key statistical parameters

<i>Predictor</i>	<i>Coefficients</i>	<i>Standard Error</i>	<i>t Stat</i>	<i>P-value</i>
Intercept	0.2060	0.0107	19.17	7.1259E-06
Temperature (°C)	-0.0006	0.0002	-3.28	0.02206419

The analysis effectively reinforced the statistical significance of temperature as a predictor of pigment absorbance and the strong model fit, $R^2 = 0.68$ (Figure 32) confirmed the predictive accuracy and reliability of the regression model. The finding that 40 °C (Figure 32) pin-pointed the optimal temperature for absorbance further emphasized the necessity of temperature regulation in pigment applications.

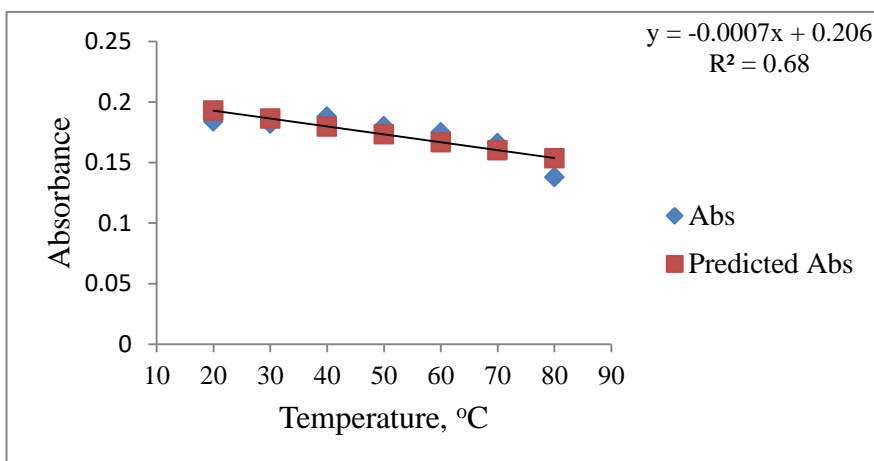


Figure 32 Line fit plot illustrating the relationship between temperature and pigment stability, showing how changes in temperature affect absorbance. The fitted line represents the trend in pigment behavior across different temperature levels, providing insights into its thermal stability

The consistent absorbance decline beyond 40 °C suggests that thermal degradation may accelerate at higher temperatures, possibly due to the breakdown of conjugated double-bonds within carotenoid structure. Maintaining controlled temperature conditions during dyeing processes is thus, crucial to preserving pigment integrity and color stability. This temperature induced instability suggests that the pigment may be less suitable for applications involving prolonged heat exposure, such as high temperature dyeing processes.

The temperature analysis in this study aligns with study reported by (Ahn et al., 2014) on alizarin and indigotin, confirming thermal degradation linked to the breakdown of conjugated double bonds. The quantitative thermal degradation data of this study also aligns with kinetic study showing first-order degradation of β -carotene with color loss and antioxidant activity decline (Kardile et al., 2020), reinforced the need for temperature controlled dyeing methods.

The assessment of the stability of *M. luteus* pigment under exposure to oxidizing (H_2O_2) and reducing (glucose) agents revealed different scenarios. Increasing H_2O_2 concentration resulted in progressive declining in absorbance and fading of pigment color (Figure 33 (A)). Oxidation intensified with higher H_2O_2 levels, indicated poor pigment tolerance to oxidative stress,

suggesting carotenoid pigments should be protected from oxidants to maintain color integrity and stability.

Conversely, the pigment exhibited no observable color change under exposure to glucose during the test period (Figure 33 (B)), highlights high pigment tolerance to reducing conditions; signifying glucose does not disrupt pigment stability. The oxidation-reduction analysis demonstrated the sensitivity of carotenoid pigments to oxidative stress while confirming their stability under reducing conditions. For optimal dyeing applications, minimizing oxidant exposure and leveraging reducing conditions could improve pigment durability.

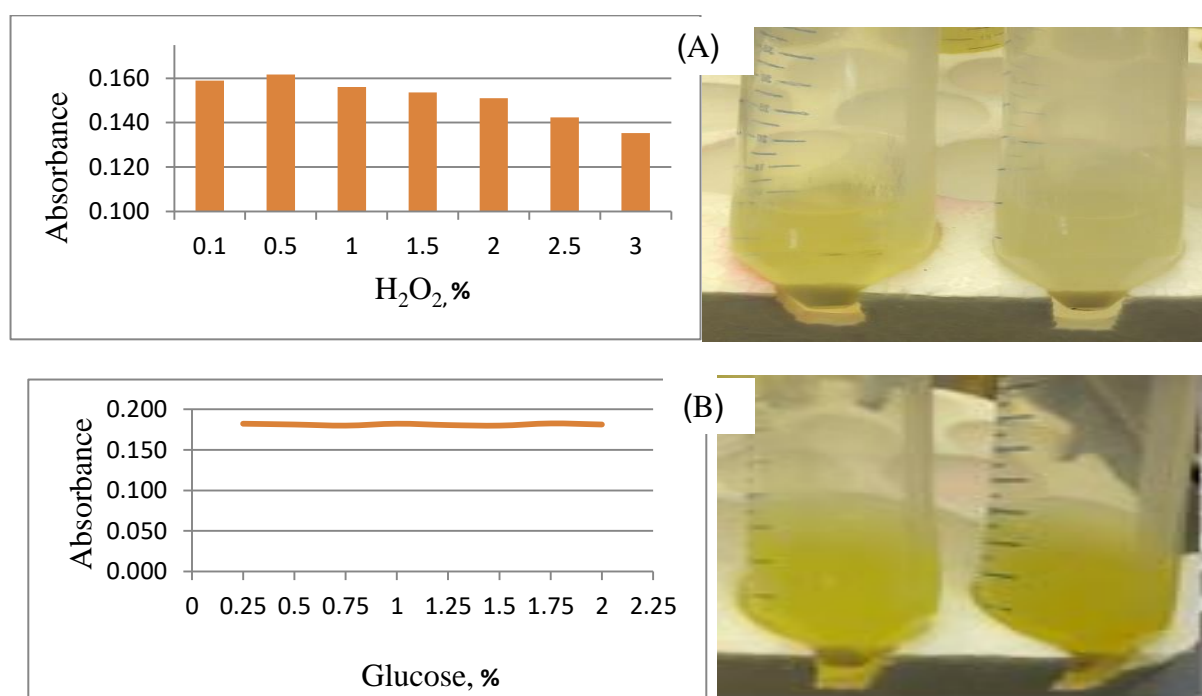


Figure 33 Influence of oxidizing and reducing agents on the stability of the pigment extracted from *M. luteus*: (A) Absorbance pattern and color intensity of the pigment solution as a function of varying concentrations of H₂O₂, and (B) Absorbance pattern and color intensity of the pigment solution as a function of varying concentrations of glucose

Each absorbance value represents the average of three replications; ensuring constancy in assessing the pigment's stability under oxidative and reductive conditions. The statistical

analysis also strongly confirmed the significant impact of H₂O₂ on pigment absorbance (Table 47), depicting the significance of differences among experimental groups. The high $F=76.215$, and extremely low $p<0.001$, confirmed a strong relationship between oxidation and pigment degradation.

Table 47 ANOVA summary table presenting the statistical analysis of variance results

<i>Source of Variation</i>	<i>SS</i>	<i>df</i>	<i>MS</i>	<i>F</i>	<i>P-value</i>	<i>F crit</i>
Between Groups	0.00159	6	0.000265	76.215	6.97E-10	2.847726
Within Groups	4.87E-05	14	3.48E-06			
Total	0.001638	20				

Key: *SS*-sum of squares, *df*-degree of freedom, *MS*-mean Square, *F*-*F*-statistic, and *F crit*-*F*-critical

The statistical analysis also indicated that while glucose has some effect on pigment stability, its impact was considerably weaker than that of H₂O₂, aligns with the color fading observation that oxidation posed greater influence on pigment integrity compared to reduction.

The statistical result in Table 48 showed variation in absorbance values across different glucose concentrations, but the influence may be more subtle or gradual compared to the pronounced degradation caused by oxidizing agents, highlighting its potential applicability in dyeing processes where antioxidant mechanisms might enhance longevity.

Table 48 ANOVA summary table presenting the statistical analysis of variance results

<i>Source of Variation</i>	<i>SS</i>	<i>df</i>	<i>MS</i>	<i>F</i>	<i>P-value</i>	<i>F crit</i>
Between Groups	2.33E-05	7	3.33E-06	3.636	0.0154	2.657197
Within Groups	1.47E-05	16	9.17E-07			
Total	3.8E-05	23				

Key: *SS*-sum of squares, *df*-degree of freedom, *MS*-mean Square, *F*-*F*-statistic, and *F crit*-*F*-critical

The analysis exhibited strong evidence that H₂O₂ significantly impacted pigment stability, demonstrated by 62% of pairwise comparisons showed significant absorbance differences

($p < 0.05$) from Bonferroni correction post-hoc tests, strengthening the assumption that carotenoid pigments are highly susceptible to oxidative degradation.

Conversely, the post-hoc test for glucose variations revealed no significant differences across 28 pairwise comparisons, suggesting that glucose exerted a negligible effect on pigment absorbance. The regression analysis (Table 49) further strengthened the deduction that H_2O_2 concentration significantly impacted pigment stability, as demonstrated by its statistical significance ($p < 0.001$) and high R^2 value of 0.89 (Figure 34). The strong model fit indicates that oxidation accounts for a substantial proportion of absorbance variability, reinforcing the critical role of oxidative stress in pigment degradation.

Table 49 Regression results table summarizing key statistical parameters

<i>Predictor</i>	<i>Coefficients</i>	<i>Standard Error</i>	<i>t Stat</i>	<i>P-value</i>
Intercept	0.1643	0.0023	68.91	1.219E-08
H_2O_2	-0.0086	0.0013	-6.51	0.0013

The line fit plot results strongly reinforced the negative linear effect of H_2O_2 on absorbance with progressive decline in pigment stability as oxidation intensified (Figure 34). This also confirmed oxidative degradation as a key factor compromising color integrity and absorbance retention.

The non-linear response of absorbance to glucose concentration (Figure 34) suggested that the impact of glucose as a reducing agent on pigment stability may involve complex interactions, making its effect less predictable. This could indicate the presence of threshold effects or secondary biochemical influences affecting pigment resilience under reducing conditions.

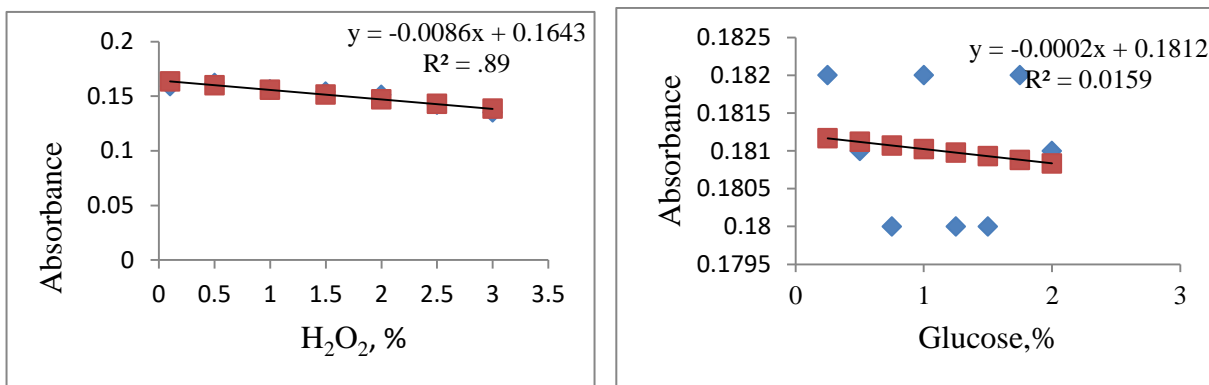


Figure 34 Line fit plot illustrating the effect of hydrogen peroxide (H₂O₂) and glucose concentrations on the stability of the extracted pigment. The fitted lines represent the trends in absorbance as a function of oxidizing (H₂O₂) and reducing (glucose) agents, providing insights into the pigment's chemical stability under varying conditions

The very weak R^2 value (0.0159) and high $p > 0.05$ (Table 50), again confirms that glucose concentration has minimal predictive power in determining pigment stability. Unlike H₂O₂ which had a strong effect, glucose's negligible impact may indicate that reducing conditions do not disrupt carotenoid structure.

Table 50 Regression results table summarizing key statistical parameters

<i>Predictor</i>	<i>Coefficients</i>	<i>Standard Error</i>	<i>t Stat</i>	<i>P-value</i>
Intercept	0.1812	0.0008	234.43	4.0649E-13
Glucose	-0.0002	0.0006	-0.31	0.77

This study demonstrated that the pigment exhibits pronounced sensitivity to oxidative stress and thermal degradation, while maintaining stability under reducing conditions. Exposure to hydrogen peroxide and elevated temperatures disrupted pigment integrity through oxidative cleavage and thermal isomerization of conjugated double bonds. These observations were consistent with recent carotenoid research which has shown that peroxide derived radicals initiate reactions like epoxidation and hydrogen abstraction, ultimately destabilizing the conjugated polyene system responsible for pigment coloration (Garcia et al., 2025; Losinska-Siçiūnienė et al., 2025).

The study reported by (Kardile et al., 2020) showed that when combined with elevated temperature, oxidative degradation is amplified as heat can enhance the oxidative reactions initiated by H₂O₂, accelerating pigment breakdown and color loss. Hence, the findings of this study reinforced the vulnerability of carotenoids to oxidative stress.

4.8 Dyeing performance of bio-pigments on textile materials

The application of extracted bacterial pigments on cotton and Tetron 6000 fabrics resulted in visibly distinct and vibrant coloration, with yellow hue extracted from *M. luteus*. The dyeing process achieved uniform color distribution across the fabrics surface, indicating good affinity between the pigment molecules and the cotton fabric. Visual inspection and photographic documentation confirmed that pigment derived dyes provided aesthetically appealing alternatives to synthetic dyes, reinforcing their potential in sustainable textile applications.

The colorfastness tests provided critical insight into the durability of the bacterial pigments on the dyed fabrics. The qualitative evaluation of washing color fastness in unicolor cotton and Tetron 6000 fabrics revealed distinct color differences compared to untreated counterparts. Bright, uniform color was observed under optimal dyeing conditions with carotenoid pigment from the isolate from initial dyeing performance (Figure 35(A, B)). The dyed fabrics exhibited vibrant coloration when compared side-by-side with un-dyed samples under bright light.

Despite promising coloration, the study also highlighted that the pigment was susceptible to fading from detergent exposure and sunlight. Prolonged sunlight exposure and repeated washing caused noticeable fading with more pronounced effect on Tetron 6000 fabric compared to cotton fabric (Figure 35 (E, F)), reflecting their weaker chemical affinity and structural complexity. The findings suggest that cotton may offer better pigment retention than Tetron 6000.

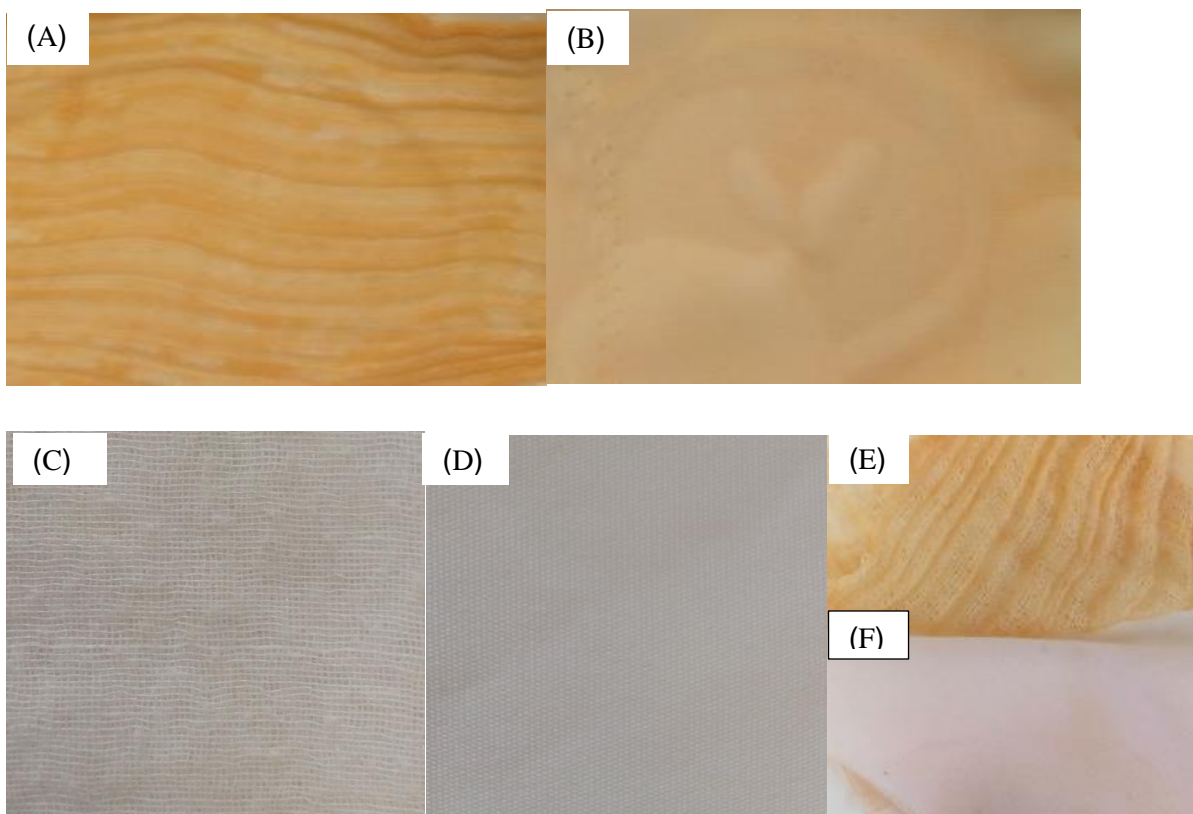


Figure 35 Actual images of cotton and Tetron 6000 fabrics before and after dyeing tests showing color difference. Panels (A) and (B) show pigment uptake by cotton and Tetron 6000 fabrics, respectively. Panels (C) and (D) show un-dyed cotton and Tetron 6000 fabrics, respectively, used as negative control for pigment uptake and retention comparison. Panels (E) and (F) depict color retention comparison between cotton and Tetron 6000 fabrics, respectively, after washing with detergent and exposure to sunlight

The quantitative pigment exhaustion analysis revealed a statistically significant difference in dye affinity between cotton and Tetron 6000 fabrics. Cotton exhibited a higher pigment uptake of 75% (Table 51), reflecting strong affinity for the pigment, whereas Tetron 6000 showed a comparatively lower uptake of 65% ($p = 0.002$). The exhaustion levels observed for cotton fall within the typical range reported for natural dyes under optimized industrial conditions (70-90%) (Zhu et al., 2025), while the performance across both fabrics surpassed that of many commercial natural dyes which often achieve 40-60% exhaustion rates depending on mordant use and fiber type (Locks et al., 2025).

Cotton fabric showed 54.6% dye fixation, ensuring better dye retention compared to Tetron 6000 fabric with 37% fixation ($p < 0.001$), demonstrating stronger dye-fiber interactions in natural fibers. This study highlighted that natural pigments bond more effectively with cotton due to its hydrophilic cellulose structure, while Tetron 6000's synthetic surface resists pigment fixation. The results align with broader findings that natural dyes struggle with synthetic fibers, reinforcing the need for fiber-specific dyeing strategies.

Table 51 Pigment's exhaustion and fixation calculation table presenting key parameters used to evaluate dye uptake and retention on fabrics

Fabric	Initial absorbance	Absorbance after dyeing	Absorbance of wash liquid	% dye absorbed	% dye fixed
Cotton	0.207	0.052	0.094	74.88	54.59
Tetron 6000	0.207	0.072	0.13	65.22	37.20

Natural pigments often exhibit lower color fastness compared to synthetic dyes as they are composed of complex mixtures of organic compounds which may not form strong chemical bonds with textile fibers, making them more prone to washing and light-induced fading. The results align with previous findings that natural fibers exhibit better bonding with microbial pigments than synthetic blends like Tetron 6000 (Samanta, 2020). Compared to synthetic dye benchmarks (84% exhaustion, 79% fixation) reported by (Siddiqua et al., 2017), the performance of this pigment, extracted from *M. luteus* isolated from environmental sample was lower, supporting the known trade-off between environmental safety and durability.

While the reported yield of 1.47 g/L is encouraging at laboratory scale, it remains below industrially viable thresholds where higher productivity is essential for economic competitiveness. Achieving commercial benchmarks will require strain improvement, advanced cultivation strategies, and metabolic engineering alongside addressing operational challenges such as pigment stability, uniform fiber compatibility, and integration with existing dyeing systems. Compared to synthetic dyes which exhibit superior fastness due to engineered covalent bonding, microbial pigments offer reduced stability under oxidative and thermal stress which can be mitigated through mordanting or encapsulation (Anshi et al., 2024). Cost competitiveness also lags behind synthetic dyes which benefit from high yields and established supply chains. However, microbial pigments hold promise if yields are enhanced

through agro-waste valorization and bioprocess optimization. Overall, microbial pigments present a sustainable and regulatory-friendly alternative, but require significant yield, fastness and scalability improvements to competing synthetic counterparts.

This study provided valuable insights into microbial pigment production but is subject to several limitations. Pigment identification was restricted to putative classification as carotenoid-like compounds based on UV-Vis, ATR-FTIR, and LC-MS data. Definitive confirmation of molecular configuration and stereochemistry will require higher-resolution analytical methods. The qualitative evaluation of the color fastness test to washing might induced observer bias and hence may not be sufficient for interpretation whether the dyeing test fits for industrial application or not. Moreover, though laboratory-scale experiments provided valuable insights, industrial applications need successful scale-up of the process to industrial-level equipment and environment. Therefore, the results of this study may not be conclusive findings that can be replicated for industrial applications.

Future research should focus on isolating more potent chromogenic bacteria to achieve higher yields, conducting quantitative dye uptake and fixation studies to further strengthen the shift towards eco-friendly textile dyeing method and investigating stabilization techniques to enhance color fastness and durability in industrial applications. In particular, genetic and metabolic engineering of *M. luteus* offers a promising route to improve pigment yield. Strategies such as overexpression of key carotenoid biosynthetic genes, elimination of competing metabolic pathways, and optimization of precursor supply could significantly enhance production efficiency. Coupled with agro-waste valorization and advanced cultivation methods, these approaches may help bridge the gap between laboratory-scale promise and industrial-scale competitiveness.

CONCLUSIONS AND RECOMMENDATIONS

This study successfully demonstrated the potential of pigment producing bacteria isolated from environmental samples as viable sources of natural dyes, particularly when cultivated on agro-waste substrates. Through careful optimization of culture conditions, significant pigment yields were achieved compared to literature values, showcasing the efficiency of low cost sustainable resources.

A group of pigment-producing microbial isolates were successfully recovered from volcanic ash sediment, quarry site soil and air samples. Morphological and biochemical characterization revealed that most isolates were Gram-positive, aerobic, non-motile, and catalase-positive, indicating strong oxidative stress resistance and suitability for pigment production. MALDI-TOF mass spectrometry enabled identification of pigment producing isolates at the genus and species level. Three non-pathogenic isolates, namely *M. luteus*, *E. aurantiacum*, and *Kocuria* sp. demonstrated better pigment yield, stability, and growth in agro-waste media, making them ideal candidates for further pigment extraction and application.

All the identified pigment-producing isolates demonstrated variable growth responses across a wide range of environmental variables, confirmed with one-way ANOVA and Pearson correlation analyses. The results highlighted that tolerance to environmental conditions is isolate-specific and critical for pigment production optimization.

Agro-waste extracts proved to be effective low-cost substrates for microbial pigment production, with orange-waste extract and tomato-waste extract supporting the highest growth and pigment yield. Among the tested isolates, *M. luteus* showed the highest growth and pigment yield (1.47 g/L) in orange waste extract. *E. aurantiacum* and *Kocuria* sp. grew well in tomato waste extract but produced lower pigment yields (0.96 g/L and 0.56 g/L, respectively).

The consistent yellowish pigment across isolates suggests that pigment biosynthesis is genetically regulated, likely involving carotenoid biosynthesis. Statistical analyses, ANOVA and linear regression confirmed significant differences in isolates' growth across agro-waste

extracts. Pairwise post-hoc comparisons revealed significant differences in OD₆₀₀ values among most agro-waste extracts, confirming variability in the isolates' growth support.

The Plackett-Burman Design was successfully employed to screen the process variables and identified those with the most significant impact on the growth of *E. aurantiacum*, evaluated via OD₆₀₀ measurement. Key influential factors identified were culture agitation rate, initial medium pH, yeast extract concentration, salt and glucose concentrations, and inoculum size. Visualization tools, the half-normal plot and Pareto chart effectively highlighted these variables as critical for optimizing pigment production. ANOVA results confirmed the statistical significance of the model ($F = 134.98$, $p < 0.001$), with $R^2 = 0.9939$ indicating excellent model fit which underscored the importance of targeted optimization in enhancing microbial growth and pigment yield.

The Face-Centered Central Composite Design refined the most influential variables as agitation speed, medium pH, and yeast extract concentration. Response variables measured were OD₆₀₀ value as indicator of bacterial growth, culture biomass as indicator of total cell mass, and pigment yield. Optimizing biomass is essential for maximizing pigment production as growth rate and cell density directly influence biosynthetic output. Optimal conditions for pigment production were found at 65 rpm agitation, pH 5, and 0.1% yeast extract, yielding the highest pigment output 0.96 g/L from *E. aurantiacum*.

Methanol (99.5%) was identified as the most efficient solvent for pigment extraction, outperforming other organic solvents in yield. ANOVA results confirmed significant differences in OD₆₀₀ and pigment yield across solvents ($p < 0.05$), validating methanol's effectiveness.

UV-Visible spectrophotometric analysis of methanolic pigment extracts revealed distinct absorption peaks: *M. luteus* λ_{\max} at 476 nm (bright yellow), *E. aurantiacum* λ_{\max} at 467 nm (orange-yellow), and *Kocuria* sp. λ_{\max} at 527 nm (creamy light yellow). All absorption peaks fell within the 400–550 nm range, typical of carotenoids, confirming the presence of conjugated chromophores responsible for yellow-orange coloration.

LC-MS analysis revealed structural diversity among pigments with variable mass to charge ratios indicating differences in molecular weights and substituents. Despite molecular variation, the pigments shared similar chromophoric structures, suggesting a common carotenoid backbone. The Chromatograms from both *M. luteus* and *E. aurantiacum* showed distinct carotenoid peaks, confirm that the pigments are carotenoid-based, with extended conjugated systems that absorb light in the visible spectrum, producing their characteristic hues.

IR spectroscopy of pigments from *M. luteus* and *E. aurantiacum* revealed peaks indicating the presence of hydroxyl, hydrocarbon, olefinic, and carbonyl groups which are consistent with carotenoid structures, supporting the classification of the pigments as carotenoid derivatives, strongly influence pigment stability, solubility and dyeing performances.

Although UV-Vis, ATR-FTIR, and LC-MS analyses provided strong evidence for carotenoid-like compounds, the designation of the pigments as "carotenoids" underscores a practical limitation in analytical depth rather than methodological inadequacy, and highlights the need for future studies to employ higher-resolution techniques for definite structural identification.

The absorbance of pigments were found influenced by various environmental factors, indicated by color fading and confirmed with statistically significant differences in absorbance before and after exposure, validating the impacts of environmental factors on pigment stability. Exposure to temperature and oxidative stress were identified as the primary destabilizing factors.

The yellow pigment extracted from *M. luteus* produced vibrant and uniform coloration on both cotton and Tetron 6000 fabrics. Cotton fabric demonstrated higher pigment uptake (75%) and better dye fixation (54.6%) compared to the Tetron 6000 fabric. Colorfastness tests revealed minor fading after washing and sunlight exposure with more pronounced fading in Tetron 6000.

Collectively, the findings contribute to the growing body of research supporting microbial pigments as sustainable alternatives to synthetic dyes, aligning with global efforts toward greener industrial practices.

Based on the findings of this study, the following recommendations are proposed to guide future research and practical applications.

- Up-scaling studies beyond laboratory optimization to pilot-scale continuous fermentation systems, integrating bioreactor design improvements for enhanced yield and reproducibility.
- Investigate buffering systems or stabilizing agents that could enhance pigment resilience under variable environmental conditions.
- Explore stabilization techniques such as natural mordants or encapsulation to enhance colorfastness and durability under industrial conditions.
- Future work should prioritize full structural elucidation of bio-pigments using advanced analytical techniques such as nuclear magnetic resonance (NMR) spectroscopy and X-ray crystallography.
- Long-term environmental impact assessments and lifecycle analysis should be undertaken to fully evaluate the ecological footprint of microbial dyeing systems.
- Conducting comprehensive analysis of the nutritional composition of agro-waste substrates that support microbial growth which enable the rational formulation of culture media and targeted supplementation strategies, thereby maximizing biomass accumulation and pigment yield.
- Incorporate 16S rRNA gene sequencing for isolates with low-confidence or unclear MALDI-TOF identifications to improve species-level resolution and taxonomic validation.
- Adopting mixed agro-waste substrate approach to guarantee both availability and nutrient sufficiency by valorizing mixtures of agro-waste residues in order to reduce dependency on a single agricultural by-product.

REFERENCES

- Abdelgawad, A. M., Shaban, E., Elsherbiny, D. A., El-Sherbiny, R. A., Farouk, H., & El-Sayed, I. E.-T. (2025). Acquiring Sustainable Coloration and Antimicrobial Properties to Natural Fabrics via Spirulina Algae/Silver Nanocomposite. *Fibers and Polymers*, 26(3), 1223–1236. <https://doi.org/10.1007/s12221-025-00880-w>
- Abdollahi, F., Jahadi, M., & Ghavami, M. (2021). Thermal stability of natural pigments produced by *Monascus purpureus* in submerged fermentation. *Food Science & Nutrition*, 9(9), 4855–4862. <https://doi.org/10.1002/fsn3.2425>
- Agarwal, H., Bajpai, S., Mishra, A., Kohli, I., Varma, A., Fouillaud, M., Dufossé, L., & Joshi, N. C. (2023). Bacterial Pigments and Their Multifaceted Roles in Contemporary Biotechnology and Pharmacological Applications. *Microorganisms*, 11(3), 614. <https://doi.org/10.3390/microorganisms11030614>
- Agudelo-Escobar, L. M., Gutiérrez-López, Y., & Urrego-Restrepo, S. (2017). Effects of aeration, agitation and pH on the production of mycelial biomass and exopolysaccharide from the filamentous fungus *Ganoderma lucidum*1. *DYNA*, 84(200), 72–79. <https://doi.org/10.15446/dyna.v84n200.57126>
- Ahmed, S., Rai, S., Datta, B., Chhetri, P., & Kumar, R. (2025). Molecular Insights into Bacterial Pigments. In R. K. Bhatia & A. Walia (Eds.), *Biocolours* (pp. 49–77). Springer Nature Singapore. https://doi.org/10.1007/978-981-95-1738-1_3
- Ahn, C., Zeng, X., Li, L., & Obendorf, S. K. (2014). Thermal degradation of natural dyes and their analysis using HPLC-DAD-MS. *Fashion and Textiles*, 1(1), 22. <https://doi.org/10.1186/s40691-014-0022-5>
- Akhtar, A. B. T., Naseem, S., Yasar, A., & Naseem, Z. (2021). Persistent Organic Pollutants (POPs): Sources, Types, Impacts, and Their Remediation. In R. Prasad (Ed.), *Environmental Pollution and Remediation* (pp. 213–246). Springer Singapore. https://doi.org/10.1007/978-981-15-5499-5_8
- Akter, T., Protity, A. T., Shaha, M., Al Mamun, M., & Hashem, A. (2023). The Impact of Textile Dyes on the Environment. In A. Ahmad, M. Jawaid, M. N. Mohamad Ibrahim, A. A. Yaqoob, & M. B. Alshammari (Eds.), *Nanohybrid Materials for Treatment of Textiles Dyes* (pp. 401–431). Springer Nature Singapore. https://doi.org/10.1007/978-981-99-3901-5_17

- Alzain, H., Kalimugogo, V., & Hussein, K. (2023). A Review of Environmental Impact of Azo Dyes. *International Journal of Research and Review*, 10(6), 64–689. <https://doi.org/10.52403/ijrr.20230682>
- Amorim, L. F. A., Gomes, A. P., & Gouveia, I. C. (2022). Design and Preparation of a Biobased Colorimetric pH Indicator from Cellulose and Pigments of Bacterial Origin, for Potential Application as Smart Food Packaging. *Polymers*, 14(18), 3869. <https://doi.org/10.3390/polym14183869>
- Amutha, K. (2025). Natural Dyes and Pigments for Sustainable Coloration of Textiles. In S. S. Muthu (Ed.), *Sustainable Coloration of Textiles* (pp. 147–170). Springer Nature Switzerland. https://doi.org/10.1007/978-3-031-91217-7_8
- Anshi, Kapil, S., Goswami, L., & Sharma, V. (2024). Unveiling the Intricacies of Microbial Pigments as Sustainable Alternatives to Synthetic Colorants: Recent Trends and Advancements. *Micro*, 4(4), 621–640. <https://doi.org/10.3390/micro4040038>
- Astudillo, Á., Rubilar, O., Briceño, G., Diez, M. C., & Schalchli, H. (2023). Advances in Agroindustrial Waste as a Substrate for Obtaining Eco-Friendly Microbial Products. *Sustainability*, 15(4), 3467. <https://doi.org/10.3390/su15043467>
- Bahram, M., Netherway, T., Frioux, C., Ferretti, P., Coelho, L. P., Geisen, S., Bork, P., & Hildebrand, F. (2021). Metagenomic assessment of the global diversity and distribution of bacteria and fungi. *Environmental Microbiology*, 23(1), 316–326. <https://doi.org/10.1111/1462-2920.15314>
- Barreto, J. V. D. O., Casanova, L. M., Junior, A. N., Reis-Mansur, M. C. P. P., & Vermelho, A. B. (2023). Microbial Pigments: Major Groups and Industrial Applications. *Microorganisms*, 11(12), 2920. <https://doi.org/10.3390/microorganisms11122920>
- Basto, B., Da Silva, N. R., Teixeira, J. A., & Silvério, S. C. (2025). Biotechnological production of natural pigments for textile dyeing. *Frontiers in Microbiology*, 16, 1677799. <https://doi.org/10.3389/fmicb.2025.1677799>
- Boateng, I. D. (2023). Application of Graphical Optimization, Desirability, and Multiple Response Functions in the Extraction of Food Bioactive Compounds. *Food Engineering Reviews*, 15(2), 309–328. <https://doi.org/10.1007/s12393-023-09339-1>
- Bonadio, M. D. P., Freita, L. A. D., & Mutton, M. J. R. (2018). Carotenoid production in sugarcane juice and synthetic media supplemented with nutrients by *Rhodotorula rubra*

102. *Brazilian Journal of Microbiology*, 49(4), 872–878.
<https://doi.org/10.1016/j.bjm.2018.02.010>
- Cappuccino, J. G., & Sherman, N. (2014). *Microbiology: A laboratory manual* (Version (10th ed.)). Pearson.
- Cavanaugh, N. T., Parthasarathy, A., Wong, N. H., Steiner, K. K., Chu, J., Adjei, J., & Hudson, A. O. (2021). Exiguobacterium sp. Is endowed with antibiotic properties against Gram positive and negative bacteria. *BMC Research Notes*, 14(1), 230.
<https://doi.org/10.1186/s13104-021-05644-2>
- Chaudhari, S. R., & Shirkhedkar, A. A. (2020). Application of Plackett-Burman and central composite designs for screening and optimization of factor influencing the chromatographic conditions of HPTLC method for quantification of efonidipine hydrochloride. *Journal of Analytical Science and Technology*, 11(1), 48.
<https://doi.org/10.1186/s40543-020-00246-2>
- Chauhan, A., & Jindal, T. (2020). Biochemical and Molecular Methods for Bacterial Identification. In A. Chauhan & T. Jindal, *Microbiological Methods for Environment, Food and Pharmaceutical Analysis* (pp. 425–468). Springer International Publishing.
https://doi.org/10.1007/978-3-030-52024-3_10
- Chavan, A., Pawar, J., Kakde, U., Venkatachalam, M., Fouillaud, M., Dufossé, L., & Deshmukh, S. K. (2025). Pigments from Microorganisms: A Sustainable Alternative for Synthetic Food Coloring. *Fermentation*, 11(7), 395.
<https://doi.org/10.3390/fermentation11070395>
- Chiu, C.-H., Lee, Y.-T., Wang, Y.-C., Yin, T., Kuo, S.-C., Yang, Y.-S., Chen, T.-L., Lin, J.-C., Wang, F.-D., & Fung, C.-P. (2015). A retrospective study of the incidence, clinical characteristics, identification, and antimicrobial susceptibility of bacteremic isolates of *Acinetobacter ursingii*. *BMC Infectious Diseases*, 15(1), 400.
<https://doi.org/10.1186/s12879-015-1145-z>
- Choi, S. Y., Lim, S., Yoon, K., Lee, J. I., & Mitchell, R. J. (2021). Biotechnological Activities and Applications of Bacterial Pigments Violacein and Prodigiosin. *Journal of Biological Engineering*, 15(1), 10. <https://doi.org/10.1186/s13036-021-00262-9>
- Chua, G. K., Mahadi, N. I. F., & Tan, F. H. Y. (2021). Bacterial Cellulose Production from Agro-Industrial and Food Wastes. In S. Shah, V. Venkatramanan, & R. Prasad (Eds.),

- Bio-valorization of Waste* (pp. 169–186). Springer Singapore.
https://doi.org/10.1007/978-981-15-9696-4_7
- Ciegler, A., Nelson, G. E. N., & Hall, H. H. (1963). Enhancement of β -Carotene Synthesis by Citrus Products. *Applied Microbiology*, *11*(2), 128–131.
<https://doi.org/10.1128/am.11.2.128-131.1963>
- Çobanoğlu, Ş., & Yazıcı, A. (2022). Isolation, Characterization, and Antibiofilm Activity of Pigments Synthesized by *Rhodococcus* sp. SC1. *Current Microbiology*, *79*(1), 15.
<https://doi.org/10.1007/s00284-021-02694-4>
- Cocato, A., Moens, L., & Vandenabeele, P. (2017). On the stability of mediaeval inorganic pigments: A literature review of the effect of climate, material selection, biological activity, analysis and conservation treatments. *Heritage Science*, *5*(1), 12.
<https://doi.org/10.1186/s40494-017-0125-6>
- Das, B. K., Jha, D. N., Sahu, S. K., Yadav, A. K., Raman, R. K., & Kartikeyan, M. (2023). Analysis of Variance (ANOVA) and Design of Experiments. In B. K. Das, D. N. Jha, S. K. Sahu, A. K. Yadav, R. K. Raman, & M. Kartikeyan, *Concept Building in Fisheries Data Analysis* (pp. 119–136). Springer Nature Singapore.
https://doi.org/10.1007/978-981-19-4411-6_7
- De Bruyne, K., Slabbinck, B., Waegeman, W., Vauterin, P., De Baets, B., & Vandamme, P. (2011). Bacterial species identification from MALDI-TOF mass spectra through data analysis and machine learning. *Systematic and Applied Microbiology*, *34*(1), 20–29.
<https://doi.org/10.1016/j.syapm.2010.11.003>
- De Oliveira, L. G., De Paiva, A. P., Balestrassi, P. P., Ferreira, J. R., Da Costa, S. C., & Da Silva Campos, P. H. (2019). Response surface methodology for advanced manufacturing technology optimization: Theoretical fundamentals, practical guidelines, and survey literature review. *The International Journal of Advanced Manufacturing Technology*, *104*(5–8), 1785–1837. <https://doi.org/10.1007/s00170-019-03809-9>
- Deng, J., Chen, Y., Lin, S., Shao, Y., Zou, Y., Zheng, Q., Guo, L., Lin, J., Chen, M., & Ye, Z. (2025). Molecular Regulation of Carotenoid Accumulation Enhanced by Oxidative Stress in the Food Industrial Strain *Blakeslea trispora*. *Foods*, *14*(9), 1452.
<https://doi.org/10.3390/foods14091452>

- Deveikaite, G., & Zvirdauskiene, R. (2023). Isolation and Characterisation of Pigments from Pigment-producing Microorganisms Isolated from Environment and Their Antibacterial Activity. *Rural Sustainability Research*, 49(344), 1–7. <https://doi.org/10.2478/plua-2023-0001>
- Dhruvi Sanghvi & Vidhu Sekhar P. (2025, March 29). *Analyzing the Contemporary Global Market Structure for Apparel and Textiles*.
- Di Salvo, E., Lo Vecchio, G., De Pasquale, R., De Maria, L., Tardugno, R., Vadalà, R., & Cicero, N. (2023). Natural Pigments Production and Their Application in Food, Health and Other Industries. *Nutrients*, 15(8), 1923. <https://doi.org/10.3390/nu15081923>
- Dutta et al. (2022). Effects of textile dyeing effluent on the environment and its treatment: A review. *Engineering and Applied Science Letters*, 5(1), 1–17. <https://doi.org/10.30538/psrp-easl2022.0080>
- Erickson, A. J., Weiss, P. T., & Gulliver, J. S. (2013). Water Sampling Methods. In A. J. Erickson, P. T. Weiss, & J. S. Gulliver, *Optimizing Stormwater Treatment Practices* (pp. 163–192). Springer New York. https://doi.org/10.1007/978-1-4614-4624-8_10
- Fahrmeir, L., Kneib, T., Lang, S., & Marx, B. D. (2021). *Regression: Models, Methods and Applications*. Springer Berlin Heidelberg. <https://doi.org/10.1007/978-3-662-63882-8>
- Failisnur, F., Sofyan, S., Kasim, A., & Tuty, A. (2018). Study of Cotton Fabric Dyeing Process With Some Mordant Methods By Using Gambier (*Uncaria gambir* Roxb) Extract. *International Journal on Advanced Science, Engineering and Information Technology*, 8(4), 1098. <https://doi.org/10.18517/ijaseit.8.4.4861>
- Fatima, M., & Anuradha, K. (2022). Isolation, Characterization, and Optimization Studies of Bacterial Pigments. *Journal of Pure and Applied Microbiology*, 16(2), 1039–1048. <https://doi.org/10.22207/JPAM.16.2.28>
- Fobiri GK. (2022). Synthetic Dye Application in Textiles: A Review on the Efficacies and Toxicities Involved. *Textile & Leather Review*, 5, 180–198. <https://doi.org/10.31881/TLR.2022.22>
- Fouillaud, M., & Dufossé, L. (2022). Microbial Secondary Metabolism and Biotechnology. *Microorganisms*, 10(1), 123. <https://doi.org/10.3390/microorganisms10010123>
- Gao, S., Surratt, J. D., Knipping, E. M., Edgerton, E. S., Shahgholi, M., & Seinfeld, J. H. (2006). Characterization of polar organic components in fine aerosols in the

- southeastern United States: Identity, origin, and evolution. *Journal of Geophysical Research: Atmospheres*, *111*(D14), 2005JD006601. <https://doi.org/10.1029/2005JD006601>
- Garcia, P. C., Esperança, M. N., Turquetti, J. R., & De Castro Peixoto, A. L. (2025). Carotenoid Degradation in Annatto Dye Wastewater Using an O₃/H₂O₂ Advanced Oxidation Process. *Processes*, *13*(3), 824. <https://doi.org/10.3390/pr13030824>
- Gemelli, S., Silveira, S. T., Paillière-Jiménez, M. E., Rios, A. D. O., & Brandelli, A. (2024). Production, Extraction and Partial Characterization of Natural Pigments from *Chryseobacterium* sp. Kr6 Growing on Feather Meal Biomass. *Biomass*, *4*(2), 530–542. <https://doi.org/10.3390/biomass4020028>
- Ghosh, S., & Banerjee, S. (2023). Microbial Pigments and Paints for Clean Environment. In A. Sarkar & I. A. Ahmed (Eds.), *Microbial products for future industrialization* (pp. 223–251). Springer Nature Singapore. https://doi.org/10.1007/978-981-99-1737-2_12
- Gillard, J. (2020). One-Way Analysis of Variance (ANOVA). In J. Gillard, *A First Course in Statistical Inference* (pp. 91–101). Springer International Publishing. https://doi.org/10.1007/978-3-030-39561-2_6
- GOMES, Gomes, M., Soares, G., & 2C2T – Centre for Textile Science and Technology, University of Minho, Campus de Azurém, Guimarães, Portugal. (2023). A Review of Bacterial Pigments: Harnessing Nature’s Colors for Functional Materials and Dyeing Processes. *Textile & Leather Review*, *6*, 167–190. <https://doi.org/10.31881/TLR.2023.016>
- Gondil, V. S., Asif, M., & Bhalla, T. C. (2017). Optimization of physicochemical parameters influencing the production of prodigiosin from *Serratia nematodiphila* RL2 and exploring its antibacterial activity. *3 Biotech*, *7*(5), 338. <https://doi.org/10.1007/s13205-017-0979-z>
- Gong, J., Ren, Y., Fu, R., Li, Z., & Zhang, J. (2017). pH-Mediated Antibacterial Dyeing of Cotton with Prodigiosins Nanomicelles Produced by Microbial Fermentation. *Polymers*, *9*(10), 468. <https://doi.org/10.3390/polym9100468>
- Grewal, J., Wołacewicz, M., Pyter, W., Joshi, N., Drewniak, L., & Pranaw, K. (2022). Colorful Treasure From Agro-Industrial Wastes: A Sustainable Chassis for Microbial

- Pigment Production. *Frontiers in Microbiology*, *13*, 832918. <https://doi.org/10.3389/fmicb.2022.832918>
- Haddix, P. L., & Shanks, R. M. Q. (2018). Prodigiosin pigment of *Serratia marcescens* is associated with increased biomass production. *Archives of Microbiology*, *200*(7), 989–999. <https://doi.org/10.1007/s00203-018-1508-0>
- Haider, A., Ringer, M., Kotroczo, Z., Mohácsi-Farkas, C., & Kocsis, T. (2023). The Current Level of MALDI-TOF MS Applications in the Detection of Microorganisms: A Short Review of Benefits and Limitations. *Microbiology Research*, *14*(1), 80–90. <https://doi.org/10.3390/microbiolres14010008>
- Hanina, M. N., Nabilah, A. S., Maryam, M. R., & Salina, M. R. (2018). *Morphological and biochemical characterization of pigment producing bacteria isolated from squid and Lala*. 020233. <https://doi.org/10.1063/1.5066874>
- Harshini, P., Varghese, R., Pachamuthu, K., & Ramamoorthy, S. (2025). Enhanced pigment production from plants and microbes: A genome editing approach. *3 Biotech*, *15*(5), 129. <https://doi.org/10.1007/s13205-025-04290-w>
- Hegazy, A. A., Abu-Hussien, S. H., Elsenosy, N. K., El-Sayed, S. M., & Abo El-Naga, M. Y. (2024). Optimization, characterization and biosafety of carotenoids produced from whey using *Micrococcus luteus*. *BMC Biotechnology*, *24*(1), 74. <https://doi.org/10.1186/s12896-024-00899-6>
- Hidayat, R. & Patricia Wulandari. (2021). Methods of Extraction: Maceration, Percolation and Decoction. *Eureka Herba Indonesia*, *2*(1), 73–79. <https://doi.org/10.37275/ehi.v2i1.15>
- Huang, X., Gan, L., He, Z., Jiang, G., & He, T. (2024). Bacterial Pigments as a Promising Alternative to Synthetic Colorants: From Fundamentals to Applications. *Journal of Microbiology and Biotechnology*, *34*(11), 2153–2165. <https://doi.org/10.4014/jmb.2404.04018>
- Iqbal Mahmud and hantanu Kaiser. (2020). Recent Progress in Waterless Textile Dyeing. *Journal of Textile Science & Engineering*, *10*(6), 1–3. <https://doi.org/10.37421/jtese.2020.10.421>
- Islam, T., Md. Rashedul Islam, K., Hossain, S., Abdul Jalil, M., & Mahbubul Bashar, M. (2024). Understanding the Fastness Issues of Natural Dyes. In B. Kumar (Ed.), *Dye*

- Chemistry—Exploring Colour From Nature to Lab.* IntechOpen.
<https://doi.org/10.5772/intechopen.1005363>
- Islam, T., Repon, Md. R., Islam, T., Sarwar, Z., & Rahman, M. M. (2022). Impact of textile dyes on health and ecosystem: A review of structure, causes, and potential solutions. *Environmental Science and Pollution Research*, 30(4), 9207–9242.
<https://doi.org/10.1007/s11356-022-24398-3>
- Jia, X., Liu, F., Zhao, K., Lin, J., Fang, Y., Cai, S., Lin, C., Zhang, H., Chen, L., & Chen, J. (2021). Identification of Essential Genes Associated With Prodigiosin Production in *Serratia marcescens* FZSF02. *Frontiers in Microbiology*, 12, 705853.
<https://doi.org/10.3389/fmicb.2021.705853>
- Johra, F. T., Bepari, A. K., Bristy, A. T., & Reza, H. M. (2020). A Mechanistic Review of β -Carotene, Lutein, and Zeaxanthin in Eye Health and Disease. *Antioxidants*, 9(11), 1046. <https://doi.org/10.3390/antiox9111046>
- Jufri, R. F. (2020). Microbial Isolation. *Journal La Lifesci*, 1(1), 18–23.
<https://doi.org/10.37899/journallalifesci.v1i1.33>
- Kamble, G. R., Hiremath, G. B., Hiremath, S. V., & Hiremath, M. B. (2022). Bacterial Pigments: An Untapped Colorful Microbial World. In S. I. Mulla & R. N. Bharagava (Eds.), *Enzymes for Pollutant Degradation* (Vol. 30, pp. 285–307). Springer Nature Singapore. https://doi.org/10.1007/978-981-16-4574-7_15
- Kandasamy, G. D., & Kathirvel, P. (2024). Production, characterization and in vitro biological activities of crude pigment from endophytic *Micrococcus luteus* associated with *Avicennia marina*. *Archives of Microbiology*, 206(1), 26.
<https://doi.org/10.1007/s00203-023-03751-1>
- Kantifedaki, A., Kachrimanidou, V., Mallouchos, A., Papanikolaou, S., & Koutinas, A. A. (2018a). Orange processing waste valorisation for the production of bio-based pigments using the fungal strains *Monascus purpureus* and *Penicillium purpurogenum*. *Journal of Cleaner Production*, 185, 882–890.
<https://doi.org/10.1016/j.jclepro.2018.03.032>
- Kantifedaki, A., Kachrimanidou, V., Mallouchos, A., Papanikolaou, S., & Koutinas, A. A. (2018b). Orange processing waste valorisation for the production of bio-based pigments using the fungal strains *Monascus purpureus* and *Penicillium purpurogenum*.

- Journal of Cleaner Production*, 185, 882–890.
<https://doi.org/10.1016/j.jclepro.2018.03.032>
- Kardile, N. B., Nanda, V., & Thakre, S. (2020). Thermal Degradation Kinetics of Total Carotenoid and Colour of Mixed Juice. *Agricultural Research*, 9(3), 400–409.
<https://doi.org/10.1007/s40003-019-00434-6>
- Kato, S., Yamagishi, A., Daimon, S., Kawasaki, K., Tamaki, H., Kitagawa, W., Abe, A., Tanaka, M., Sone, T., Asano, K., & Kamagata, Y. (2018). Isolation of Previously Uncultured Slow-Growing Bacteria by Using a Simple Modification in the Preparation of Agar Media. *Applied and Environmental Microbiology*, 84(19), e00807-18.
<https://doi.org/10.1128/AEM.00807-18>
- Kazi, Z., Hungund, B. S., Yaradoddi, J. S., Banapurmath, N. R., Yusuf, A. A., Kishore, K. L., Soudagar, M. E. M., Khan, T. M. Y., Elfasakhany, A., & Buyondo, K. A. (2022). Production, Characterization, and Antimicrobial Activity of Pigment from *Streptomyces* Species. *Journal of Nanomaterials*, 2022, 1–8.
<https://doi.org/10.1155/2022/3962301>
- Khattab, T. A., Abdelrahman, M. S., & Rehan, M. (2020). Textile dyeing industry: Environmental impacts and remediation. *Environmental Science and Pollution Research*, 27(4), 3803–3818. <https://doi.org/10.1007/s11356-019-07137-z>
- Kirby, B. M., Barnard, D., Marla Tuffin, I., & Cowan, D. A. (2011). Ecological Distribution of Microorganisms in Terrestrial, Psychrophilic Habitats. In K. Horikoshi (Ed.), *Extremophiles Handbook* (pp. 839–863). Springer Japan. https://doi.org/10.1007/978-4-431-53898-1_41
- Konar, A., & Datta, S. (2022). Strain Improvement of Microbes. In P. Verma (Ed.), *Industrial Microbiology and Biotechnology* (pp. 169–193). Springer Singapore. https://doi.org/10.1007/978-981-16-5214-1_6
- Kowalska, P., Mierzejewska, J., Skrzyszewska, P., Witkowska, A., Oksejuk, K., Sitkiewicz, E., Krawczyk, M., Świadek, M., Głuchowska, A., Marlicka, K., Sobiepanek, A., & Milner-Krawczyk, M. (2024). Extracellular vesicles of *Janthinobacterium lividum* as violacein carriers in melanoma cell treatment. *Applied Microbiology and Biotechnology*, 108(1), 529. <https://doi.org/10.1007/s00253-024-13358-1>

- Kramar, A., & Kostic, M. M. (2022). Bacterial Secondary Metabolites as Biopigments for Textile Dyeing. *Textiles*, 2(2), 252–264. <https://doi.org/10.3390/textiles2020013>
- Kusumlata, Ambade, B., Kumar, A., & Gautam, S. (2024). Sustainable Solutions: Reviewing the Future of Textile Dye Contaminant Removal with Emerging Biological Treatments. *Limnological Review*, 24(2), 126–149. <https://doi.org/10.3390/limnolrev24020007>
- Lau, W. X., Carvajal-Zarrabal, O., Nolasco-Hipólito, C., Kohej, M., Gregory, Z. A-A., Abdullah, M. O., Toh, S. C., & Lihan. S. (2018). Production of pigments by *Rhodotorula mucilaginosa*. *Malaysian Journal of Microbiology*. <https://doi.org/10.21161/mjm.144188>
- Lee, C.-C. (2025). Microbial Pigments: Fermentative Production and Biological Activities. In K. Sharma (Ed.), *Bio-prospecting of Novel Microbial Bioactive Compounds for Sustainable Development* (pp. 43–65). Springer Nature Switzerland. https://doi.org/10.1007/978-3-031-82178-3_4
- Lellis, B., Fávaro-Polonio, C. Z., Pamphile, J. A., & Polonio, J. C. (2019). Effects of textile dyes on health and the environment and bioremediation potential of living organisms. *Biotechnology Research and Innovation*, 3(2), 275–290. <https://doi.org/10.1016/j.biori.2019.09.001>
- Locks, E., Guelli Ulson De Souza, S. M. D. A., Da Silva Júnior, A. H., De Oliveira, C. R. S., & De Aguiar, C. R. L. (2025). Reactive Dyeing of Cotton Yarns by Exhaustion Method in an Oil-Based Medium Using Crude and Refined Soybean Oil. *Colorants*, 4(2), 11. <https://doi.org/10.3390/colorants4020011>
- López, G.-D., Álvarez-Rivera, G., Carazzone, C., Ibáñez, E., Leidy, C., & Cifuentes, A. (2023). Bacterial Carotenoids: Extraction, Characterization, and Applications. *Critical Reviews in Analytical Chemistry*, 53(6), 1239–1262. <https://doi.org/10.1080/10408347.2021.2016366>
- Lopez Marin, M. A., Strejcek, M., Junkova, P., Suman, J., Santrucek, J., & Uhlik, O. (2021). Exploring the Potential of *Micrococcus luteus* Culture Supernatant With Resuscitation-Promoting Factor for Enhancing the Culturability of Soil Bacteria. *Frontiers in Microbiology*, 12, 685263. <https://doi.org/10.3389/fmicb.2021.685263>

- López-Mora, D. J., Flores-Dávalos, A. G., Lorenzo-Santiago, M. A., Guardado-Fierros, B. G., Rodríguez-Campos, J., & Contreras-Ramos, S. M. (2025). Maximizing Biomass Production and Carotenoid-like Pigments Yield in *Kocuria sediminis* As04 Through Culture Optimization. *Microorganisms*, 13(7), 1555. <https://doi.org/10.3390/microorganisms13071555>
- Losinska-Sičiūnienė, R., Strazdaitė-Žiilienė, Ž., Pranckevičiūtė, S., & Servienė, E. (2025). Light and Temperature Effects on the Accumulation of Carotenoids in *Rhodotorula* spp. Yeasts. *Fermentation*, 11(7), 412. <https://doi.org/10.3390/fermentation11070412>
- Lu, W., Maidannyk, V. A., & Lim, A. S. L. (2020). Carotenoids degradation and precautions during processing. In *Carotenoids: Properties, Processing and Applications* (pp. 223–258). Elsevier. <https://doi.org/10.1016/B978-0-12-817067-0.00007-5>
- Lu, X., Li, W., Wang, Q., Wang, J., & Qin, S. (2023). Progress on the Extraction, Separation, Biological Activity, and Delivery of Natural Plant Pigments. *Molecules*, 28(14), 5364. <https://doi.org/10.3390/molecules28145364>
- Lyu, X., Lyu, Y., Yu, H., Chen, W., Ye, L., & Yang, R. (2022). Biotechnological advances for improving natural pigment production: A state-of-the-art review. *Bioresources and Bioprocessing*, 9(1), 8. <https://doi.org/10.1186/s40643-022-00497-4>
- Machmudah, S., & Goto, M. (2013). Methods for Extraction and Analysis of Carotenoids. In K. G. Ramawat & J.-M. Mérillon (Eds.), *Natural Products* (pp. 3367–3411). Springer Berlin Heidelberg. https://doi.org/10.1007/978-3-642-22144-6_145
- Maiorano, A. E., Da Silva, E. S., Perna, R. F., Ottoni, C. A., Piccoli, R. A. M., Fernandez, R. C., Maresma, B. G., & De Andrade Rodrigues, M. F. (2020). Effect of agitation speed and aeration rate on fructosyltransferase production of *Aspergillus oryzae* IPT-301 in stirred tank bioreactor. *Biotechnology Letters*, 42(12), 2619–2629. <https://doi.org/10.1007/s10529-020-03006-9>
- Manjula, D., Jeevitha, P., Ramya, I., Hemapriya, J., & Ravi, A. (2018). Biotechnological Applications of Halophilic Pigments – An Overview. *International Journal of Current Microbiology and Applied Sciences*, 7(07), 4392–4398. <https://doi.org/10.20546/ijcmas.2018.707.512>
- Maoka, T. (2020). Carotenoids as natural functional pigments. *Journal of Natural Medicines*, 74(1), 1–16. <https://doi.org/10.1007/s11418-019-01364-x>

- Marinkovic, V. (2020). A novel desirability function for multi-response optimization and its application in chemical engineering. *Chemical Industry and Chemical Engineering Quarterly*, 26(3), 309–319. <https://doi.org/10.2298/CICEQ190715007M>
- McDonough, R. J. (1997). Agitation in fermenters and bioreactors. In E. Goldberg (Ed.), *Handbook of Downstream Processing* (pp. 357–416). Springer Netherlands. https://doi.org/10.1007/978-94-009-1563-3_15
- McGoverin, C., Steed, C., Esan, A., Robertson, J., Swift, S., & Vanholsbeeck, F. (2021). Optical methods for bacterial detection and characterization. *APL Photonics*, 6(8), 080903. <https://doi.org/10.1063/5.0057787>
- McPherson, M. R., Wang, P., Marsh, E. L., Mitchell, R. B., & Schachtman, D. P. (2018). Isolation and Analysis of Microbial Communities in Soil, Rhizosphere, and Roots in Perennial Grass Experiments. *Journal of Visualized Experiments*, 137, 57932. <https://doi.org/10.3791/57932>
- Mehta, M., Sharma, M., Pathania, K., Jena, P. K., & Bhushan, I. (2021). Degradation of synthetic dyes using nanoparticles: A mini-review. *Environmental Science and Pollution Research*, 28(36), 49434–49446. <https://doi.org/10.1007/s11356-021-15470-5>
- Mendes-Silva, T. D. C. D., Andrade, R. F. D. S., Ootani, M. A., Mendes, P. V. D., Sá, R. A. D. Q. C. D., Silva, M. R. F. D., Souza, K. S., Correia, M. T. D. S., Silva, M. V. D., & Oliveira, M. B. M. D. (2020). Biotechnological Potential of Carotenoids Produced by Extremophilic Microorganisms and Application Prospects for the Cosmetics Industry. *Advances in Microbiology*, 10(08), 397–410. <https://doi.org/10.4236/aim.2020.108029>
- Mohammed, A. M. (2018). UV-Visible Spectrophotometric Method and Validation of Organic Compounds. *European Journal of Engineering Research and Science*, 3(3), 8. <https://doi.org/10.24018/ejers.2018.3.3.622>
- Mohd Said, F. (2025). Production of Microbial Pigment in a Bioreactor. In J.-M. Mérillon & K. G. Ramawat (Eds.), *Plant Specialized Metabolites* (pp. 1135–1152). Springer Nature Switzerland. https://doi.org/10.1007/978-3-031-51158-5_40
- Molina, A. K., Corrêa, R. C. G., Prieto, M. A., Pereira, C., & Barros, L. (2023). Bioactive Natural Pigments' Extraction, Isolation, and Stability in Food Applications. *Molecules*, 28(3), 1200. <https://doi.org/10.3390/molecules28031200>

- Mouro, C., Gomes, A. P., Costa, R. V., Moghtader, F., & Gouveia, I. C. (2023). The Sustainable Bioactive Dyeing of Textiles: A Novel Strategy Using Bacterial Pigments, Natural Antibacterial Ingredients, and Deep Eutectic Solvents. *Gels*, 9(10), 800. <https://doi.org/10.3390/gels9100800>
- Możejko-Ciesielska, J. (2025). Eco-Innovations in Biopigment Production by Bacteria—Challenges and Future Prospects. *Sustainability*, 17(21), 9897. <https://doi.org/10.3390/su17219897>
- Munsell. (2010). *Munsell Soil Color Charts*. Grand Rapids. Munsell Color System; Color Matching from Munsell Color Company
- Muthusamy, S., Udhayabaskar, S., Udayakumar, G. P., Kirthikaa, G. B., & Sivarajasekar, N. (2020). Properties and Applications of Natural Pigments Produced from Different Biological Sources—A Concise Review. In V. Sivasubramanian, A. Pugazhendhi, & I. G. Moorthy (Eds.), *Sustainable Development in Energy and Environment* (pp. 105–119). Springer Singapore. https://doi.org/10.1007/978-981-15-4638-9_9
- Nagendrappa, G. (2010). Sir William Henry Perkin: The man and his ‘Mauve.’ *Resonance*, 15(9), 779–793. <https://doi.org/10.1007/s12045-010-0088-3>
- Napoli, C., Marcotrigiano, V., & Montagna, M. T. (2012). Air sampling procedures to evaluate microbial contamination: A comparison between active and passive methods in operating theatres. *BMC Public Health*, 12(1), 594. <https://doi.org/10.1186/1471-2458-12-594>
- Nasha Musa, N., & Zulaikha Yusof, N. (2019). Chemical and Physical Parameters Affecting Bacterial Pigment Production. *Materials Today: Proceedings*, 19, 1608–1617. <https://doi.org/10.1016/j.matpr.2019.11.189>
- Negi, A. (2025). Environmental Impact of Textile Materials: Challenges in Fiber–Dye Chemistry and Implication of Microbial Biodegradation. *Polymers*, 17(7), 871. <https://doi.org/10.3390/polym17070871>
- Negi, A. (2025). Natural Dyes and Pigments: Sustainable Applications and Future Scope. *Sustainable Chemistry*, 6(3), 23. <https://doi.org/10.3390/suschem6030023>
- Neha, T., Shishir, T., & Ashutosh, D. (2017). Fourier transform infrared spectroscopy (FTIR) profiling of red pigment produced by *Bacillus subtilis* PD5. *African Journal of Biotechnology*, 16(27), 1507–1512. <https://doi.org/10.5897/AJB2017.15959>

- Ngamwonglumlert, L., Devahastin, S., & Chiewchan, N. (2017). Natural colorants: Pigment stability and extraction yield enhancement via utilization of appropriate pretreatment and extraction methods. *Critical Reviews in Food Science and Nutrition*, 57(15), 3243–3259. <https://doi.org/10.1080/10408398.2015.1109498>
- Njuguna, M. J., Muriuki, M., & Karenga, S. (2022). Attenuated Total Reflectance –Fourier Transform Infrared (ATR-FTIR) Analysis of *Ocimum kenyense* Essential Oils. *International Journal of Pure and Applied Chemistry*, 1(1), 1–10. <https://doi.org/10.37284/ijpac.1.1.722>
- Nor, N. M., Mohamed, M. S., Loh, T. C., Foo, H. L., Rahim, R. A., Tan, J. S., & Mohamad, R. (2017). Comparative analyses on medium optimization using *one-factor-at-a-time*, response surface methodology, and artificial neural network for lysine–methionine biosynthesis by *Pediococcus pentosaceus* RF-1. *Biotechnology & Biotechnological Equipment*, 31(5), 935–947. <https://doi.org/10.1080/13102818.2017.1335177>
- Omar et al. (2019). Agro-industrial Orange Waste as a Low Cost Substrate for Carotenoids Production by *Rhodotorula mucilagenosa*. *Assiut Journal of Agricultural Sciences*, 50(1), 62–74. <https://doi.org/10.21608/ajas.2019.33459>
- Ontman, R., Groffman, P. M., Driscoll, C. T., & Cheng, Z. (2023). Surprising relationships between soil pH and microbial biomass and activity in a northern hardwood forest. *Biogeochemistry*, 163(3), 265–277. <https://doi.org/10.1007/s10533-023-01031-0>
- Pacciani-Mori, L., Giometto, A., Suweis, S., & Maritan, A. (2020). Dynamic metabolic adaptation can promote species coexistence in competitive microbial communities. *PLOS Computational Biology*, 16(5), e1007896. <https://doi.org/10.1371/journal.pcbi.1007896>
- Padhan, B., Poddar, K., Sarkar, D., & Sarkar, A. (2021). Production, purification, and process optimization of intracellular pigment from novel psychrotolerant *Paenibacillus* sp. BPW19. *Biotechnology Reports*, 29, e00592. <https://doi.org/10.1016/j.btre.2021.e00592>
- Parrilli, E., Tutino, M. L., & Marino, G. (2022). Biofilm as an adaptation strategy to extreme conditions. *Rendiconti Lincei. Scienze Fisiche e Naturali*, 33(3), 527–536. <https://doi.org/10.1007/s12210-022-01083-8>

- Paul, T., Mondal, A., Bandyopadhyay, T. K., & Bhunia, B. (2024). Prodigiosin production and recovery from *Serratia marcescens*: Process development and cost–benefit analysis. *Biomass Conversion and Biorefinery*, *14*(3), 4091–4110. <https://doi.org/10.1007/s13399-022-02639-2>
- Peerhossaini, H. (2022). Effects of Turbulent Mixing and Orbitally Shaking on Cell Growth and Biomass Production in Active Fluids. *American Journal of Biomedical Science & Research*, *15*(4). <https://doi.org/10.34297/AJBSR.2022.15.002129>
- Pei, L., Zhu, H., Gong, S., Dong, W., Zhu, L., & Wang, J. (2024). Comprehensive analysis of dye adsorption and supramolecular interaction between dyes and cotton fibers in non-aqueous media/less water dyeing system. *Industrial Crops and Products*, *222*, 119955. <https://doi.org/10.1016/j.indcrop.2024.119955>
- Pisareva, E. I., & Kujumdzieva, A. V. (2010). Influence of Carbon and Nitrogen Sources on Growth and Pigment Production by *Monascus Pilosus* C₁ Strain. *Biotechnology & Biotechnological Equipment*, *24*(sup1), 501–506. <https://doi.org/10.1080/13102818.2010.10817890>
- Pitt, T. L., Malnick, H., Shah, J., Chattaway, M. A., Keys, C. J., Cooke, F. J., & Shah, H. N. (2007). Characterisation of *Exiguobacterium aurantiacum* isolates from blood cultures of six patients. *Clinical Microbiology and Infection*, *13*(9), 946–948. <https://doi.org/10.1111/j.1469-0691.2007.01779.x>
- Pizzicato, B., Pacifico, S., Cayuela, D., Mijas, G., & Riba-Moliner, M. (2023). Advancements in Sustainable Natural Dyes for Textile Applications: A Review. *Molecules*, *28*(16), 5954. <https://doi.org/10.3390/molecules28165954>
- Poddar, K., Padhan, B., Sarkar, D., & Sarkar, A. (2021). Purification and optimization of pink pigment produced by newly isolated bacterial strain *Enterobacter* sp. PWN1. *SN Applied Sciences*, *3*(1), 105. <https://doi.org/10.1007/s42452-021-04146-x>
- Ramamurthy, K., Priya, P. S., Murugan, R., & Arockiaraj, J. (2024). Hues of risk: Investigating genotoxicity and environmental impacts of azo textile dyes. *Environmental Science and Pollution Research*, *31*(23), 33190–33211. <https://doi.org/10.1007/s11356-024-33444-1>

- Ramesh, C., Prasastha, V. R., Venkatachalam, M., & Dufossé, L. (2022). Natural Substrates and Culture Conditions to Produce Pigments from Potential Microbes in Submerged Fermentation. *Fermentation*, 8(9), 460. <https://doi.org/10.3390/fermentation8090460>
- Ramesh, C., Vinithkumar, N., Kirubakaran, R., Venil, C., & Dufossé, L. (2019). Multifaceted Applications of Microbial Pigments: Current Knowledge, Challenges and Future Directions for Public Health Implications. *Microorganisms*, 7(7), 186. <https://doi.org/10.3390/microorganisms7070186>
- Ramos, G. L. de P. A., Vigoder, H. C., & Nascimento, J. dos S. (2021). Kocuria spp. in Foods: Biotechnological Uses and Risks for Food Safety. *Applied Food Biotechnology*, 8(2), 79–88. <https://doi.org/10.22037/afb.v8i2.30748>
- Rao, A. S., Deka, S. P., More, S. S., Nair, A., More, V. S., & Ananthjaraju, K. S. (2021). A Comprehensive Review on Different Microbial-Derived Pigments and Their Multipurpose Activities. In A. Vaishnav & D. K. Choudhary (Eds.), *Microbial Polymers* (pp. 479–519). Springer Singapore. https://doi.org/10.1007/978-981-16-0045-6_20
- Rehman, N. N. M. A., & Dixit, P. P. (2020). Influence of light wavelengths, light intensity, temperature, and pH on biosynthesis of extracellular and intracellular pigment and biomass of *Pseudomonasaeruginosa* NR1. *Journal of King Saud University - Science*, 32(1), 745–752. <https://doi.org/10.1016/j.jksus.2019.01.004>
- Repon, Md. R., Dev, B., Rahman, M. A., Jurkonienė, S., Haji, A., Alim, Md. A., & Kumpikaitė, E. (2024). Textile dyeing using natural mordants and dyes: A review. *Environmental Chemistry Letters*, 22(3), 1473–1520. <https://doi.org/10.1007/s10311-024-01716-4>
- Ribeiro, D., Freitas, M., Silva, A. M. S., Carvalho, F., & Fernandes, E. (2018). Antioxidant and pro-oxidant activities of carotenoids and their oxidation products. *Food and Chemical Toxicology*, 120, 681–699. <https://doi.org/10.1016/j.fct.2018.07.060>
- Rifna, E. J., Misra, N. N., & Dwivedi, M. (2023). Recent advances in extraction technologies for recovery of bioactive compounds derived from fruit and vegetable waste peels: A review. *Critical Reviews in Food Science and Nutrition*, 63(6), 719–752. <https://doi.org/10.1080/10408398.2021.1952923>

- Rothschild, L. J., & Mancinelli, R. L. (2001). Life in extreme environments. *Nature*, 409(6823), 1092–1101. <https://doi.org/10.1038/35059215>
- Saha, S., Singh, J., Paul, A., Sarkar, R., Khan, Z., & Banerjee, K. (2020). Anthocyanin Profiling Using UV-Vis Spectroscopy and Liquid Chromatography Mass Spectrometry. *Journal of AOAC INTERNATIONAL*, 103(1), 23–39. <https://doi.org/10.5740/jaoacint.19-0201>
- Sajjad, W., Din, G., Rafiq, M., Iqbal, A., Khan, S., Zada, S., Ali, B., & Kang, S. (2020). Pigment production by cold-adapted bacteria and fungi: Colorful tale of cryosphere with wide range applications. *Extremophiles*, 24(4), 447–473. <https://doi.org/10.1007/s00792-020-01180-2>
- Samanta, P. (2020). A Review on Application of Natural Dyes on Textile Fabrics and Its Revival Strategy. In A. Kumar Samanta, N. S. Awwad, & H. Majdooa Algarni (Eds.), *Chemistry and Technology of Natural and Synthetic Dyes and Pigments*. IntechOpen. <https://doi.org/10.5772/intechopen.90038>
- Sebastian, L., Paul, A. M., & Jayanthi, D. (2022). Isolation and Production of Prodigiosin Pigments from *Streptomyces* spp. In D. Dharumadurai (Ed.), *Methods in Actinobacteriology* (pp. 683–693). Springer US. https://doi.org/10.1007/978-1-0716-1728-1_100
- Sen, T., Barrow, C. J., & Deshmukh, S. K. (2019). Microbial Pigments in the Food Industry—Challenges and the Way Forward. *Frontiers in Nutrition*, 6, 7. <https://doi.org/10.3389/fnut.2019.00007>
- Sengupta, S., & Bhowal, J. (2022). Characterization of a blue-green pigment extracted from *Pseudomonas aeruginosa* and its application in textile and paper dyeing. *Environmental Science and Pollution Research*, 30(11), 30343–30357. <https://doi.org/10.1007/s11356-022-24241-9>
- Shahin, Y. H., Elwakil, B. H., Ghareeb, D. A., & Olama, Z. A. (2022). *Micrococcus lylae* MW407006 Pigment: Production, Optimization, Nano-Pigment Synthesis, and Biological Activities. *Biology*, 11(8), 1171. <https://doi.org/10.3390/biology11081171>
- Sharma, A., Dev, K., Sourirajan, A., & Choudhary, M. (2021). Isolation and characterization of salt-tolerant bacteria with plant growth-promoting activities from saline agricultural

- fields of Haryana, India. *Journal of Genetic Engineering and Biotechnology*, 19(1), 99. <https://doi.org/10.1186/s43141-021-00186-3>
- Siddiqua, U., Ali, S., Hussain, T., Bhatti, H., & Asghar, M. (2017). The Dyeing Process and the Environment: Enhanced Dye Fixation on Cellulosic Fabric Using Newly Synthesized Reactive Dye. *Polish Journal of Environmental Studies*, 26(5), 2215–2222. <https://doi.org/10.15244/pjoes/68430>
- Silva-Castro, G. A., Moyo, A. C., Khumalo, L., Van Zyl, L. J., Petrik, L. F., & Trindade, M. (2019). Factors influencing pigment production by halophilic bacteria and its effect on brine evaporation rates. *Microbial Biotechnology*, 12(2), 334–345. <https://doi.org/10.1111/1751-7915.13319>
- Simsek Geyik, M., Efe, D., & Gormez, A. (2024). Identification of Bacteria Producing Red Pigments and Their Application in the Textile Industry. *Arabian Journal for Science and Engineering*. <https://doi.org/10.1007/s13369-024-09290-1>
- Singha, K., Pandit, P., Maity, S., & Sharma, S. R. (2021). Harmful environmental effects for textile chemical dyeing practice. In *Green Chemistry for Sustainable Textiles* (pp. 153–164). Elsevier. <https://doi.org/10.1016/B978-0-323-85204-3.00005-1>
- Slama, H. B., Chenari Bouket, A., Pourhassan, Z., Alenezi, F. N., Silini, A., Cherif-Silini, H., Oszako, T., Luptakova, L., Golińska, P., & Belbahri, L. (2021). Diversity of Synthetic Dyes from Textile Industries, Discharge Impacts and Treatment Methods. *Applied Sciences*, 11(14), 6255. <https://doi.org/10.3390/app11146255>
- Soren, J. P., Paul, T., Banerjee, A., Mondal, K. C., & Mohapatra, P. K. D. (2020). Exploitation of Agricultural Waste as Sole Substrate for Production of Bacterial L-Glutaminase Under Submerged Fermentation and the Proficient Application of Fermented Hydrolysate as Growth Promoting Agent for Probiotic Organisms. *Waste and Biomass Valorization*, 11(8), 4245–4257. <https://doi.org/10.1007/s12649-019-00761-3>
- Su, L., Nian, Y., & Li, C. (2023). Microencapsulation to improve the stability of natural pigments and their applications for meat products. *Food Materials Research*, 3(1), 0–0. <https://doi.org/10.48130/FMR-2023-0010>
- Szadkowski, B., Kuśmierk, M., Śliwka-Kaszyńska, M., & Marzec, A. (2022). Structure and Stability Characterization of Natural Lake Pigments Made from Plant Extracts and

- Their Potential Application in Polymer Composites for Packaging Materials. *Materials*, 15(13), 4608. <https://doi.org/10.3390/ma15134608>
- Udensi, J., Loughman, J., Loskutova, E., & Byrne, H. J. (2022). Raman Spectroscopy of Carotenoid Compounds for Clinical Applications—A Review. *Molecules*, 27(24), 9017. <https://doi.org/10.3390/molecules27249017>
- Venil, C. K., Devi, P. R., & Ahmad, W. A. (2020). Agro-Industrial Waste as Substrates for the Production of Bacterial Pigment. In Z. A. Zakaria, R. Boopathy, & J. R. Dib (Eds.), *Valorisation of Agro-industrial Residues – Volume I: Biological Approaches* (pp. 149–162). Springer International Publishing. https://doi.org/10.1007/978-3-030-39137-9_7
- Venil, C. K., Dufossé, L., & Renuka Devi, P. (2020). Bacterial Pigments: Sustainable Compounds With Market Potential for Pharma and Food Industry. *Frontiers in Sustainable Food Systems*, 4, 100. <https://doi.org/10.3389/fsufs.2020.00100>
- Venil, C. K., Dufossé, L., Velmurugan, P., Malathi, M., & Lakshmanaperumalsamy, P. (2021). Extraction and Application of Pigment from *Serratia marcescens* SB08, an Insect Enteric Gut Bacterium, for Textile Dyeing. *Textiles*, 1(1), 21–36. <https://doi.org/10.3390/textiles1010003>
- Venil, C. K., Yusof, N. Z., Aruldass, C. A., & Ahmad, W.-A. (2016). Application of violet pigment from *Chromobacterium violaceum* UTM5 in textile dyeing. *Biologia*, 71(2), 121–127. <https://doi.org/10.1515/biolog-2016-0031>
- Venil, C. K., Zakaria, Z. A., & Ahmad, W. A. (2013). Bacterial pigments and their applications. *Process Biochemistry*, 48(7), 1065–1079. <https://doi.org/10.1016/j.procbio.2013.06.006>
- Villa, F., Wu, Y.-L., Zerboni, A., & Cappitelli, F. (2022). In Living Color: Pigment-Based Microbial Ecology At the Mineral–Air Interface. *BioScience*, 72(12), 1156–1175. <https://doi.org/10.1093/biosci/biac091>
- Vishnivetskaya, T. A., Kathariou, S., & Tiedje, J. M. (2009). The *Exiguobacterium* genus: Biodiversity and biogeography. *Extremophiles*, 13(3), 541–555. <https://doi.org/10.1007/s00792-009-0243-5>
- Wang, G., Li, Q., Zhang, Z., Yin, X., Wang, B., & Yang, X. (2023). Recent progress in adaptive laboratory evolution of industrial microorganisms. *Journal of Industrial*

- Microbiology and Biotechnology*, 50(1), kuac023.
<https://doi.org/10.1093/jimb/kuac023>
- Wang, X., Jiang, J., & Gao, W. (2022). Reviewing textile wastewater produced by industries: Characteristics, environmental impacts, and treatment strategies. *Water Science and Technology*, 85(7), 2076–2096. <https://doi.org/10.2166/wst.2022.088>
- Wang, Y., Liu, J., Yi, Y., Zhu, L., Liu, M., Zhang, Z., Xie, Q., & Jiang, L. (2024). Insights into the synthesis, engineering, and functions of microbial pigments in *Deinococcus* bacteria. *Frontiers in Microbiology*, 15, 1447785. <https://doi.org/10.3389/fmicb.2024.1447785>
- Wani, A. K., Akhtar, N., Sher, F., Navarrete, A. A., & Américo-Pinheiro, J. H. P. (2022). Microbial adaptation to different environmental conditions: Molecular perspective of evolved genetic and cellular systems. *Archives of Microbiology*, 204(2), 144. <https://doi.org/10.1007/s00203-022-02757-5>
- Wechselberger, P., Sagmeister, P., & Herwig, C. (2013). Real-time estimation of biomass and specific growth rate in physiologically variable recombinant fed-batch processes. *Bioprocess and Biosystems Engineering*, 36(9), 1205–1218. <https://doi.org/10.1007/s00449-012-0848-4>
- White, R. A., Soles, S. A., Gavelis, G., Gosselin, E., Slater, G. F., Lim, D. S. S., Leander, B., & Suttle, C. A. (2019). The Complete Genome and Physiological Analysis of the Eurythermal Firmicute *Exiguobacterium chiriqhucha* Strain RW2 Isolated From a Freshwater Microbialite, Widely Adaptable to Broad Thermal, pH, and Salinity Ranges. *Frontiers in Microbiology*, 9, 3189. <https://doi.org/10.3389/fmicb.2018.03189>
- Whitman, W. B., Rainey, F. A., Kämpfer, P., Trujillo, M. E., DeVos, P., Hedlund, B., & Dedysh, S. (Eds.). (2015). *Bergey's Manual of Systematics of Archaea and Bacteria* (1st ed.). Wiley. <https://doi.org/10.1002/9781118960608>
- Wijesekara, T., & Xu, B. (2024). A critical review on the stability of natural food pigments and stabilization techniques. *Food Research International*, 179, 114011. <https://doi.org/10.1016/j.foodres.2024.114011>
- Xu, F., Zhang, Z., Zhao, Z., Ji, X., Liu, J., & Song, X. (2024). Dyeing Performance and Color Evaluation of Cotton Fabrics Dyed with *Caesalpinia sappan* L. and *Galla chinensis*

- Mill. Extract, and the Evaluation of Binary Sequential Dyeing Method. *Fibers and Polymers*, 25(3), 1023–1046. <https://doi.org/10.1007/s12221-024-00481-z>
- Yadav, K. S., & Prabha, R. (2014). Effect of Ph and Temperature on Carotenoid Pigments produced from *Rhodotorula Minuta*. *International Journal of Fermented Foods*, 3(2), 105. <https://doi.org/10.5958/2321-712X.2014.01312.X>
- Yang, X., Hu, W., Xiu, Z., Jiang, A., Yang, X., Saren, G., Ji, Y., Guan, Y., & Feng, K. (2020). Effect of salt concentration on microbial communities, physicochemical properties and metabolite profile during spontaneous fermentation of Chinese northeast sauerkraut. *Journal of Applied Microbiology*, 129(6), 1458–1471. <https://doi.org/10.1111/jam.14786>
- Yaseen, D. A., & Scholz, M. (2019). Textile dye wastewater characteristics and constituents of synthetic effluents: A critical review. *International Journal of Environmental Science and Technology*, 16(2), 1193–1226. <https://doi.org/10.1007/s13762-018-2130-z>
- Yuan, N., Wang, C., & Pei, Y. (2016). Bacterial toxicity assessment of drinking water treatment residue (DWTR) and lake sediment amended with DWTR. *Journal of Environmental Management*, 182, 21–28. <https://doi.org/10.1016/j.jenvman.2016.07.053>
- Zhang, R., Zhang, Y., Zhang, T., Xu, M., Wang, H., Zhang, S., Zhang, T., Zhou, W., & Shi, G. (2022). Establishing a MALDI-TOF-TOF-MS method for rapid identification of three common Gram-positive bacteria (*Bacillus cereus*, *Listeria monocytogenes*, and *Micrococcus luteus*) associated with foodborne diseases. *Food Science and Technology*, 42, e117021. <https://doi.org/10.1590/fst.117021>
- Zhu, R., Cao, Y., Chen, L., Shi, G., Huang, Z., Xiao, M., Wang, X., Gong, J., Cai, Z., & Zhai, S. (2025). Sustainable and high-exhaustion dyeing for cotton fabrics using biomass-based keratin modification. *Cellulose*, 32(3), 2055–2071. <https://doi.org/10.1007/s10570-025-06378-1>

APPENDICES

Supplementary Table 1 Triplicate OD₆₀₀ measurements of three isolates across utilized AWEs

AWE	Isolate	read 1	read 2	read 3
cabbage	<i>Kocuria</i> sp.	0.445	0.442	0.443
cabbage	<i>Micrococcus luteus</i>	0.544	0.544	0.543
cabbage	<i>Exiguobacterium aurantiacum</i>	0.404	0.405	0.405
nutrient broth	<i>Kocuria rosea</i>	0.615	0.612	0.62
nutrient broth	<i>Micrococcus luteus</i>	0.646	0.645	0.646
nutrient broth	<i>Exiguobacterium aurantiacum</i>	0.524	0.523	0.523
onion	<i>Kocuria</i> sp.	0.199	0.198	0.198
onion	<i>Micrococcus luteus</i>	0.299	0.299	0.298
onion	<i>Exiguobacterium aurantiacum</i>	0.215	0.212	0.214
papaya	<i>Kocuria</i> sp.	0.235	0.234	0.235
papaya	<i>Micrococcus luteus</i>	0.24	0.241	0.24
papaya	<i>Exiguobacterium aurantiacum</i>	0.165	0.165	0.163
cannon ball cabbage	<i>Kocuria</i> sp.	0.455	0.453	0.45
cannon ball cabbage	<i>Micrococcus luteus</i>	0.545	0.544	0.543
cannon ball cabbage	<i>Exiguobacterium aurantiacum</i>	0.435	0.433	0.436
watermelon	<i>Kocuria</i> sp.	0.375	0.372	0.374
watermelon	<i>Micrococcus luteus</i>	0.423	0.424	0.424
watermelon	<i>Exiguobacterium aurantiacum</i>	0.435	0.425	0.435
carrot	<i>Kocuria</i> sp.	0.355	0.356	0.352
carrot	<i>Micrococcus luteus</i>	0.333	0.332	0.332
carrot	<i>Exiguobacterium aurantiacum</i>	0.335	0.334	0.335
tomato	<i>Kocuria</i> sp.	0.555	0.552	0.556
tomato	<i>Micrococcus luteus</i>	0.624	0.625	0.625
tomato	<i>Exiguobacterium aurantiacum</i>	0.525	0.522	0.526
potato	<i>Kocuria</i> sp.	0.325	0.325	0.326
potato	<i>Micrococcus luteus</i>	0.308	0.309	0.309
potato	<i>Exiguobacterium aurantiacum</i>	0.455	0.465	0.465
orange	<i>Kocuria</i> sp.	0.545	0.547	0.546
orange	<i>Micrococcus luteus</i>	0.861	0.863	0.862
orange	<i>Exiguobacterium aurantiacum</i>	0.514	0.51	0.512
bread leftover	<i>Kocuria</i> sp.	0.078	0.082	0.079
bread leftover	<i>Micrococcus luteus</i>	0.071	0.069	0.072
bread leftover	<i>Exiguobacterium aurantiacum</i>	0.063	0.062	0.063
banana	<i>Kocuria</i> sp.	0.051	0.053	0.051

banana	<i>Micrococcus luteus</i>	0.045	0.046	0.044
banana	<i>Exiguobacterium aurantiacum</i>	0.061	0.06	0.06
beetroot	<i>Kocuria</i> sp.	0.075	0.074	0.073
beetroot	<i>Micrococcus luteus</i>	0.068	0.071	0.071
beetroot	<i>Exiguobacterium aurantiacum</i>	0.056	0.055	0.054

Supplementary dummy Table 2 Quantitative analysis of dye exhaustion and fixation

Fabric	Initial absorbance of the dye bath at λ_{max} (Ao)	Absorbance of remaining dye bath (Af)	Absorbance of wash liquid (Aw)	% dye absorbed (Ao-Af)/Ao*100	% dye fixed (Ao-Aw)/Ao*100
cotton	0.207	0.052	0.094		
Tetron 6000	0.207	0.072	0.13		

Supplementary Table 3 Bacterial isolates tolerance to Environmental factors (OD₆₀₀ values), which reflect their growth under each condition

Isolate	Temperature (°C)					
	20	25	28	32	37	45
PPPI-1	0.293	0.556	0.664	0.615	0.6	0.231
PPPI-2	0.122	0.252	0.278	0.493	0.656	0.43
PPPI-3	0.203	0.327	0.392	0.456	0.345	0.168
PPPI-4	0.057	0.28	0.435	0.636	0.723	0.532
PPPI-5	0.026	0.042	0.452	0.677	0.86	0.725
PPPI-6	0.495	0.642	0.754	0.707	0.735	0.45
Isolate	pH					
	4.5	6	7	8	10	
PPPI-1	0.022	0.26	0.631	0.511	0.392	
PPPI-2	0.032	0.359	0.64	0.511	0.327	
PPPI-3	0.115	0.376	0.615	0.544	0.327	
PPPI-4	0.064	0.206	0.522	0.45	0.4	
PPPI-5	0.028	0.253	0.585	0.409	0.392	
PPPI-6	0.197	0.375	0.602	0.545	0.38	
Isolate	Salt Conc. (% NaCl)					
	0.5	1	2	3	4	5
PPPI-1	0.092	0.19	0.237	0.245	0.275	0.295
PPPI-2	0.121	0.199	0.185	0.135	0.156	0.115
PPPI-3	0.131	0.244	0.194	0.22	0.268	0.223

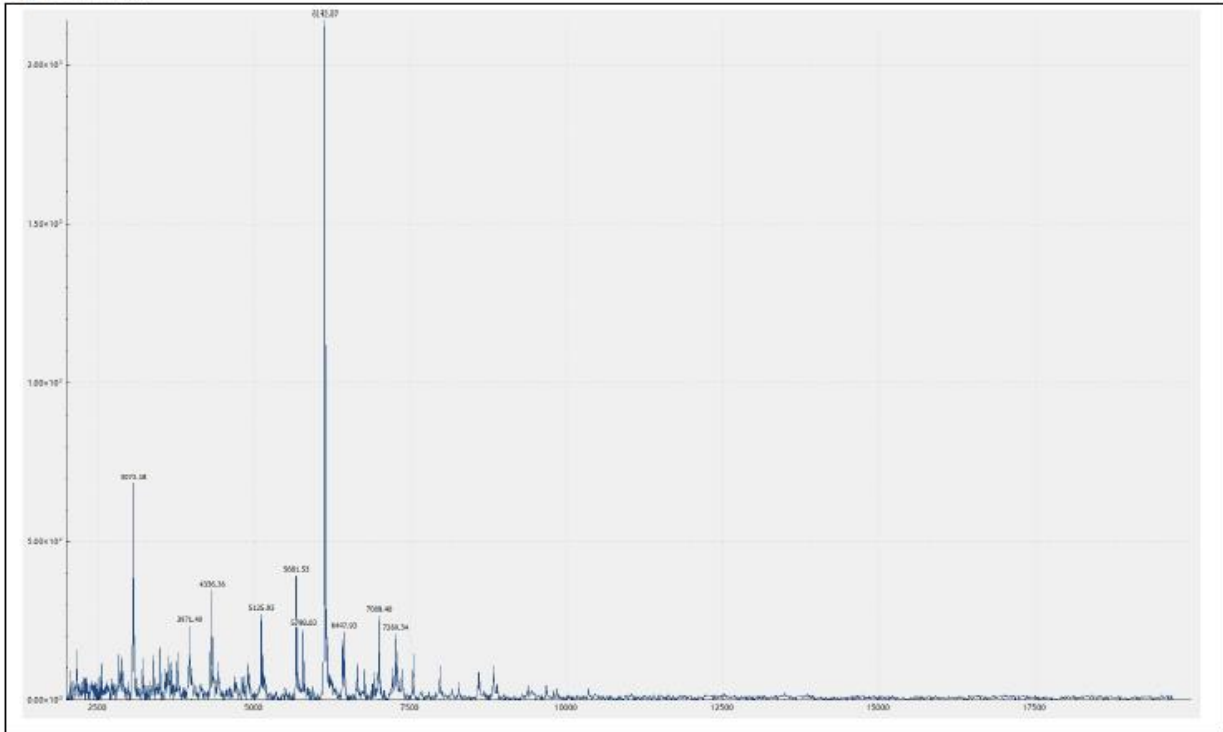
PPPI-4	0.169	0.298	0.341	0.329	0.334	0.4
PPPI-5	0.129	0.351	0.355	0.365	0.455	0.468
PPPI-6	0.134	0.145	0.279	0.289	0.31	0.355
Isolate	Agitation (rpm)					
	30	60	90	120	150	
PPPI-1	0.125	0.145	0.255	0.155	0.132	
PPPI-2	0.095	0.125	0.255	0.175	0.122	
PPPI-3	0.115	0.165	0.194	0.19	0.125	
PPPI-4	0.12	0.18	0.241	0.105	0.152	
PPPI-5	0.125	0.178	0.276	0.192	0.155	
PPPI-6	0.125	0.19	0.2	0.177	0.172	
Isolate	Carbon source (1%)					
	Glucose	Fructose	Lactose	Maltose	Sucrose	
PPPI-1	0.255	0.25	0.197	0.145	0.223	
PPPI-2	0.221	0.199	0.187	0.135	0.235	
PPPI-3	0.23	0.155	0.194	0.125	0.198	
PPPI-4	0.269	0.158	0.141	0.155	0.2	
PPPI-5	0.229	0.165	0.168	0.165	0.255	
PPPI-6	0.245	0.172	0.145	0.147	0.232	
Isolate	Nitrogen source (0.1%)					
	Yeast extract		Peptone	Tryptone	Urea	
PPPI-1	0.265		0.245	0.197	0.145	
PPPI-2	0.255		0.2	0.187	0.135	
PPPI-3	0.235		0.185	0.194	0.125	
PPPI-4	0.27		0.178	0.141	0.155	
PPPI-5	0.275		0.195	0.168	0.165	
PPPI-6	0.285		0.19	0.145	0.147	

Supplementary Fig 1 MALDI-TOF data

Identification Result:

Genus	<i>Kocuria</i>
Species	<i>rosea</i>
Score	1.74
Scoring Criteria	< 1.7 Unreliable; 1.7-2.0 Probable Genus; > 2.0 Probable Species

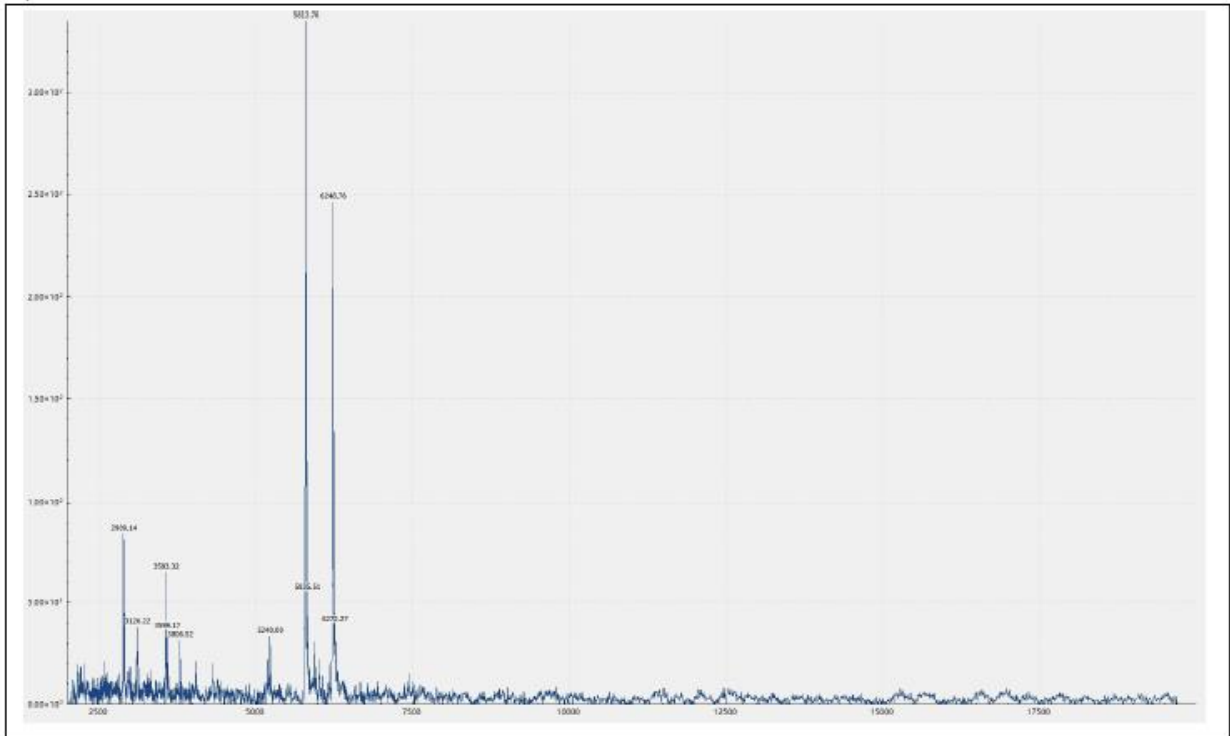
Spectrum:



Identification Result:

Genus	<i>Acinetobacter</i>
Species	<i>ursingii</i>
Score	1.84
Scoring Criteria	< 1.7 Unreliable; 1.7-2.0 Probable Genus; > 2.0 Probable Species

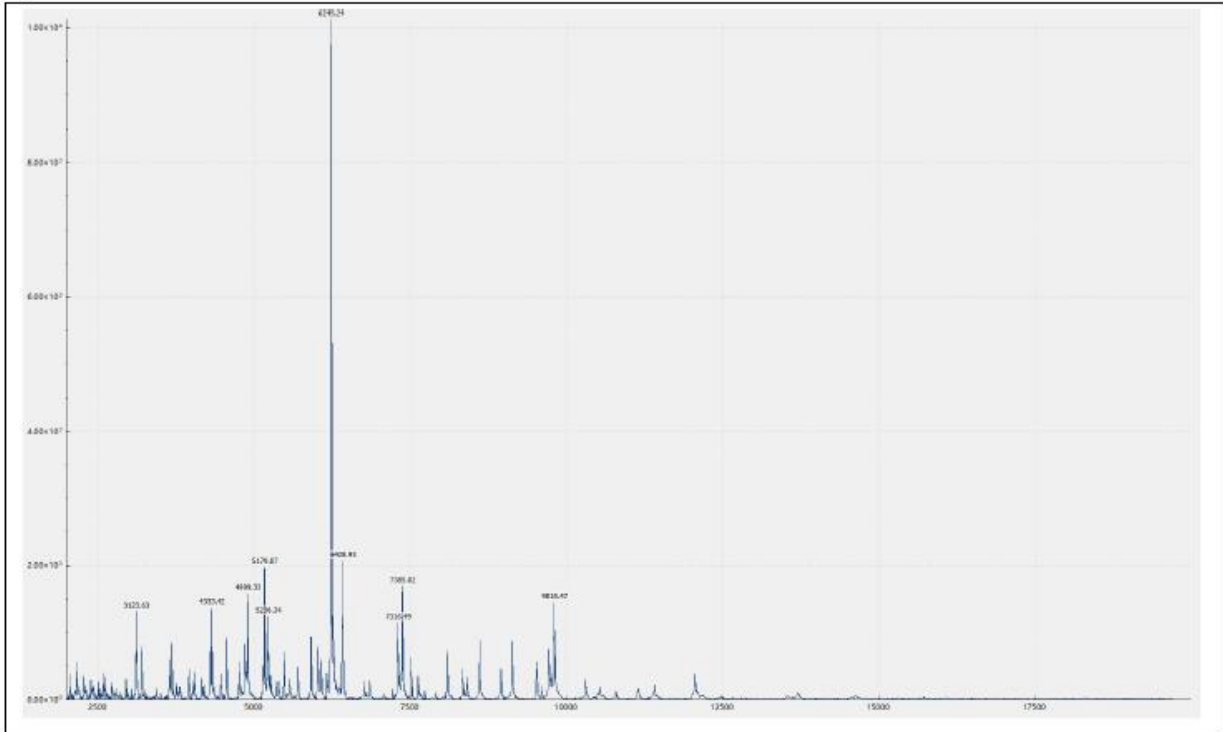
Spectrum:



Identification Result:

Genus	<i>Micrococcus</i>
Species	<i>luteus</i>
Score	2.19
Scoring Criteria	< 1.7 Unreliable; 1.7-2.0 Probable Genus; > 2.0 Probable Species

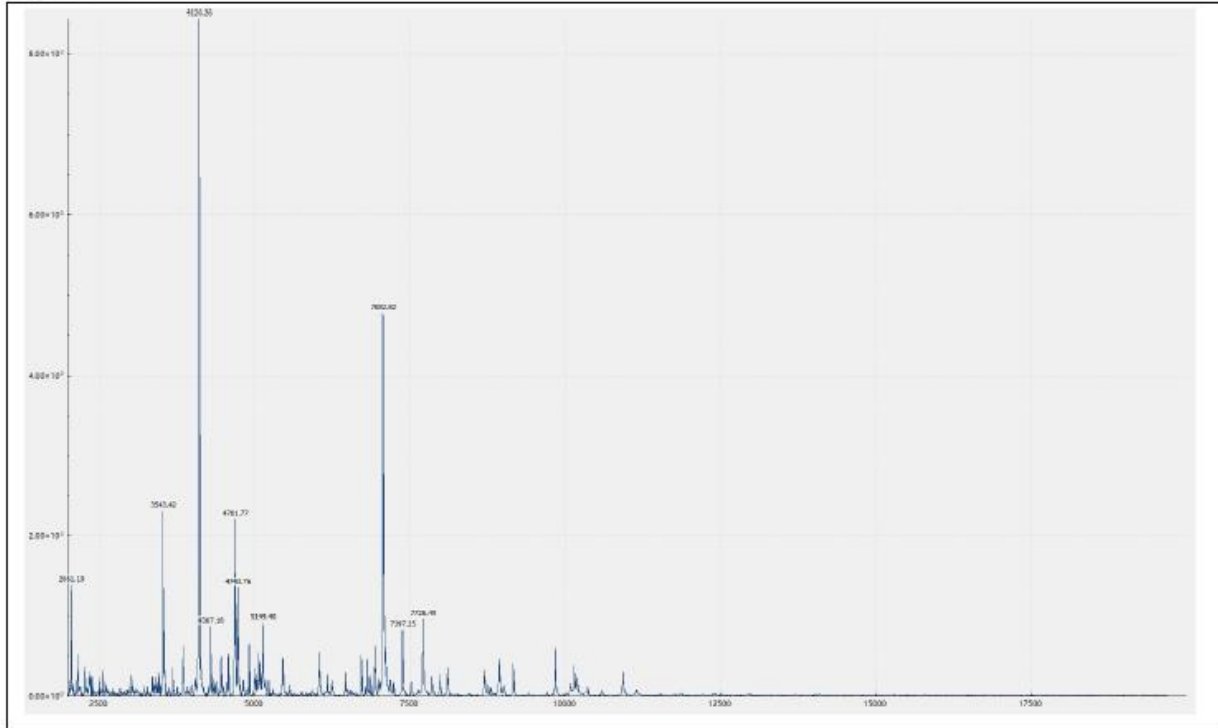
Spectrum:



Identification Result:

Genus	<i>Exiguobacterium</i>
Species	<i>aurantiacum</i>
Score	2.25
Scoring Criteria	< 1.7 Unreliable; 1.7-2.0 Probable Genus; > 2.0 Probable Species

Spectrum:



Supplementary Fig 2 ATR-FTIR data

